Centro de Investigación en Alimentación y Desarrollo, A. C.

NANOENCAPSULADOS DE COMPUESTOS FENÓLICOS DE ORÉGANO (*Lippia graveolens*) CON POLÍMEROS CATIÓNICOS PEGILADOS CON ACTIVIDAD POTENCIAL ANTINEOPLÁSICA

Por:

Melissa Garcia Carrasco

TESIS APROBADA POR LA

COORDINACIÓN EN CIENCIA Y TECNOLOGÍA DE PRODUCTOS AGRÍCOLAS DE ZONAS TROPICALES Y SUBTROPICALES

Como requisito parcial para obtener el grado de

DOCTORA EN CIENCIAS

Culiacán, Sinaloa Junio, 2024

APROBACIÓN

Los miembros del comité designado para la revisión de la tesis de la MC. Melissa Garcia Carrasco, la han encontrado satisfactoria y recomiendan que sea aceptada como requisito parcial para obtener el grado de Doctora en Ciencias.

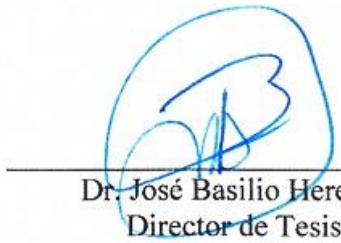

Dr. José Basilio Heredia
Director de Tesis

Dr. Ángel Licea Claverie
Co-director de tesis

Dr. Erick Paul Gutiérrez Grijalva
Integrante del comité de tesis

Dr. Lorenzo Antonio Picos Corrales
Integrante del comité de tesis

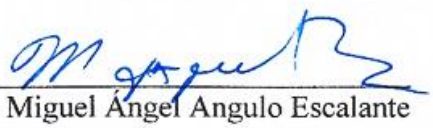

Dr. Miguel Ángel Angulo Escalante
Integrante del comité de tesis

DECLARACIÓN INSTITUCIONAL

La información generada en la tesis "Nanoencapsulados de Compuestos Fenólicos de Orégano *(Lippia graveolens)* con Polímeros Catiónicos Pegilados con Actividad Potencial Antineoplástica" es propiedad intelectual del Centro de Investigación en Alimentación y Desarrollo, A.C. (CIAD). Se permiten y agradecen las citas breves del material contenido en esta tesis sin permiso especial de la autora MC. Melissa García Carrasco, siempre y cuando se dé crédito correspondiente. Para la reproducción parcial o total de la tesis con fines académicos, se deberá contar con la autorización escrita de quien ocupe la titularidad de la Dirección General del CIAD.

La publicación en comunicaciones científicas o de divulgación popular de los datos contenidos en esta tesis, deberá dar los créditos al CIAD, previa autorización escrita del director(a) de tesis.

CIAD

Coordinación de Programas Académicos

Dra. Graciela Caire Juvera
Directora General

AGRADECIMIENTOS

Al Consejo Nacional de Humanidades, Ciencias y Tecnologías (CONAHCYT) por la beca de manutención #763248 que me permitió desarrollar mis estudios.

Al Centro de Investigación en Alimentación y Desarrollo (CIAD) subsede Culiacán por darme la oportunidad de ser parte de su cuerpo estudiantil. Por la formación académica brindada a través de sus integrantes.

Al proyecto CONAHCyT Ciencia Básica #252416 [“Biodisponibilidad y Potencial Antiinflamatorio de Compuestos Fenólicos de Orégano (*Hedeoma patens* Jones)], del cual se deriva y financia este trabajo de investigación.

A mi director de tesis, Dr. José Basilio Heredia, por recibirme en su grupo de investigación, por todo el apoyo brindado durante este proyecto. Muchas gracias por su confianza, su tiempo, por compartirme su conocimiento y consejos.

A mi co-director de tesis al Dr. Ángel Licea Claveríe, por aceptar realizar el presente trabajo, y por todos estos años de aprendizaje que he tenido en su grupo de trabajo, muchas gracias por darme su confianza, sus consejos y tiempo a lo largo de estos años, al igual que al Dr. Lorenzo A. Picos Corrales, muchas gracias por todos estos años apoyando cada una de estas etapas.

A la Dra. Ma. Priscila Quiñonez, al Dr. Luis J. Salazar y al Dr. Eduardo Hermosillo, por seguir apoyándome a la distancia, gracias por convertirse en mi segundo hogar.

A los miembros del comité, Dr. Erick P. Gutiérrez Grijalva y Dr. Miguel Ángel Angulo Escalante, gracias por su tiempo y por contribuir con su experiencia al desarrollo de este trabajo.

A la nueva familia que se formó con los compañeros de LAFN, en especial a la Dra. Laura, Dra. Nayely, Dra. Marilyn, MC. Alicia y MC. Brianda por su amistad, consejos y risas en los últimos años, asi como a mis compañeros de laboratorio, muchas gracias por todo.

DEDICATORIA

A mi familia que aprecio con todo mi corazón gracias por apoyarme siempre.
Los amo.

CONTENIDO

CONTENIDO (continuación)

LISTADO DE FIGURAS

Figura **Página**

RESUMEN

Los compuestos fenólicos extraídos de orégano mexicano (*Lippia graveolens*), han presentado diferentes propiedades biológicas, entre las que destacan capacidad antioxidante, antiinflamatoria y anticancerígena. No obstante, estos compuestos tienden a ser inestables y poco solubles en medio acuoso, además de disminuir o perder sus propiedades biológicas cuando se encuentran a expuestos a la luz o bien a cambios en el pH del medio. Es por ello que en la presente investigación se desarrollaron diferentes matrices catiónicas a base de quitosano (QS) y poli(*N*,*N*-diaminoetil metacrilato) (PDEAEAM). Se utilizaron 3 diferentes matrices, QS, QS modificado con poli(etilenglicol) metacrilato (PEGMA) (QS-*b*-PPEGMA) y bloques de poli(etilenglicol) con PDEAEM (PEG-*b*-PDEAEM). El tamaño de partícula obtenido de las matrices cargadas fue de 955 nm, 458 nm y 122.4 nm, respectivamente. El contenido cargado de compuestos fenólicos de los tres sistemas no sobrepasó el 70%. En los perfiles de liberación se observó que el sistema que libero poco más del 80% de los compuestos fenólicos contenidos fue QS-*b*-PPEGMA debido a la alta solubilidad que presentaron en medio acuoso. Se determinó el contenido de compuestos fenólicos mediante UPLC/MS, teniendo como compuestos mayoritarios naringenina, floridzina y cirsimaristina, compuestos que han presentado propiedades antiinflamatorias y antitumorales. Después del ensayo gastrointestinal (GI) *in vitro*, se observó que la actividad antioxidante de los compuestos encapsulados aumento, caso contrario en los compuestos fenólicos sin encapsular, con lo cual estas matrices le estarían confiriendo protección al pasar por la fase GI. Se determinó que una concentración ≤500 μg mL^{-1} de compuestos fenólicos en bloques PEGilados no presentaron citotoxicidad en fibroblastos CCD18, mientras que en células Caco-2 inhibieron la proliferación de estas, después de 72 h se pudo observar que el efecto de los compuestos cargados fue muy similar al del fármaco modelo (5FU) utilizado. Por último, también se determinó la estabilidad de estos cargados la cual no se afectó después de 4 meses de almacenamiento. Por lo que las matrices cargadas con extractos fenólicos de orégano mexicano (*Lippia graveolens*) podrían utilizarse como posible tratamiento coadyuvante contra el cáncer de colon.

Palabras claves: Nanoemulsiones, Compuestos fenólicos, matrices PEGiladas, Caco-2, CCD18-co.

ABSTRACT

The phenolic compounds extracted from Mexican oregano (*Lippia graveolens*) have presented different biological properties, among which antioxidant, anti-inflammatory, and anti-cancer. However, these compounds tend to be unstable and poorly soluble in aqueous medium, in addition to decreasing or losing their biological properties when exposed to light or changes in the pH of the medium. That is why in the present investigation different cationic matrices based on chitosan (QS) and poly(*N*,*N*-diaminoethyl methacrylate) (PDEAEAM) were developed. Three different matrices were used, QS, QS modified with poly(ethylene glycol) methacrylate (PEGMA) (QS-*b*-PPEGMA), and poly(ethylene glycol) blocks with PDEAEM (PEG-*b*-PDEAEM). The particle size obtained from the loaded matrices was 955 nm, 458 nm, and 122.4 nm, respectively. Regarding the content of phenolic compounds in the three systems, it did not exceeded 70%. In the release profiles, it was observed that the system with a higher percentage was the QS-*b*-PPEGMA block, releasing just over 80% of the phenolic compounds contained, due to the high solubility these blocks presented in aqueous medium. The content of phenolic compounds was determined by UPLC/MS, with naringenin, phloridzin, and cirsimaristin being the main compounds, that have shown anti-inflammatory and anti-tumor properties. After the *in vitro* gastrointestinal (GI) tests, it was observed that the antioxidant activity of the encapsulated compounds was increased, the opposite of the free phenolic compounds, so it that these matrices confer protection when passing through the GI phase. It was determined that the PEGylated blocks containing 500 µg mL^{-1} or less of phenolic compounds did not present cytotoxicity in CCD18 fibroblasts, While in Caco-2 cells, they showed inhibition of the proliferation, it was observed that the loaded compounds had an activity very similar to the model drug (5FU) after 72 hours. Finally, the stability of these loads was also determined, which was not affected after 4 months of storage. Phenolic extract from Mexican oregano (*Lippia graveolens*) loaded in cationic matrices may be a good coadjutant to colon cancer treatment.

Key words: Nanoemulsions, Phenolic compounds, PEGylated matrixes, Caco-2, CCD18-co

1. SIPNOSIS

1.1. Justificación

El cáncer es una enfermedad crónico-degenerativa caracterizada por un crecimiento descontrolado y anormal de células, las cuales pueden diseminarse a otras partes del cuerpo. La quimioterapia es uno de los tratamientos más utilizados y a pesar de que existen un sinfín de fármacos comerciales para los diferentes tipos de cáncer, estos no son completamente efectivos, son extremadamente invasivos y dañan tejido sano provocando efectos adversos a los pacientes que los consumen, por ello se han investigado alternativas de dichos fármacos. Las plantas medicinales han atraído la atención en los últimos años ya que estas presentan una amplia gama de productos naturales con actividad biológica y propiedades terapéuticas. En la actualidad se han encontrado varios agentes anticancerígenos de origen vegetal como lo son el taxol, vincristina, derivados de la camptotecina, topotecán e irinotecán, así como epipodofilotoxinas. Estos han sido utilizados de manera sinérgica con otros fármacos que ayudan a controlar la proliferación células cancerígenas. Este mecanismo está estrechamente relacionado con el proceso de inflamación celular, ya que estas células cancerígenas producen citoquinas que son capaces de activar diferentes rutas de señalización que ayudan a que estas obtengan los nutrientes necesarios para seguir reproduciéndose. En los últimos años se ha descubierto que una gran cantidad de metabolitos secundarios vegetales presentan propiedades antinflamatorias, dentro de estos se encuentran los compuestos fenólicos que se producen en diferentes plantas y hierbas como el orégano mexicano (*Lippia graveolens*). También se sabe que este tipo de compuestos tienen baja biodisponibilidad y pueden perder su actividad cuando entran en contacto con diferentes estímulos presentes en el ambiente (luz, pH, etc.). Es por ello que en el presente trabajo se encapsularon estos compuestos fenólicos en nanogeles y micelas de poli(etilenglicol)-poli(metacrilato de *N*,*N*-dimetilaminoetilo) (PEG-PDEAEM) y poli(etilenglicol)-quitosano (PEG-QS), los cuales pueden presentar cambios en su fase a bajo la influencia de diferentes estímulos como cambios en el pH y temperatura del medio, así como realizar estudios de liberación controlada *in vitro* y en la línea celular Caco-2.

1.2. Antecedentes

1.2.1 Cáncer como Problema de Salud Pública

El cáncer es una de las enfermedades que ataca a millones de personas alrededor del mundo, en un estudio estadístico realizado en Estados Unidos publicado en el 2024, se presentan un estimado del número de personas que podrían contraer cáncer (Figura 1-a), así como el porcentaje de muertes posible a causa de lo mismo (Figura 1-b)(Siegel *et al.*, 2024).

a)

Próstata	299,010,	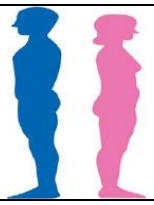	Mama	310,720
Pulmón	116,310		Pulmón	118,270
Colón	81,540		Colón	71,270
Leucemia	36,450		Tiroides	31,520

Total de personas: 1,029,080 hombres y 972,060 mujeres

b)

Pulmón	65,790	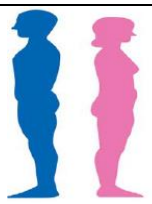	Pulmón	59,280
Próstata	35,250		Mama	42,250
Colón	28,700		Colón	24,310
Leucemia	13,640		Leucemia	10,030

Total de personas: 322,800 hombres y 288,920 mujeres

Figura 1. Casos de a) Incidencia y b) Muerte de hombres y mujeres a causa de los principales tipos de cáncer en USA, 2024.

Comparando los resultados con los de años anteriores se puede observar que hay una disminución de la mortalidad prevista y esto se asocia a la disminución en el consumo de tabaco, así como en la detección temprana de algunos tipos de cáncer, además de la mejora en los tratamientos de elección, así como el uso de tratamientos coadyuvantes (Siegel *et al.*, 2024). Por otra parte, en México hasta el año 2022 del total de defunciones registradas ante la INEGI el 10.6% de casos fue debido a tumores malignos, teniendo un aumento del 4.86% de defunciones entre el 2012 y el 2022 (INEGI, 2024).

La incidencia de los diferentes tipos de cáncer en México incrementa con la edad, tanto en hombres como en mujeres; sin embargo, es superior en mujeres, y se ha asociado con riesgos conductuales y metabólicos. En el censo realizado hasta el año 2022 en pacientes de 0 a 29 años el principal tipo de cáncer que causó la muerte de los pacientes fue leucemia, mientras que para pacientes de 30 años en adelante el cáncer con mayores defunciones fue el de próstata y de mama, para hombres y mujeres, respectivamente, siendo el cáncer colo-rectal encontrándose entre el tercer y cuarto puesto, respectivamente (INEGI, 2024). En cuanto la incidencia de casos hasta el año 2022 la Organización Mundial de la Salud (Figura 2) mostró los primeros tres principales tipos de cáncer presentados en la población mexicana son cáncer de mama, próstata y colo-rectal (GLOBOCAN, 2022).

Próstata	26,565		Mama	31,043
Colo-rectal	8,359		Cérvico uterino	10,348
Linfoma de Hodgkin	5,173		Tiroides	9,057
Pulmon	5,062		Colo-rectal	7,723

Total de personas: 95,954 (hombres), 111,200 (mujeres)

Figura 2. Casos de Incidencia de cáncer en hombre y mujeres en México en el año 2022 (GLOBOCAN 2022)

1.2.2 El Cáncer y la Inflamación

La inflamación (Figura 3a) es una respuesta que el sistema inmune activa después de recibir un daño o encontrar algún agente extraño, inicialmente se activan señales químicas para iniciar y mantener la respuesta del hospedero designado a sanar el tejido dañado. Esto provoca la activación y la migración de leucocitos (neutrófilos, monocitos y eosinófilos) provenientes de sistema circulatorio hacia el sitio donde se encuentra el daño. Se cree que los neutrófilos coordinan la migración de células endoteliales y fibroblastos con un mecanismo de cuatro pasos, en el cual se forma un andamio con matriz extracelular provisional donde estas células proliferan, esta especie de nido formado ayuda reconstituir al microambiente. Estos pasos involucran la activación de

moléculas de adhesión de la familia de las selectinas (L-, P- y E-selectina), las cuales facilitan la vascularización del endotelio, desencadenando una activación y sobreexpresión de integrinas leucocitarias mediadas por citoquinas y moléculas activadores de leucocitos; la inmovilización de neutrófilos en la superficie de endotelio vascular por medio de una fuerte adhesión de integrinas $\alpha_4\beta_1$ y $\alpha_4\beta_7$ que se unen a la molécula de adhesión celular endotelial vascular-1 (VCAM-1) y MadCAM-1, respectivamente; y transmigración a través del endotelio a sitios de lesión, presumiblemente facilitados por proteasas extracelulares, como las metaloproteasas de matriz (MMPs) (Coussent y Werb, 2002).

Una familia de citocinas quimiotácticas (quimiocinas), poseen un alto grado de especificidad para el quimioatrayente de leucocitos específicos (Balkwil y Mantovani, 2001; Rossi y Zlotnik, 2000, Muller *et al.*, 2002), dictan la evolución natural de la respuesta inflamatoria. El desarrollo de enfermedades crónicas se debe a expresión regular de estas citocinas. La citocina pro-inflamatoria TNF-α (factor de necrosis tumoral-α) controla las poblaciones de células inflamatorias, además de mediar otros aspectos de los procesos inflamatorios. TGF-β_1 también es importante, influyendo tanto positiva como negativamente en los procesos de inflamación y reparación (Moustakas *et al.*, 2002). La inflamación normal asociada con la cicatrización de heridas, generalmente es autolimitada; sin embargo, la desregulación de cualquier factor de convergencia puede conducir a anomalías y, en última instancia, la patogénesis, este parece ser el caso durante la progresión neoplásica (Figura 3b).

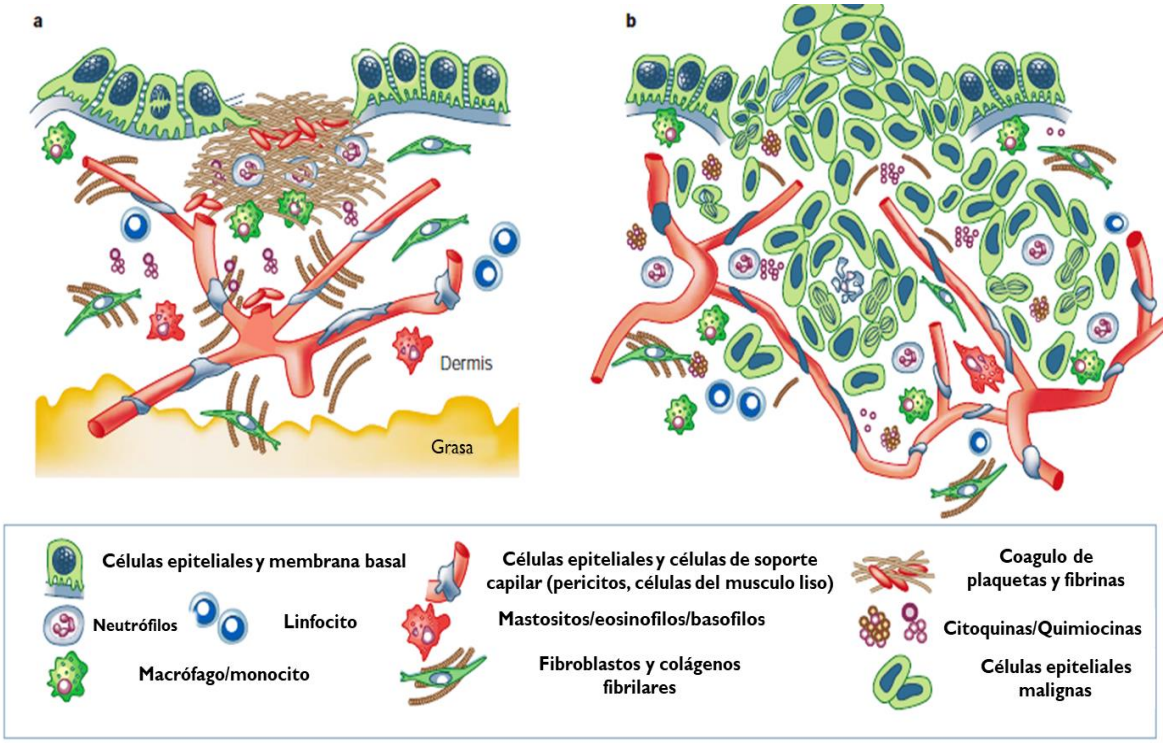

Figura 3. Proceso de inflamación a) normal y b) en proliferación celular (Coussent y Werb, 2002).

Las células tumorales por su parte producen algunas citoquinas y quimiocinas que atraen leucocitos (neutrófilos, células dendríticas, macrófagos, eosinófilos, mastocitos y/o linfocitos), los cuales son capaces de producir citoquinas, mediadores citotóxicos como las especies reactivas de oxígeno (ROS), proteasas de serina y cisteína, MMPs y agentes de perforación de membrana, así como mediadores solubles de muerte celular, TNF-α, interleucinas (IL) e interferones (IFNs) (Kuper *et al.*, 2000; Wahl y Kleinman, 1998). Dependiendo de la cantidad de citocinas y quimiocinas que se produzcan se ve comprometido el crecimiento de estas células (Figura 4).

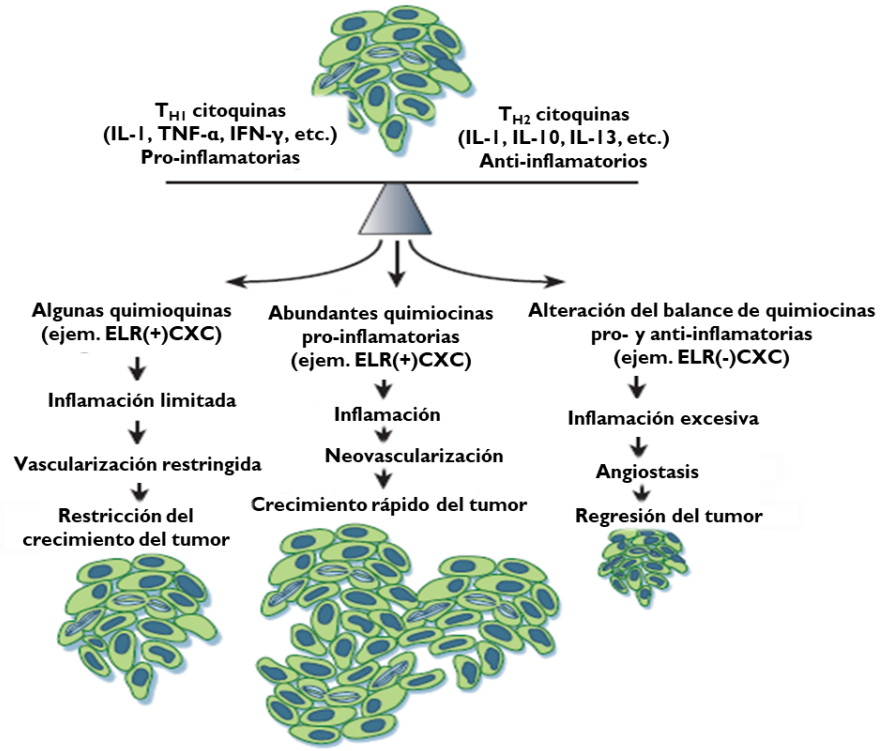

Figura 4. Regulación de la proliferación celular mediante citoquinas y quimiocinas (Coussent y Werb, 2002).

1.2.3 Tratamientos contra el Cáncer

En la actualidad la existencia de diferentes tipos de cáncer hace que también existan diferentes tratamientos, dentro de los tratamientos convencionales se encentran: la quimioterapia, la cirugía y la radiación (Figura 5):

- **Quimioterapia:** Es el tratamiento de primera opción y que por elección se le da a la mayoría de los pacientes que padecen de algún tipo de cáncer, pero este al ser sistémico, ataca no solamente a células cancerígenas, si no también células normales.
- **Cirugía:** Este tratamiento se utiliza solamente en algunos tipos de cáncer, donde se forman tumores localizados, lo cuales puedes ser extirpados total o parcialmente, del sitio en el que se encuentre. Ayuda de igual manera a mitigar los síntomas contra el cáncer (NIC, 2015).
- **Radiación:** La terapia por radiación es uno de los tratamientos más comunes contra el cáncer, y en este se utilizan partículas u ondas de alta energía que ayudan a eliminar o dañar células cancerosas.

Esta radiación actúa directamente sobre el ADN de estas células produciendo roturas que evitan que la célula se siga dividiendo (NIC, 2018)

Figura 5. Tipos de tratamientos convencionales contra el cáncer.

1.2.4 Agentes Fitoquímicos

Desde la antigüedad se han utilizado extractos de plantas como medicamentos por sus propiedades bactericidas, fungicida, antiparasitarios y otras propiedades medicinales tales como analgésicos, sedantes, espasmódicos, anestésicos locales y antiinflamatorios (Adorjan y Buchbauer, 2010; Bakkali *et al.*, 2008; Buchbaer *et al.*, 1993) y se han desarrollado un gran número de medicamentos modernos a partir de ellos (Kharb *et al.*, 2012). Dentro de los productos naturales, los metabolitos secundarios (Figura 6) de origen vegetal han sido ampliamente utilizados en todo el mundo, para el tratamiento de diversas enfermedades crónicas. Las hierbas medicinales han jugado un papel importante en la prevención y el tratamiento del cáncer que ejecutan sus múltiples efectos terapéuticos al inhibir el cáncer activando enzimas y hormonas, estimulando la reparación del ADN mecanismo, promoviendo la producción de enzimas protectoras, induciendo la acción antioxidante y mejorando la inmunidad, por lo tanto mostrando efecto anticancerígeno (Thakore *et al.* 2012).

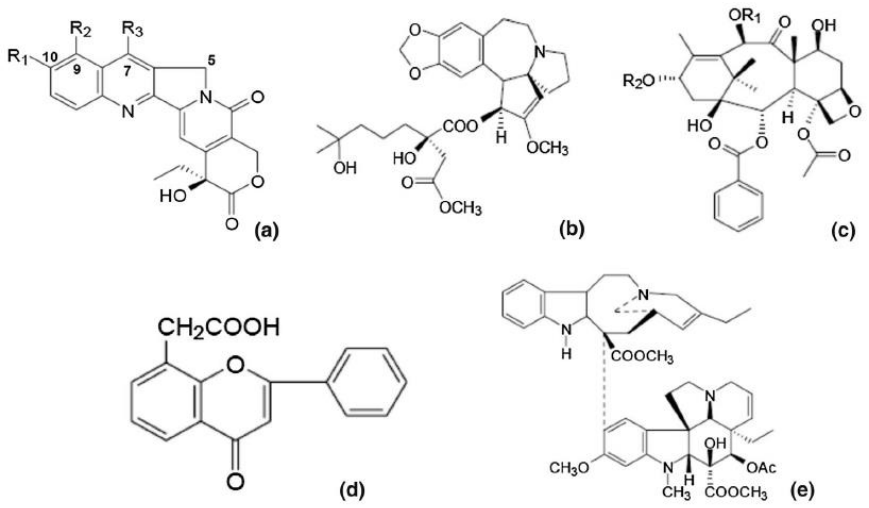

Figura 6. Metabolitos secundarios a) Camptotecina, b) Homoharringtonina, c) Taxol, d) Acido flavona-8-acético y e) Vinorelbina

Además de las alteraciones mutagénicas de las células cancerígenas, estas secretan cascadas de señalizaciones que inducen el proceso de inflamación para así poder obtener los nutrientes necesarios para seguir reproduciéndose. Es por ello que también se han estudiado alternativas antiinflamatorias en la medicina natural, *Artemisia herba alba* y *Magnolia officinalis* han sido ampliamente utilizadas ya que inhiben y estimulan la producción de IL-12 e IL-4, respectivamente, además disminuyen la producción de óxido nitroso (NO) (Messaoudene *et al.,* 2011). En México es muy común el uso de infusión de hierbas, en las que recientemente la *Buddleia scordioides* (Sevilla), *Chamaemelum nobile* (Manzanilla) y *Listea glaucescens* (Laurel), mostraron respuestas de inhibición sobre marcadores antiinflamatorios, aliviando estrés oxidativo y una baja regulación de COX -2, TNF-α, NF-κB e IL-8 (Herrera-Carrera *et al.*, 2015). La mayoría de los compuestos que exhiben propiedades quimiopreventivas (antiproliferación, apoptosis, prevención de la oxidación y actividad antiinflamatoria, entre otras) son compuestos fenólicos (Figura 7), estos se pueden subdividir en ácidos fenólicos, flavonoides y no flavonoides. Los flavonoides están conformados por dos anillos fenólicos unidos por tres carbonos, los cuales normalmente están oxigenados. Las propiedades antiinflamtorias y antioxidantes de estos compuestos son atribuidas a su estructura química, ya que son capaces de donar electrones o hidrógeno, neutralizar radicales libres o algunas otras especies reactivas de oxígeno (Zhang y Tsao, 2016). Los mecanismos propuestos de estos compuestos son por su actividad estrogénica/antiestrogénica (Veeramuthu *et al*., 2017).

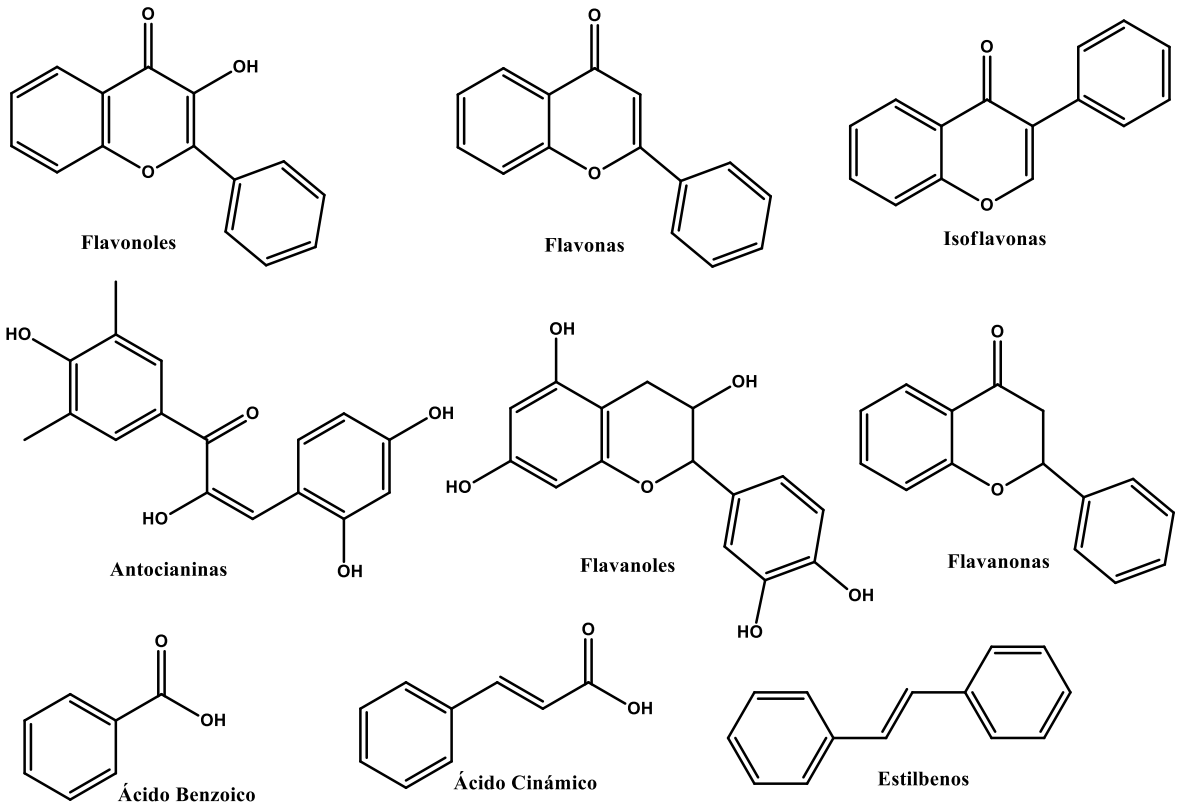

Figura 7. Estructura de compuestos fenólicos

1.2.5 Agentes Fitoquímicos en Orégano (*Lippia graveolens*)

En orégano se han encontrado diferentes tipos de fitoquímicos, los cuales se agrupan dependiendo de sus propiedades hidrófilicas o hidrofóbicas, en aceites esenciales o compuestos fenólicos, respectivamente (Ambriz-Pérez *et al.*, 2019). Los compuestos fenólicos son un grupo heterogéneo de compuestos derivados del metabolismo secundario de las plantas. Estos se caracterizan estructuralmente porque tienen al menos un anillo aromático al que uno o más grupos hidroxilo se encuentran unidos a estructuras aromáticas y alifáticas.

Estos compuestos pueden clasificarse en flavonoides y no flavonoides. Los flavonoides están compuestos por dos anillos aromáticos unidos a través de un heterociclo, los cuales dependiendo del grado de hidrogenación se pueden subclasificar en flavonoles, flavonas, isoflavonas, entre otros. Dentro de los no flavonoides se encuentran los derivados del ácido hidroxibenzoico e

hidroxicinámico y a estos se les conoce comúnmente como ácidos fenólicos. En los últimos años se ha incrementado el interés de la ciencia y la industria alimentaria en estos compuestos debido a sus beneficios en la salud (Gutierrez-Grijalva *et al.*, 2018). El aumento en la ingesta de compuestos del tipo flavonoide ha disminuido la aparición de algunas enfermedades crónicas como la diabetes, enfermedades cardiovasculares, Alzheimer, Parkinson e inflamación (Bravo, 1998; Mhamed, 2014). El aislamiento de estos compuestos se realiza con ayuda de solventes, estos se elegirán dependiendo de la polaridad y la afinidad de los compuestos con el solvente, dentro de los comúnmente utilizados para la extracción de estos son los de tipo metanólico.

1.2.6 Liberación de Fármacos a partir de Nanopartículas

Los tratamientos tradicionales contra el cáncer quedan limitados en muchos de los casos solo a la cirugía, la radiación y la quimioterapia, lo cual lleva consigo un alto riesgo de daño a tejido sano o bien no erradicar por completo el cáncer, por lo que la nanotecnología ha desarrollado en las últimas décadas terapias dirigidas lo cual facilitaría la administración de fármacos en quimioterapia, ya que ofrece un medio adecuado para la liberación controlada de una gran variedad de fármacos y otros agentes bioactivos (Hamidi *et al.* 2008; Estanqueiro *et al.* 2015; Benjamin *et al.* 2017). Desde un punto de vista terapéutico, una liberación controlada en respuesta a señales específicas puede resultar ventajosa en un buen número de situaciones como en el que la inestabilidad, alta citotoxicidad y liberación en tejidos específicos de un principio activo se ve comprometida (Chamundeesware, *et al.* 2019).

1.2.7 Sistemas de Liberación Controlada

Con el fin de mejorar la calidad de vida de los pacientes con cáncer se han propuesto nuevos tratamientos y el desarrollo de nuevas tecnologías biomédicas para disminuir los efectos adversos presentados por los fármacos utilizados en quimioterapia. La nanomedicina es una rama de la

ciencia que se dedica al diseño, construcción y utilización de estructuras funcionales a escala nanométricas para ayudar al tratamiento, diagnóstico y control de sistemas biológicos. En la terapia contra el cáncer, uno de los sistemas más prometedores son las nanocápsulas, que poseen propiedades fisicoquímicas únicas tales como estabilidad en un amplio intervalo de valores de pH y temperaturas, buen grado de flexibilidad y alta relación superficie/volumen con capacidad para almacenar fármacos (Sanna *et al.* 2014; Kang *et al.,* 2015). Todas estas características hacen que estas partículas sean idóneas para su utilización en el suministro controlado de antineoplásicos.

El uso de nanopartículas para el transporte de fármaco dentro del cuerpo humano permite que el fármaco tenga una mayor probabilidad de llegar a su sitio de acción, por lo que hoy en día se han preparado diferentes tipos de nanocápsulas para ayudar a que esto sea posible. Como nanoacarreadores tradicionales, tenemos aquellos que están basados en los sistemas liposomales, estos han tenido un gran éxito como transportadores de fármacos, así como co-administradores de fármacos quimioterapéuticos y agentes génicos, muchos investigadores han informado de sus logros utilizando liposomas catiónicos modificados (Chen *et al*., 2008; Fulton y Najahi-Missaoui, 2023*)* Dentro de los nanoacarreadores no tradicionales se encuentran los dendrímeros que son macromoléculas hiperramificadas y monodispersas las cuales presentan pesos moleculares definidos. Estos pueden interactuar con moléculas de fármacos y genes por encapsulaciones simples, interacciones electrostáticas y conjugaciones covalentes ya que poseen cavidades internas vacías donde es posible hospedar una molécula huésped y una densidad alta de superficie (González-Ayón *et al.*, 2015).

También existe una clase de nanoacarreadores a base de polímeros reticulados como los nanohidrogeles que son redes poliméricas que tienden a hincharse y a su vez poseen propiedades fisicoquímicas únicas en el entorno acuoso, presentan una buena estabilidad en una amplia gama de valores de pH y temperaturas, buen grado de flexibilidad y alto volumen para la encapsulación de fármacos bioactivos (Kakizawa y Kataoka, 2002). Así mismo, existen estrellas poliméricas, que son similares a las micelas las cuales tienen alrededor brazos que ayudan a la estabilidad de la misma (Licea-Claveríe *et al.,* 2009). Las micelas son nanoacarreadores capaces de proteger el contenido, evitando su degradación así como de evitar su liberación prematura. La mayoría de los complejos micelares se basan en un autoensamblaje de bloques hidrofóbicos para formar el interior

y bloques hidrófilicos para formar la cubierta de la micela (Van der Meel *et al.*, 2014). Por otra parte, las vesículas son agregados que cuentan con una doble capa. Estas se auto-ensamblan como resultado del efecto hidrófobo cuando las moléculas anfipáticas, normalmente fosfolípidos, son presentadas en un entorno acuoso (Chen *et al.*, 2010). En la Figura 8 se muestran algunos de los tipos diferentes de nanocápsulas mencionados anteriormente.

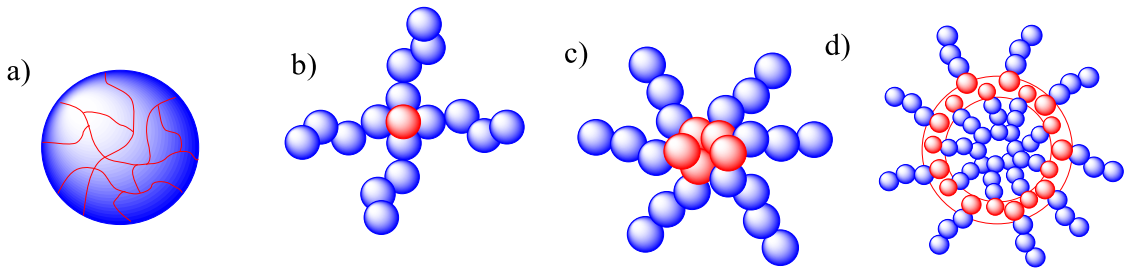

Figura 8. Ilustración esquemática de cuatro tipos principales de nanoacarreadores: a) Nanogel, b) Estrellas, c) Micelas y d) Vesículas.

1.2.8 Monómeros Utilizados para la Síntesis de Nanocápsulas Catiónicas

Para que los nanoacarreadores mencionados anteriormente sean capaces de responder a ciertos estímulos como el pH o a la temperatura, deben de contener polímeros que respondan de igual manera a esos estímulos. Estos polímeros presentan un cambio de volumen reversible como respuesta a una variación pequeña de un parámetro del medio acuoso donde se encuentren (Picos-Corrales *et al.*, 2012)

Cuando la variable es la temperatura, la respuesta se origina en la llamada temperatura crítica inferior de solución (LCST) de las cadenas de polímeros que forman las nanocápsulas. Esta debe estar optimizada dentro del intervalo en el que se quiere trabajar. Algunos de estos polímeros también pueden presentar respuestas a otros estímulos externos del medio como los cambios de pH, alterando la conformación de la nanocápsula y su estructura química, dejando salir el o los principios activos que se encuentren dentro de la nanocápsula (Figura 9), dependiendo de los grupos contenidos en los polímeros estos pueden ser aniónicos o catiónicos, estas características

hace que estas nanocápsula sean catalogadas como polímeros inteligentes, ya que cuando el estímulo cesa estas vuelven a su forma original (Khan *et al.*, 2023; Singh y Nayak, 2023).

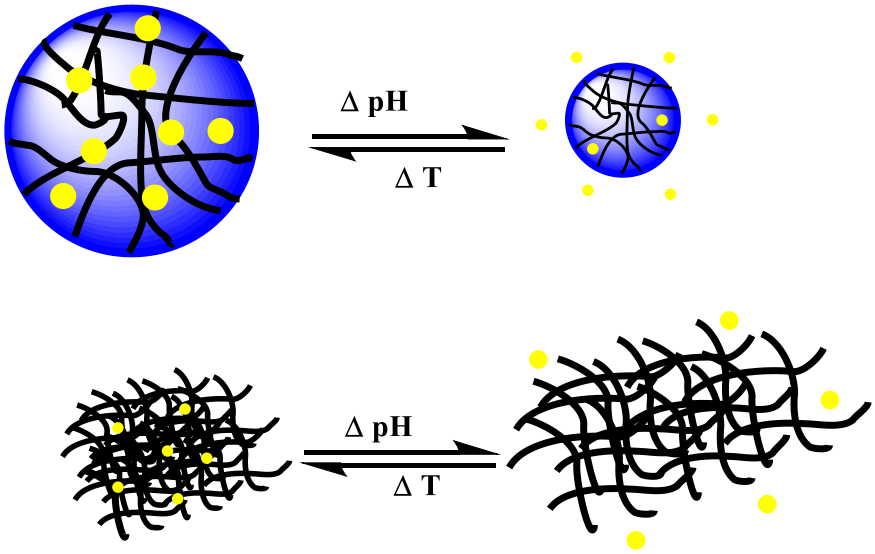

Figura 9. Variación del tamaño en función de la temperatura o del pH.

Los monómeros utilizados para la síntesis de estos sistemas nanoacarreadores sensibles a estímulos (por ejemplo, a la temperatura y/o pH) son de gran importancia ya que, dependiendo de ellos, los nanoacarreadores pueden presentar un cierto porcentaje o nula toxicidad y por supuesto biocompatibilidad al entrar en contacto con las células vivas.

1.2.8.1 Poli(etilenglicol) (PEG). El poli(etilenglicol) (PEG) ha sido uno de los polímeros que en los últimos años ha ido ganando importancia debido a la biocompatibilidad alta que presenta, aumentar el tiempo en circulación de nanoacarreadores, disminuir el reconocimiento y eliminación por parte del sistema fagocítico mononuclear (Shi et al., 2021; Shi et al., 2022). Otro factor relevante para las características del PEG es la longitud de cadenas que este contenga, porque dependiendo del tamaño estos polímeros son solubles en agua y también presentan LCST (Molina y Bergueiro, 2015). Esta última puede verse modificada por los grupos terminales que el PEG tenga ya sean del tipo ácido, amino o hidroxilo (Kataoka et al., 2003).

Por ello el metacrilato de poli(etilenglicol) metil éter (PEGMA) (Figura 10), ha sido ampliamente

utilizado. Cuando este comienza a degradarse, algunas de sus propiedades cambian, esto permite un cambio en el tamaño de los subproductos degradados, lo cual es muy favorable para la aplicación médica, ya que estos subproductos pueden ser fácilmente excretados por filtración renal (Chen *et al.*, 2017).

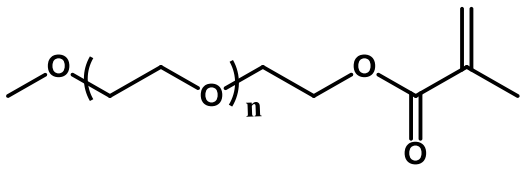

Figura 10. Estructura del metacrilato de poli(etilenglicol) metil éter (PEGMA).

El PEG como el PEGMA son polímeros hidrofílicos, normalmente se copolimerizan con polímeros hidrofóbicos, los cuales ayudan a mantener por más tiempo una mayor cantidad del fármaco o agente que se quiere transportar a un sitio específico.

1.2.8.2 Metacrilato de (*N*,*N*-dimetilamino)etilo (DEAEM). Otro de los monómeros que ha sido ampliamente utilizado en los últimos años es el metracrilato de (*N*,*N*-dietilamino) etilo (DEAEM) (Figura 11), el cuál forma polímeros que presentan cambios en su conformación con variaciones del pH del medio, en otras palabras son sensibles a cambios de pH (Manzanares-Guevara et al., 2017).

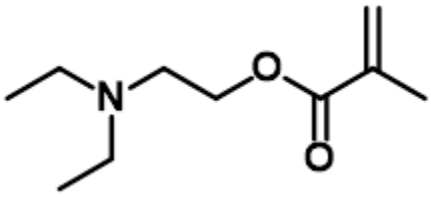

Figura 11. Estructura del metracrilato de (*N*,*N*-dietilamino) etilo (DEAEM).

La combinación del DEAEM y el PEG da como resultado copolímeros que son sensibles a

estímulos del medio que los rodea, como se puede observar en la estructura del PDEAEM este posee una amina terciaria, que puede ser fácilmente cuaternizada para producir un polímero catiónico, esto hace que los grupos amino terciarios actúen como ligandos para muchos metales (Amalvy *et al.*, 2004). También se ha confirmado que este polímero es sensible al pH con un pK_a cercano a 7.

1.2.8.3 Quitosano (QS). El quitosano (QS) se deriva de fuentes de origen natural, como lo son el exoesqueleto de los insectos, crustáceos y hongos (Dash et al., 2011). El QS (Figura 12) es un copolímero lineal compuesto de β-(1-4) D-glucosamina ligada y N-acetil-D-glucosamina al azar, obtenido a partir de la desacetilación de la quitina, se describe así como un polielectrolito catiónico. La naturaleza catiónica del quitosano es especial ya que la mayoría de los polisacáridos son neutros o presentan carga negativa cuando se encuentran a pH bajos. Esta propiedad ayuda la formación de complejos electrostáticos o estructuras multicapa con otros polímeros sintéticos o naturales con carga negativa (Venkatesan y Kim, 2010).

Este biopolímero presenta una variedad de propiedades físicas, químicas y biológicas como biodegradable, biocompatible, bioadhesivo y no tóxico (Kumar *et al.*, 2004). Dichas propiedades le confieren numerosas aplicaciones en campos tales como cosméticos, productos farmacéuticos, ingeniería biomédica, la oftalmología, la biotecnología, la agricultura, los textiles, la enología, la elaboración de alimentos y nutrición; también es útil en el tratamiento de aguas para eliminar partículas y contaminantes disueltos (Dash *et al*., 2011). Los principales parámetros que influyen en las caracteristicas y propiedades de quitosano son su peso molecular, el grado de desacetilacion, lo que represeta la fraccion molar de unidades desacetilada, y su cristalinidad (Renault *et al*., 2009).

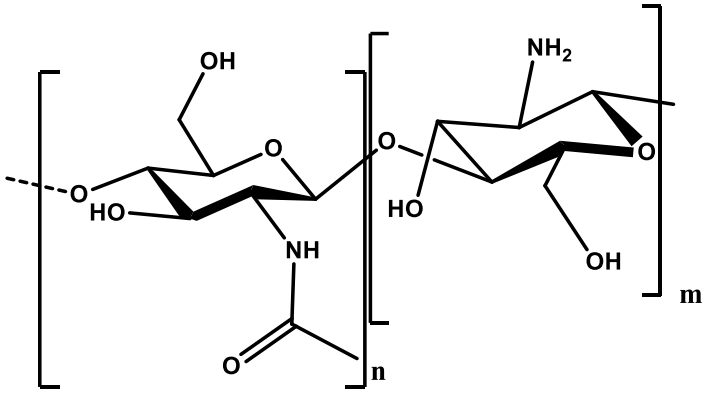

Figura 12. Estructura del Quitosano

1.2.9 Síntesis de Polímeros

1.2.9.1 Polimerización por radicales libres. Para la obtención de los diferentes tipos de morfologías de los nanoacarreadores existen diferentes tipos de polimerización, para la obtención de nanoacarreadores tipo micela se utiliza de convencionalmente la polimerización por radicales libres, la cual consiste agregar una gran cantidad de iniciador el cual va a producir una gran cantidad de radicales lo cual ayudará a la obtención en primera instancia de un homopolímero. Después de obtener el primer homopolímero, en la siguiente etapa de polimerización se adiciona un monómero diferente que se activará con radicales libres del iniciador y se irá adicionando al homopolímero previamente obtenida, teniendo como resultado un copolímero el bloque (Odian,1991) (Figura 13). Con ello estos polímeros pueden obtener diferentes propiedades dependiendo de la relación entre ambos polímeros, entre las que se encuentran variaciones en la solubilidad, sensibilidad al pH y/o a la temperatura, entre otras.

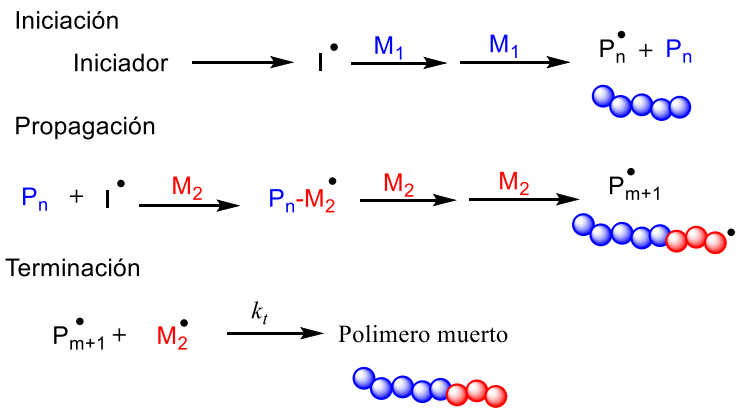

Figura 13. Esquema de la polimerización por radicales libres.

1.2.9.2 Polimerización por Transferencia de Cadena Reversible Adición-Fragmentación (RAFT). Para la obtención de bloques copoliméricos se utilizó la polimerización RAFT, la cual es muy similar a la de radicales libres, con la diferencia que en esta se puede controlar el crecimiento de las cadenas de polímero y esto es posible con la ayuda de un agente de transferencia de cadena (CTA) como se muestra en la Figura 14. Los compuestos insaturados de estructura general 1 o 4 pueden actuar como agentes de transferencia de cadena mediante un mecanismo de fragmentación por adición de dos pasos. En estos compuestos, C=X debe ser un doble enlace que sea reactivo a la adición de radicales. X es más a menudo CH_2 o S. Z es un grupo elegido para dar al agente de transferencia una reactividad apropiada hacia los radicales de propagación y transmitir la estabilidad apropiada a los radicales intermedios (2 o 5, respectivamente).

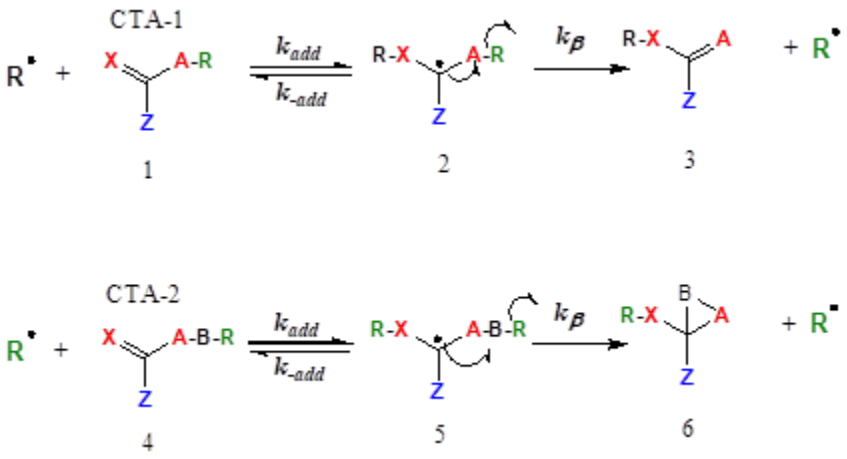

Figura 14. Mecanismo de transferencia de cadena reversible de adición-fragmentación.

Algunos ejemplos de A son CH_2, CH_2=$CHCH_2$, O o S. R es un grupo saliente homolítico y R● debe ser capaz de reiniciar la polimerización de manera eficiente. En todos los ejemplos conocidos de transferencia los agentes, B son O. Dado su funcionalidad se puede introducir en los productos en los pasos de transferencia (típicamente desde Z) y reiniciación (desde R), estos reactivos ofrecen una ruta a una variedad de polímeros de función terminal, incluidos los telequélicos (Moad *et al.*, 2008).

En 1995 se informó que las polimerizaciones de monómeros metacrílicos en presencia de macromonómeros metacrílicos (X=CH_2, Z=CO_2-R) en condiciones en las que el monómero es muy activo muestran muchas de las características de la polimerización viviente (Krstina *et al.*, 1995; Krstina *et al.*, 1996). Estos sistemas involucran el mecanismo RAFT (Figura 15).

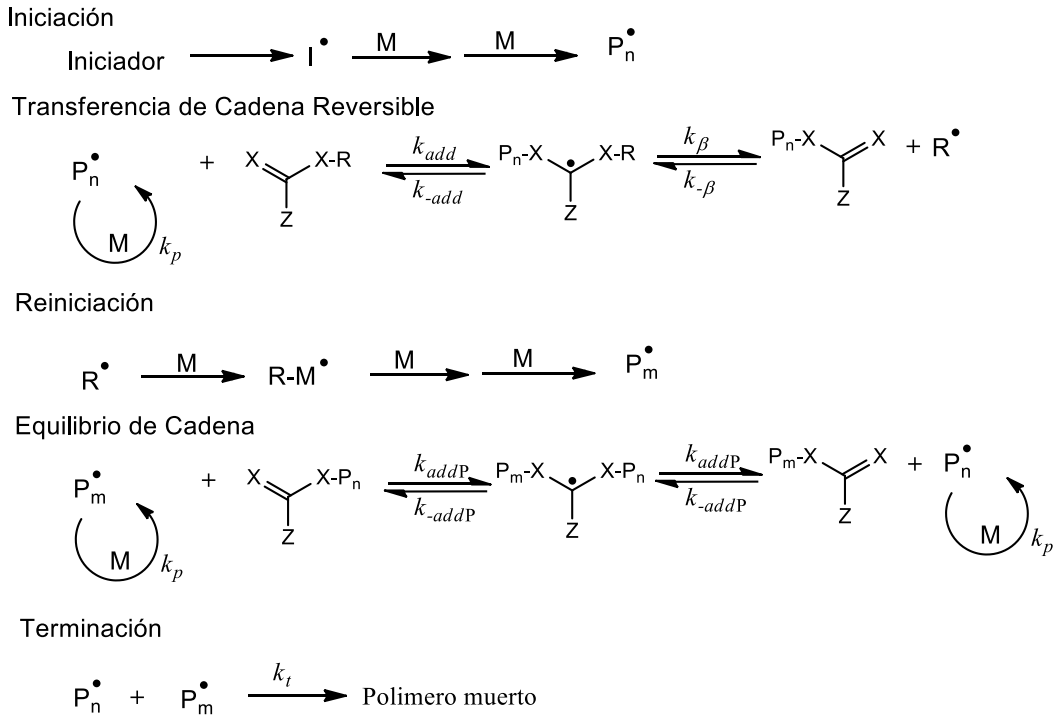

Figura 15. Mecanismo de la polimerización RAFT.

1.2.9.2.1 Polimerización RAFT para formar Bloques con PEG. La polimerización RAFT es uno de los métodos más versátiles para la preparación de copolímeros en bloque con una distribución de

pesos moleculares estrecha. De acuerdo al mecanismo y a los trabajos experimentales, se ha encontrado que cuando se parte de un macro-CTA tipo tritiocarbonato para formar un copolímero en bloques, el grupo tiocarboniltio queda en el extremo del segundo bloque (Moad *et al.*, 2005; Lambeth *et al.*, 2006). De acuerdo a lo reportado en la literatura, cuando se quiere preparar un copolímero en bloques es necesario partir de un macro-CTA en el cual se permita el equilibrio del polímero radical saliente sea más estable y a su vez permita la adición de un segundo bloque. Como se hizo en el trabajo ya publicado por Cortez-Lemus *et al.* (2017), donde obtienen un macro-CTA con metoxi-polietilenglicol (M_n=2000 g mol^{-1}) el cual posteriormente se hace reaccionar con DEAEM, para la obtención de bloques copoliméricos anfifílicos (Figura 16).

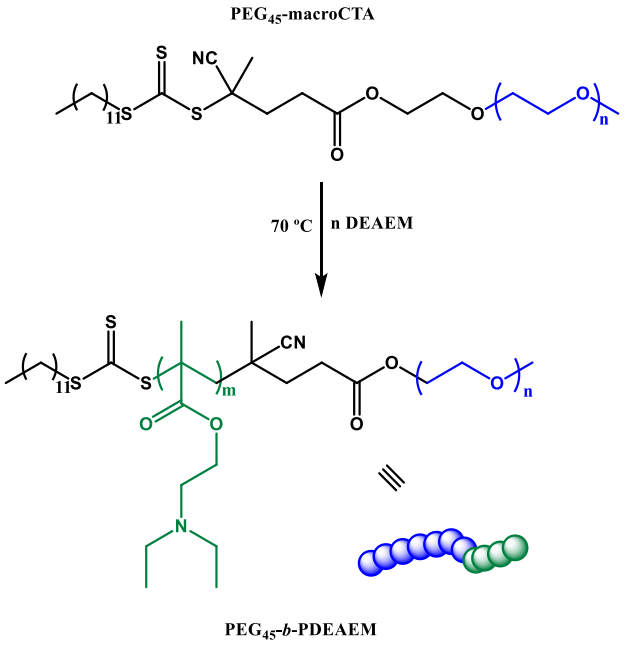

Figura 16. Síntesis de copolímeros en bloque vía RAFT.

1.3. Hipótesis

1. Al menos 10% de PDEAEM en un copolímero en bloques permite obtener un polímero sensible a cambios de pH.
2. La solubilidad de las matrices poliméricas en medio acuoso ayudara a que los compuestos

fenólicos sean liberados en un mayor porcentaje.

3. La interacción de las aminas libres con los –OH libres en el extracto ayuda al encapsulamiento de este agente fitoquímico, al tener un mayor contenido de –OH el contenido de compuestos fenólicos podría ser mayor.
4. Una concentración de al menos 100 µg mL^{-1} no presenta citotoxicidad en células normales teniendo una concentración del 20% en peso del PDEAEM
5. Los compuestos fenólicos presentes en el encapsulado a una concentración mínima de 50 µg mL^{-1} tienen efectos antiproliferativos.

1.4. Objetivo General

Evaluar la eficiencia de encapsulación de compuestos polifenólicos del orégano, usando polímeros catiónicos PEGilados y su actividad antiproliferativa en la línea celular de cáncer de colon (Caco-2).

1.5. Objetivos Específicos

1. Sintetizar copolímeros en bloque de PEG y monómeros catiónicos (PDEAEM >30%, o QS).
2. Determinar factores que favorecen la liberación de compuestos fenólicos encapsulados de manera controlada.
3. Determinar el contenido de flavonoides antes y después de la digestión gastrointestinal *in vitro* por UPLC/MS.
4. Evaluar la citotoxicidad de los bloques de QS-*b*-PPEGMA y PEG-*b*-PDEAEM cargados y sin cargar en línea celular de fibroblastos (CCD18).
5. Evaluar la capacidad antiproliferativa de bloques de QS-*b*-PPEGMA y PEG-*b*-PDEAEM cargados en línea celular de cáncer de colon (Caco-2).

1.6. Sección Integradora del Trabajo

La información presente en este manuscrito está dividida en secciones denominadas capítulos a continuación se describe el contenido.

En el artículo 1 se describe las potenciales propiedades antioxidantes y antinflamatorias que los compuestos fenólicos de orégano mexicano (*Lippia graveolens*) presentan bajo diferentes ensayos colorimétricos (ABTS, TRC y ORAC), antes y después de pasar por el sistema gastrointestinal *in vitro*; de igual manera se describe la modificación del quitosano con PPEGMA, el cual aumenta la solubilidad de quitosano en medio acuoso. Se determinaron sus propiedades térmicas, así como el contenido de cargado de compuestos fenólicos, su liberación y la protección de estos utilizando quitosano modificado y sin modificar antes y después de la digestión *in vitro*, encontrando que el sistema de quitosano modificado con PPEGMA aumenta la solubilidad de estos compuestos en medio acuoso, así como les brinda protección térmica y protección en fase gástrica, por lo que lo hace un buen reservorio para este tipo de compuestos. Este artículo se encuentra publicado en Polymers.

En el artículo 2 se describe la síntesis de copolímeros en bloque a base de PEG con polímeros catiónicos como el PDEAEM y el QS, así como la caracterización del potencial antioxidante por medio de ensayos colorimétricos como el TEAC y ORAC de los compuestos fenólicos encapsulados en las diferentes matrices catiónicas PEGiladas, antes y después de pasar por la simulación gastrointestinal *in vitro*, también se determinó el contenido de compuestos fenólicos antes y después mediante UPLC/MS. Se reporta un alto contenido de naringenina, floridzina y crisimaristina, las cuales han presentado propiedades antiinflamatorias y antitumorales. También describe la actividad en fibroblastos CCD18 y células CACO-2 en el que se determinó que a 500 $\mu g\ mL^{-1}$ estas matrices cargadas no presentan citotoxicidad en células de colon normales, pero si exhiben capacidad antiproliferativa en CACO-2. La actividad es similar a la del fármaco modelo utilizado (5FU) después de 72 h, por lo cual se puede inferir que los compuestos encapsulados en las matrices catiónicas pudieran ser en buen coadyuvante en el tratamiento contra el cáncer de colon. Este artículo fue enviado a la revista “Journal of Drug Delivery Science and Technology”

1.7. Referencias

Adorjan, B.; Buchbauer, G. 2010. “Biological properties of essential oils: an updated review,” Flavour Fragrance J., 25(6):407–426.

Ahmed, E. M. 2013. Hydrogel: Preparation, characterization, and applications: A review. Adv. Res., 6:105-121.

Amalvy, J. I.; Wanless, E. J.; Li, Y.; Michailidou, V.; Armes, S. P. 2004 Synthesis and Characterization of Novel pH-Responsive Microgels Based on Tertiary Amine Methacrylates. Langmuir. 20:8992-8999.

Ambriz-Pérez, D. L; Leyva Lopez, N.; Gutierrez-Grijalva, R. P.; Basilio Heredia, J. 2019. Phenolic compounds: Natural alternative in inflammation treatment, a Review. Cogent Food Agric. 2:1-14

Aspden, T.J.; Mason, J.D.; Jones, N.S.; Lowe, J.; Skaugrud, O.; Illum, L. 1997 Chitosan as a nasal delivery system: the effect of chitosan solutions on in vitro and in vivo mucociliary transport rates in human turbinates and volunteers. J. Pharm. Sci. 86:509–513.

Balkwill. F.; Mantovani, A. 2001. Inflammation and cancer: back to Virchow. Lancet 357:539-545

Bakkali, F.; Averbeck, S.; Averbeck, D.; Idaomar, M. 2008. “Biological effects of essential oils—a review”. Food and Chemical Toxicology. 46(2):446–475.

Benjamin, N. HO.; Claire, M. P.; Amareshwar, T.K. S. 2017. Update on Nanotechnology-based Drug Delivery Systems in Cancer Treatment. Anticancer Res. 27(11):5975-5981.

Bravo, L. 1998 Polyphenols: Chemistry, dietary sources, metabolism, and nutritional significance. Nutr. Rev. 56:317–333.

Buchbauer, G.; Jirovetz, L.: Jager, W.; Plank, C. y Dietrich, H. 1993. “Fragrance compounds and essential oils with sedative effects upon inhalation”. J. Pharm. Sci. 82(6):660–664.

Cheng, Y.; Xu, Z. H.; Ma, M. L.; Xu, T. W. 2008. Dendrimers as drug carriers: Applications in different routes of drug administration. J. Pharm. Sci. 97:123–143.

Chen, T.; Ferris, R.; Zhang, J.; Ducker, R.; Zauscher, S. 2010 Stimulus-responsive polymer brushes on surfaces: Transduction mechanisms and applications. Nat. Mater. 35:94-112.

Chen, Q.; Li, S.; Feng, Z.; Wang, M., Cai, C., Wang, J.; Zhang, L. 2017 Poly(2-(diethylamino)ethyl methacrylate)-based, pH-responsive, copolymeric mixed micelles for targeting anticancer drug control release. Int. J. Nanomedicine 12:6857-6870.

Cortez-Lemus, N. A.; García-Soria, S. V.; Paraguay-Delgado, F.; Licea-Claveríe, A. 2017. Synthesis of gold nanoparticles using poly(ethyleneglycol)-b-poly(N,N-diethylaminoethylmethacrylate) as nanoreactors. Polym. Bull. 74:3527-3544.

Coussens, L. M.; Wer, Z. 2002 Inflammation and cancer. Nature. 40:860-867.

Dash, M.; Chiellini, F.; Ottenbrite, R. M. y Chienillini, E. 2011, Chitosan-A versatile semi-synthetic polymer in biomedical applications. Prog. Polym. Sci. 36:981-1014.

Estanqueiro, M.; Amaral, M- H.; Conceição, J.; Sousa, L. J. M. 2015. Nanotechnological carriers for cancer chemotherapy: The state of the art. Colloids Surf. B: Biointerfaces. 126:631-648.

Ferlay, J.; Ervik, M.; Lam, F.; Laversanne, M.; Colombet, M.; Mery, L.; Piñeros, M.; Znaor, A.; Soerjomataram, I.; Bray, F. 2024. Global Cancer Observatory: Cancer Today. Lyon, France: International Agency for Research on Cancer. Disponible en: https://gco.iarc.who.int/media/globocan/factsheets/populations/484-mexico-fact-sheet.pdf Acceso: 30/04/2024.

Fulton, M. D.; Najahi-Missaoui, W. 2023. Liposomes in Cancer Therapy: How Did We Start and Where Are We Now. Int. J. Mol. Sci. 24(7):6615.

García–Soria, S. V. Síntesis de copolímeros en dibloque funcionalizados con nanopartículas de oro con potencial para aplicaciones biomédicas. Tesis de Maestría en Ciencias en Química, Instituto Tecnológico de Tijuana, Centro de Graduados e Investigación en Química, Tijuana, B.C., 2014.

Gutiérrez-Grijalva, E. P.; Angulo-Escalante, M. A.; León-Félix, J.; Basilio, H. J. 2017. Effect of In Vitro Digestion on the Total Antioxidant Capacity and Phenolic Content of 3 Species of Oregano (Hedeoma patens, Lippia graveolens, Lippia palmeri). J. Food Sci. 82:2832-2839.

Gutierrez-Grijalva, R. P.; Picos-Salas, M. A.; Leyva Lopez, N., Criollo-Mendoza, M. S.; Vazquez-Olivo, G.; Basilio Heredia, J. 2018. Flavonoids and Phenolic Acids from Oregano: Occurrence, Biological Activity and Health Benefits. Plants 2:1-23.

González-Ayón, M.; Sañudo-Barajas, J. A.; Picos-Corrales, L. A.; Licea-Claveríe, A. 2015. PNVCL-PEGMA Nanohydrogels with Tailored Transition Temperature for Controlled Delivery of 5-Fluorouracil. J. Polym. Sci., Part A: Polym. Chem. 53:2662-2672.

Hamidi M., Azadi A.; Rafiei P. 2008. Hydrogel nanoparticles in drug delivery. Adv. Drug Deliv. Rev. 60:1638–1649.

Herrera-Carrera, E.; Moreno-Jiménez, M. R.; Rocha-Guzmán, N. E.; Gallegos-Infante; J. A., Díaz-Rivas, J. O.; Gamboa-Gómez, C. I.; González-Laredo, R. F. 2015. Phenolic composition of selected herbal infusions and their anti-inflammatory effect on a colonic model in vitro in HT-29 cells. Cogent Food Agric. 1(1):10591033

Horney, B.; Muller, A.; Zlonik, A. 2002. Chemokines: agents for the immunotherapy of cancer?. Nature 2:175-184.

Instituto Nacional de Estadística y Geografía (INEGI). Ultima fecha de actualización: 02/02/2024. Disponible en: https://www.inegi.org.mx/contenidos/saladeprensa/aproposito/2024/EAP_CANCER24.pdf Acesso: 25/04/2024.

Kang, L.; Gao, Z.; Huang, W.; Jin, M.; Wang, Q. 2015. Nanocarrier-mediated co-delivery of chemotherapeutic drugs and gene agents for cancer treatment. Acta Pharm. Sin. B 3:169-175.

Kakizawa Y.; Kataoka K. 2002. Block copolymer micelles for delivery of gene and related compounds. Adv. Drug Deliv. Rev. 54:203–22.

Kataoka, K.; Nagasaki, Y.; Otsuka, H. 2003 PEGylated nanoparticles for biological and pharmaceutical applications. Adv. Drug Deliv. Rev. 55:403-419.

Khan, R.U., Shao, J., Liao, JY.; Quian, L. 2023. pH-triggered cancer-targeting polymers: From

extracellular accumulation to intracellular release. Nano Res. 16:5155–5168.

Kharb, M.; Jat, R. K.; Gupta A. 2012. A review on medicinal plants used as a source of anticancer agents. Int. J. Drug Res. Technol. 2:177–18.

Kim, J.H.; Kim, Y.S.; Kim, S.; Park, J. H.; Kim, K.; Choi, K.; Chung, H.; Jeong, S. Y.; Park, R.W.; Kim, I.S.; Kwon, I. C. J. 2006 Hydrophobically modified glycol chitosan nanoparticles as carriers for paclitaxel. J. Control. Rel. 111:228-234.

Krstina, J.; Moad, G.; Rizzardo, E.; Winzor, C. L.; Berge, C. T.; Fryd, M. 1995 Narrow Polydispersity Block Copolymers by Free-Radical Polymerization in the Presence of Macromonomers. Macromolecules 28:5381.

Krstina, J.; Moad, C.L.; Moad, G.; Rizzardo, E.; Berge, C.T.; Fryd, M. 1996 A new form of controlled growth free radical polymerization. Macromol. Symp. 111:11-23.

Kumar, M.N.; Muzzarelli, R.A.; Muzzarelli, C.; Sashiwa, H.; Domb, A.J. 2004. Chitosan chemistry and pharmaceutical perspectives. Chem. Rev. 104: 6017–6084.

Kwon, S.; Park, J. H.; Chung, H.; Kwon, I. C.; Jeong, S. Y.; Kim, I.S. 2003. Physicochemical Characteristics of Self-Assembled Nanoparticles Based on Glycol Chitosan Bearing 5β-Cholanic Acid. Langmuir 19:10188-10193.

Lambeth, R. H.; Ramakrishnan, S.; Mueller, R.; Poziemski, J. P., Miguel, G. S.; Markoski, L. J.; Zukoski, C. F.; Moore, J. S. 2006. Synthesis and aggregation behavior of thermally responsive stars polymers. Langmuir 22:6352-6360.

Lea, T. 2015. Caco-2 Cell line En: Verhoeckx, K.; Cotter, P.; Lopez-Expósito, C. K.; Lea, T.; Mackie, A.; Requena, T.; Swiatecka, D.; Wichers, H (eds.).The impact of food Bioactives on Health. Springer International Publishing, Switzerland, 103-111 pp.

Lee K.Y.; Yuk S.H. 2007. Polymeric protein delivery systems. Prog. Polymer Sci. 32:669-697.

Lin, C.; Anseth, K. S. 2009. PEG hydrogels for the controlled release of biomolecules in regenerative medicine. Pharm. Res. 26:631-643.

Licea-Claveríe, A.; Alvarez-Sanchez, J.; Picos-Corrales, L. A.; Obeso-Vera C.; Flores, C. M.; Cornejo-Bravo, J. M.; Hawker, J. C.; Frank, W. C. 2009. The Use of the RAFT-Technique for the Preparation of Temperature/pH Sensitive Polymers in Different Architectures. Macromol. Symp. 283-284:56-66.

Mazanares-Guevara, L.A; Licea-Claverìe, A.; Paraguay-Delgado, F. 2017. Synthesis and Characterization of Novel pH-Responsive Microgels Based on Tertiary Amine Methacrylates. Soft Mater. 16:37–50.

Messaoudene, D.; Belguendouz, H.; Ahmedi, M. L.; Benabdekader, T.; Otmani, F.; Terahi, M.; Touil-boukoffa, C. 2011. Ex vivo effects of flavonoïds extracted from Artemisia herba alba on cytokines and nitric oxide production in Algerian patients with Adamantiades- Behçet's disease. J. Inflammation (London, U. K.) 8:35.

Moad, G.; Rizzardo, E.; Thang, S. H. 2008. Radical addition-fragmentation chemistry in polymer synthesis. Polymer 49:1079-1131.

Mohamed, S. 2014. Functional foods against metabolic syndrome (obesity, diabetes, hypertension and dyslipidemia) and cardiovascular disease. Trends Food Sci. Technol. 35:114–128.

Molina, M.; Bergueiro, J. 2015. Aplicaciones biomédicas de nanogeles dendríticos termosensibles. Rev. Iberoam. Polim. 16:164-172.

Moustakas, A.; Pardalu, K.; Gaal, A. y Helding, C. H. 2002. Mechanisms of TGF-β signaling in regulation of cell growth and differentiation. Immunol. Lett. 82:85-91.

Muslin, T.; Morimoto, M; Saimoto H.; Okamono, Y.; Minami, S.;Shigemasa, Y. 2001. Synthesis ad bioactivities of poly(ethylene glicol)-chitosan hybrids. Carbohydr. Polym. 46:323-330.

National Cancer Institute. Cancer Treatments. Ultima fecha de actualización 29/04/2015. Disponible en: https://www.cancer.gov/espanol/cancer/tratamiento/tipos Acceso 29/04/2024

National Cancer Institute. Cancer Treatments. Ultima fecha de actualización 08/01/2019. Disponible en: https://www.cancer.gov/espanol/cancer/tratamiento/tipos/radioterapia Acceso 29/04/2024

Odian, G. 1991. "Principles of Polymerization" 3rd Ed., John Wiley and Sons, Inc., New York.

Picos-Corrales, L. A., 2012, Nanogeles Sensibles Preparados vía RAFT e Irradiación para el Suministro Controlado de Fármacos. Tesis de Doctorado en Ciencias en Química, Instituto Tecnológico de Tijuana, Centro de Graduados e Investigación, Tijuana, B.C. México.

Pimentel-Moral S.; Teixeira M.C.; Fernandes A.R.; Arráez-Román D.; Martínez-Férez A.; Segura-Carretero A.; Souto E.B. 2018. Lipid nanocarriers for the loading of polyphenols – A comprehensive review. Adv. Colloid Interface Sci. 260:85-94

Renault F, Sancey B, Badot P, Crini G. 2009. Chitosan For Coagulation/Flocculation Processes – An Eco-Friendly Approach. Eur. Polym. J. 45:1337-1348.

Rossi, D.; Zlonik, A. 2000 The biology of chemokines and their receptors. Annu. Rev. Inmmunol. 18:217-242.

Sanna, V.; Pala, N.; Sechi, M. 2014. Targeted therapy using nanotechnology: focus on cancer. Int. J. Nanomedicine. 9. 467-483.

Siegel, R. L.; Giaquinto, A. N.; Jemal, A. 2024. Cancer statistics. CA Cancer J. Clin. 74:1. 12-49

Singh, J.; Nayak, P. 2023. pH-responsive polymers for drug delivery: Trends and opportunities. J. Polym. Sci. 61(22):2828-2850.

Shi, D.; Beasock, D.; Fessler, A.; Szebeni, J.; Ljubimova, J. Y.; Afonin, K. A.; Dobrovolskaia, M. A. 2022. To PEGylate or not to PEGylate: Immunological properties of nanomedicine's most popular component, polyethylene glycol and its alternatives. Adv. Drug Delivery Rev. 180: 114079.

Shi, L.; Zhang, J.; Zhao, M.; Tang, S.; Cheng, X.; Zhang, W.; Li, W.; Liu, X.; Peng, H.; Wang, Q. 2021. Effects of polyethylene glycol on the surface of nanoparticles for targeted drug delivery. Nanoscale. 13:10748-10764

Thakore, P.; Mani, R.K.; Singh, J.; Kavitha. 2012. A brief review of plants having anti-cancer property. Int. J. Pharm. Res. Dev. 3:129–136.

Van der Meel, R.; Marcel, H.A.; Fens, M.; Vader, P.; Wouter W.; Van, S.; Omolola, E. A.; Raymond, M.; Schiffelers, S. 2014. Extracellular vesicles as drug delivery systems: lessons from the liposome field. J. Control. Rel. 195:72-85.

Veeramuthu, D.; Tharsius-Raja, W. R.; Al-Dhabi, N. A. y Savarimuthu I. 2017, Flavonoids: Anticancer Properties. En: Gonzalo C. Justino. Flavonoids-From Biosynthesis to Human Health. IntechOpen, London, 287-303.

Venkatesan, J.; Kim, S.K. 2010. Chitosan composites for bone tissue engineering—An overview. Mar. Drugs. 8:2252–2266.

Youan B.B.C. 2004. Chronopharmaceutics: gimmick or clinically relevant approach to drug delivery?. J. Control. Rel. 98:337-353.

Zhang, J.; Wang, Q. y Wang, A. Synthesis and characterization of chirosan-*g*-poly(acrylic acid)/attapulgite superabsorbent composites. Carbohyd. Polym. 68:367-374.

Zhang, H. y Tsao, R. 2016, Dietary polyphenols, oxidative stress and antioxidant and anti-inflammatory effects. Curr. Opin. Food Sci. 8:33-42.

2. LOADING AND RELEASE OF PHENOLIC COMPOUNDS PRESENT IN MEXICAN OREGANO (*Lippia graveolens*) IN DIFFERENT CHITOSAN BIO-POLYMERIC CATIONIC MATRIXES

Melissa Garcia-Carrasco[1], Lorenzo A. Picos-Corrales[2], Erick P. Gutiérrez-Grijalva[3], Miguel A. Angulo-Escalante[1], Angel Licea-Claverie[4,*] and J. Basilio Heredia[1,*]

[1]Nutraceuticals and Functional Foods Laboratory, Centro de Investigación en Alimentación y Desarrollo, A.C., Carretera a Eldorado Km. 5.5, Col. Campo El Diez, Culiacán 80110, Sinaloa, Mexico

[2]Facultad de Ingeniería Culiacán, Universidad Autónoma de Sinaloa, Ciudad Universitaria, Culiacán 80013, Sinaloa, Mexico

[3]Cátedras CONACYT-Centro de Investigación en Alimentación y Desarrollo, A.C., Carretera a Eldorado Km. 5.5, Col. Campo El Diez, Culiacán 80110, Sinaloa, Mexico

[4]Centro de Graduados e Investigación en Química, Tecnológico Nacional de Mexico/Instituto Tecnológico de Tijuana, A.P. 1166, Tijuana 22000, Baja California, Mexico

[*]aliceac@tectijuana.mx and jbheredia@ciad.mx.

Artículo publicado:

1ro de septiembre 2022

En la revista:

Polymers

https://doi.org/10.3390/ polym14173609

polymers

MDPI

Article

Loading and Release of Phenolic Compounds Present in Mexican Oregano (*Lippia graveolens*) in Different Chitosan Bio-Polymeric Cationic Matrixes

Melissa Garcia-Carrasco [1], Lorenzo A. Picos-Corrales [2], Erick P. Gutiérrez-Grijalva [3], Miguel A. Angulo-Escalante [1], Angel Licea-Claverie [4,*] and J. Basilio Heredia [1,*]

[1] Nutraceuticals and Functional Foods Laboratory, Centro de Investigación en Alimentación y Desarrollo, A.C., Carretera a Eldorado Km. 5.5, Col. Campo El Diez, Culiacán 80110, Sinaloa, Mexico
[2] Facultad de Ingeniería Culiacán, Universidad Autónoma de Sinaloa, Ciudad Universitaria, Culiacán 80013, Sinaloa, Mexico
[3] Cátedras CONACYT-Centro de Investigación en Alimentación y Desarrollo, A.C., Carretera a Eldorado Km. 5.5, Col. Campo El Diez, Culiacán 80110, Sinaloa, Mexico
[4] Centro de Graduados e Investigación en Química, Tecnológico Nacional de Mexico/Instituto Tecnológico de Tijuana, A.P. 1166, Tijuana 22000, Baja California, Mexico
* Correspondence: aliceac@tectijuana.mx (A.L.-C.); jbheredia@ciad.mx (J.B.H.)

Abstract: Mexican oregano (*Lippia graveolens*) polyphenols have antioxidant and anti-inflammatory potential, but low bioaccessibility. Therefore, in the present work the micro/nano-encapsulation of these compounds in two different matrixes of chitosan (CS) and chitosan-*b*-poly(PEGMA$_{2000}$) (CS-*b*-PPEGMA) is described and assessed. The particle sizes of matrixes of CS (~955 nm) and CS-*b*-PPEGMA (~190 nm) increased by 10% and 50%, respectively, when the phenolic compounds were encapsulated, yielding loading efficiencies (LE) between 90–99% and 50–60%, correspondingly. The release profiles in simulated fluids revealed a better control of host–guest interactions by using the CS-*b*-PPEGMA matrix, reaching phenolic compounds release of 80% after 24 h, while single CS retained the guest compounds. The total reducing capacity (TRC) and Trolox equivalent antioxidant capacity (TEAC) of the phenolic compounds (PPHs) are protected and increased (more than five times) when they are encapsulated. Thus, this investigation provides a standard encapsulation strategy and relevant results regarding nutraceuticals stabilization and their improved bioaccessibility.

Keywords: chitosan; polyethylene glycol methacrylate; oregano; phenolic compounds; nanoencapsulation; bioaccessibility

Citation: Garcia-Carrasco, M.; Picos-Corrales, L.A.; Gutiérrez-Grijalva, E.P.; Angulo-Escalante, M.A.; Licea-Claverie, A.; Heredia, J.B. Loading and Release of Phenolic Compounds Present in Mexican Oregano (*Lippia graveolens*) in Different Chitosan Bio-Polymeric Cationic Matrixes. *Polymers* **2022**, *14*, 3609. https://doi.org/10.3390/polym14173609

Academic Editor: Ki Hyun Bae

Received: 1 July 2022
Accepted: 25 August 2022
Published: 1 September 2022

1. Introduction

The secondary metabolites present in plants, such as phenolic compounds, better known as phytochemicals, have gained great interest in recent years since they play an important role in the prevention of different diseases such as cancer, diabetes, and obesity, which are related to oxidative stress [1]. Mexican oregano (*L. graveolens*) is an endemic species from northwestern Mexico mostly known for its culinary uses but is also a rich source of phenolic compounds that can bring great benefits to human health due to their pharmacological properties, which include the anti-inflammatory, antifungal, and antibacterial activities, among others [2–4]. In this subject, essential oils and polyphenols are the major secondary metabolites found in oregano that are responsible for its biological properties [2,5]. Previous works have shown that oregano polyphenols have low bioaccessibility, and in-vitro digestion assays have demonstrated that phenolic acids, flavones, and flavanones of oregano seem to be susceptible to the pH changes during each digestion stage [6–8]. Thus, despite the bioactive properties of oregano polyphenols, they may be affected during their journey through the gastrointestinal (GI) tract, mainly due to pH

changes favoring the ionization of these compounds or they are degraded, and thus the active compounds could lose their properties [1,9,10].

The low bioaccessibility of polyphenols is a subject highly reported; hence, different alternatives have been proposed to protect these metabolites from degradation. Among the technologies useful for this purpose are: (1) spray drying (for microencapsulation), (2) biopolymeric-type systems such as pectin, alginate, gums, and chitosan used to encapsulate different phytochemical compounds such as curcumin, thymol, and carvacrol [11–17]. Although most of these loading and release studies have been carried out with isolated compounds, it has also been found that when there is a combination of phenolic compounds, they can create synergism between them and enhance their activity [18].

The biopolymer chitosan (CS), which is obtained from a natural polysaccharide called chitin, represents a biocompatible and biodegradable platform with outstanding performance in sorption-oriented processes. This is one of the main polymeric matrixes used for the encapsulation of synthetic or natural agents due to polyelectrolyte character, which means that the charge of its functional groups can be modified depending on the pH of the medium, where the amino and the hydroxyl groups give this character [19–22]. However, this biopolymer is insoluble in normal deionized water, limiting biological applications; regarding this, some studies have been focused on modifying these molecules with different polymers to improve their solubility, such as polyethylene glycol (PEG). PEG has been one of the polymers with better biocompatibility [23]. Modified biopolymers have shown the capacity to adhere to peptide sequences [24], growth factors [25], and the ability to control mechanical properties regardless of polymerization conditions [26].

As it is well known, PEG is one of the few polymers approved by the U.S. FDA; moreover, the polyethylene glycol methyl methacrylate (PEGMA) properties are attributed to PEG due to their similar structures [27]. In addition, in case a certain percentage passes into the blood system, these particles avoid a response by the immune system, thus expanding the areas of application [28,29]. In some approaches, the use of PEGMA is related to the increase in the lower critical solution temperature (LCST) of the synthesized copolymers, increasing the LCST at temperatures greater than 32 °C, which ensures that the matrix can remain stable at temperatures higher than the LCST in aqueous medium [30].

Based on the abovementioned, in the present work the encapsulation of phenolic compounds extracted from the aerial part of Mexican oregano (*L. graveolens*) was carried out in systems based on chitosan (CS) and chitosan modified with PEGMA (Chitosan-*block*-poly($PEGMA_{2000}$) (CS-*b*-PPEGMA), their release profiles at different pH levels were studied and their antioxidant activity before and after encapsulation was assessed. For that, a simple encapsulation method involving mechanical stirring was used.

2. Materials and Methods

2.1. Reagents

Polyethylene glycol methyl methacrylate 2000 g mol^{-1} (PEGMA), ammonium persulfate (APS, 98%, Sigma Aldrich, Toluca, Mexico), sodium chloride (NaCl, Jalmek, San Nicolás de los Garza, Mexico), chitosan (Low weight, 98%, Sigma Aldrich), glacial acetic acid (99.7%, Fermont, Monterrey, Mexico), deuterium chloride/deuterium oxide (D_2O/DCl 35% by weight, 99.9% deuterium, Sigma Aldrich), Folin-Ciocalteu reagent, aluminum chloride, potassium acetate, quercetin, DPPH radical, ABTS radical, potassium persulfate, HPLC grade water, and formic acid were purchased from Sigma-Aldrich (Toluca, Mexico). Moreover, sodium hydroxide (97.8%, Chemical Products of Monterrey SA de CV, Monterrey, Mexico) was purchased through a local provider.

2.2. Chitosan Purification

CS was dissolved in an aqueous acetic acid solution at 1% in volume, up to a concentration of 10 mg mL^{-1}; afterward, the mixture was filtered under reduced pressure with Büchner. CS was precipitated from the acidic solution using 1 M sodium hydroxide solution. The alkaline CS suspension was filtered under reduced pressure with a 5 µm

particle cutoff filter. The CS was washed with deionized water until neutralization, frozen, and finally lyophilized (Labconco, FreeZone® 1 L, Kansas City, MI, USA).

2.3. Plant Material and Extraction of Free Polyphenols

Oregano (*L. graveolens*) was collected in Santa Gertrudis, Durango, Mexico. Dried oregano leaves were ground using an Ika Werke M20 grinder (IKA, Staufen, Germany) until a fine powder consistency was obtained. Oregano powder was stored at −4 °C until use. The extract of phenolic compounds was obtained using 25 mL of absolute ethanol for 1 g of oregano powder, where the mixture was stirred and homogenized on a stirring plate (Thermo Scientific Cimarec, Waltham, MA, USA) at room temperature for 18 h. Subsequently, the extract obtained was centrifuged at 10,000 rpm for 15 min, and the supernatant was collected and stored at 4 °C until use. This technique was performed repeatedly to obtain approximately 1 L of extract. Figure 1 is a schematic representation for the process involving the extraction of phenolic compounds.

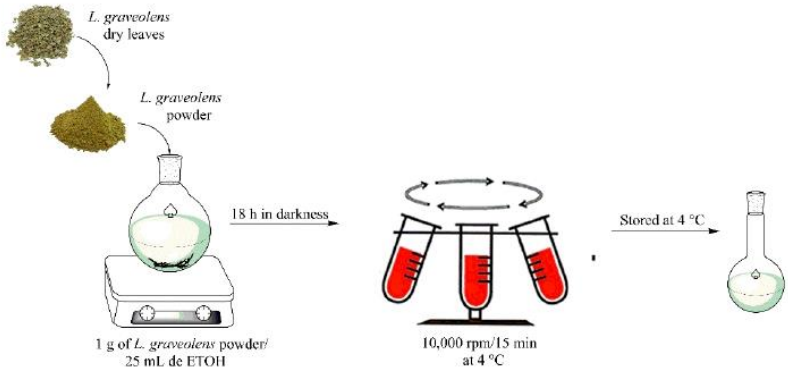

Figure 1. Schematic representation for free phenolic compounds extraction.

2.4. Characterization of the Extract of L. graveolens

2.4.1. Total Reducing Capacity

The total reducing capacity was evaluated through phenolic content analysis using the Folin–Ciocalteu (FC) method proposed by Swain and Hillis [31], with some modifications. The procedure consisted of mixing 10 µL of the samples, 230 µL of distilled water, and 10 µL of FC reagent in a 96-well microplate. The mixture was incubated for 3 min, and then 25 µL of 4N Na_2CO_3 were added, incubating again at room temperature for 2 h in the darkness. After incubation, absorbance at 725 nm was measured (Synergy HT microplate reader). Calculations were made using a gallic acid standard curve (from 0 to 0.4 mg mL^{-1}) and the results were expressed in milligrams of gallic acid equivalents per gram of powder obtained (mg AG g^{-1}). Each sample was measured in triplicate (n = 3).

2.4.2. Total Flavonoids Content (TFC)

The total flavonoid content was performed according to the methodology described by Ghasemi, et al. [32], with slight modifications. The process consists of taking 30 µL of the extract, then 250 µL of distilled water are added, and then 10 µL of aluminum chloride and 10 µL of 1 M potassium acetate, and it is left incubating in the darkness for 30 min; after incubation, absorbance is read at 415 nm in a Synergy HT microplate reader (Synergy HT, Bio-Tek Instruments, Inc., Winooski, VT, USA). The content of total flavonoids is determined from a quercetin standard curve (from 0 to 0.4 mg mL^{-1}); the results are expressed in equivalent mg of quercetin per gram of dry extract (mg QE g^{-1} of dry sample). Each sample was measured in triplicate (n = 3).

2.4.3. Antioxidant Capacity Methods

Inhibition of the 2,2-Diphenyl-1-Picrylhydrazyl Radical (DPPH)

This method uses the DPPH radical, which reduces its purple chromogen by the action of an antioxidant compound to hydrazine, a compound that colors a pale-yellow tone. This DPPH radical scavenging assay was carried out according to Karadag, et al. [33], for which 20 µL of the sample was placed in a 96-well flat-bottomed transparent microplate. Then, 280 µL of the DPPH radical were added and incubated for 30 min in the absence of white light. Finally, the absorbance at 515 nm was measured (Synergy HT microplate reader). A Trolox curve from 0.1 to 1 mmol TE g^{-1} was used to calculate the results, which are expressed as mmol Trolox equivalent per gram of powder (mmol TE g^{-1}). Each sample was measured in triplicate (n = 3).

Trolox Equivalent Antioxidant Capacity (TEAC)

The antioxidant capacity by the TEAC assay of the encapsulated sample was determined as described by Thaipong, et al. [34]. ABTS was dissolved in distilled water at a concentration of 7.4 mM (stock solution). The ABTS●+ radical was produced by mixing the ABTS stock solution with 2.6 mM potassium persulfate (1:1 *v*/*v*) and incubating the mixture in the dark at 25 °C for 12–16 h before use. Subsequently, the reaction solution was prepared by taking 100 µL of the radical and dissolving in 2900 µL of solvent to adjust the absorbance. For the assay, aliquots of 15 µL of extract and 285 µL of the reaction solution were added and homogenized using a vortex. Subsequently, it was incubated in the darkness for 2 h. After the time elapsed, the absorbance at 734 nm was read in a Synergy HT microplate using transparent 96-well flat-bottom plates. The reaction solution was taken as a blank. A Trolox curve from 0.1 to 1 mmol TE g^{-1} was used to calculate the results, which are expressed as mmol Trolox equivalent per gram of powder (mmol TE g^{-1}). Each sample was measured in triplicate (n = 3).

2.5. Identification of Phenolic Compounds by Ultra High-Resolution Liquid Chromatography/Mass Spectrometry (UPLC/MS)

Mass-liquid chromatography was used to carry out the separation for the identification of individual phenolic compounds from unencapsulated oregano extract. The analysis was performed in a class H UPLC unit (Waters Corporation, Milford, MA, USA) coupled to a G2-XS QT of mass analyzer (quadrupole and time of flight). The separation of phenolic acids was performed with a UPLC BEH C18 column (1.7 µm × 2.1 mm × 100 mm) at 40 °C, with gradient elution solution A (water-0.1% formic acid) and solution B (methanol), which is supplied at a flow rate of 0.3 mL min^{-1}. On the other hand, the separation of flavonoids was performed with a different set of conditions, including a UPLC BEH C18 column (1.7 µm × 2.1 mm × 100 mm) at 30 °C, with gradient elution solution A (water-0.05% formic acid) and solution B (acetonitrile), which is supplied at a flow rate of 0.3 mL min^{-1}. The ionization of the compounds was performed by electrospray (ESI), and the parameters used consisted of a capillary voltage of 1.5 kV, sampling cone: 30 V, desolvation gas of 800 (L h^{-1}), and a temperature of 500 °C. A collision ramp of 0–30 V was used. The Massbank of North America (MoNA) database was used for compound identification. The identification of phenolic compounds by UPLC was performed in duplicate (n = 2).

2.6. Synthesis of Chitosan-Block-Poly(PEGMA)

The methodology for the synthesis of CS-*b*-PPEGMA blocks was carried out as published by Ganji and Abdekhodaie [35], with slight modifications. Briefly, the preparation was done using conventional free radical polymerization with a weight ratio of 50:50 CS:PEGMA and 0.01 M free radical initiator (KPS). CS (0.5 g), PEGMA (0.46 mL, 0.5 g), KPS (0.135 g, 0.01 M), an inert atmosphere (N_2) in a three-necked flask with a magnetic stir bar, and 50 mL of water containing 1% (*v*/*v*) acetic acid were used. First, CS and initiator (KPS) were added followed by stirring for 30 min at 60 °C using an oil bath, and then the $PEGMA_{2000}$ was added dropwise, and the reaction was stirred (350 rpm) for 6 h. After the reaction time, the flask was removed from the oil bath and placed in a cold-water bath. For the purification of the solution, NaOH 4M was first added to the solution to precipitate the CS; next, the product was filtered and subsequently washed with acetone to

remove the residual $PEGMA_{2000}$. Finally, the sample was dialyzed for 48 h, with changes of water periodically; after that, the recovered sample was lyophilized and weighed to determine the yield of the reaction, resulting around 70%. Chitosan-*b*-PPEGMA; ^{1}H-NMR (400 MHz, $CDCl_3$, δ, ppm): 4.00–4.30 ($HOCH_2CH_2OCHCH_2OH$ of the polysaccharide ring of Chitosan), 3.87 (CH_2CH_2O of the PEG chain), 5.13 (CHNH of acetylglucosamine ring), 3.50 ($CHNH_2$ of glucosamine ring), 2.29 (CH_2 aliphatic from the CS backbone).

2.7. Preparation of Nanometric Polymer Aggregates

The copolymer aggregates were prepared through a direct dissolution consisting of the solubilization of the bulk copolymer CS-*b*-PPEGMA (10 mg) in distilled water (10 mL) under magnetic stirring at room temperature for 24 h. For CS, a solution of 1 wt% was prepared in 15 mL of water with 1% (*v*/*v*) of acetic acid under magnetic stirring at room temperature for 24 h.

2.8. Loading of Phenolics Compounds

The loading was performed based on a solvent evaporation method [36] and adapted from the methodology reported by Picos-Corrales, et al. [37]. Briefly, 10 mg of block copolymers were dissolved in 10 mL of distilled water, and 1.5 mg of phenolic compounds were dissolved in 5 mL of ethanol. The phenolic compounds (PPHs) solution was added dropwise into the polymer solution and left under magnetic stirring for 24 h. The phenolic compounds that were not loaded were removed by centrifugation for 20 min. The purified material was filtered using a disc filter with a pore size of 1 μM and then frozen and freeze-dried. The mass of phenolic compounds loaded in the CS and block copolymers was determined by preparing a 0.3 mg mL^{-1} solution in PBS pH 2, measuring the absorbance by UV analysis at a wavelength (λ_{max}) of 280 nm, and then quantified by using a calibration curve of phenolic compounds in PBS pH 2. The loading efficiency of phenolic compounds (LE) and the loaded PPHs content (LC) were calculated using Equations (1) and (2).

$$LE(\%) = (\text{mass of PPHs in polymer}/\text{mass of PPHs in loading solution}) \times 100 \quad (1)$$

$$LC(\%) = (\text{mass of PPHs in polymers}/\text{mass of dry polymer}) \times 100 \quad (2)$$

2.9. Measurements

Hydrogen nuclear magnetic resonance (^{1}H-NMR) spectra were collected on a Bruker AMX-400 (Bruker Corporation, Billerica, MA, USA) (400 MHz) spectrometer and reported in ppm using tetramethylsilane (TMS) as the NMR reference standard. The solvent used was deuterium chloride (37%), D_2O + DCl, for all samples.

Thermogravimetric analysis (TGA) was performed on a TA-Instruments Discovery-TGA equipment (TA-Instruments, New Castle, DE, USA). Measurements were performed for cationic matrixes and phenolic compounds loaded by heating under nitrogen flow from room temperature up to 600 °C using a heating rate of 10 °C min^{-1}.

Differential Scanning Calorimetry (DSC) was performed on a TA Instrument DSC2000, New Castle, DE, USA). Measurements were performed for cationic matrixes and were used to determine the melting point (T_m), the glass transition temperature (T_g) and thermal decomposition temperatures (T_d). For measurements, samples were cooled to −10 °C; maintained isothermally for 5 min, and afterward heated with modulation (±0.5 °C every 60 s) at a rate of 5 °C min^{-1} to 375 °C in a nitrogen atmosphere using. Two cycles of measurement were run, and the results reported corresponded to the second cycle.

Dynamic light scattering (DLS) measurements were carried out on 1.0 mg mL^{-1} block copolymer and 1 wt% of CS solutions at 25 °C using a Malvern Instruments Nano-ZS Nanosizer (ZEN 3690) (Malvern, Worcestershire, UK) equipment. The instrument is equipped with a helium-neon laser (633 nm) with size detection between 0.6 nm and 5 μm. DLS experiments were performed at the scattering angle of 90°, and the distribution of sizes was calculated using Malvern Instruments dispersion technology software, based on CONTIN analysis and Stokes-Einstein equation for spheres as usual.

UV–Vis spectra of Phenolics Compounds (PPHs) dispersions for the measurement were acquired using a UV-Vis Varian Cary 100 spectrophotometer system (Agilent Technologies, Santa Clara, CA, USA) at room temperature from aqueous dispersion.

The Zeta potential (ζ) of PPHs and PPHs-loaded polymeric matrixes dispersions (at 1 mg mL^{-1}) was measured using a Malvern ZetaSizer Nano ZS instrument (Malvern, Worcestershire, UK). The measurements were the average of three runs performed at 25 °C and distilled water.

2.10. In Vitro Release Studies

For release profile studies, 0.3 mg mL^{-1} of PPHs-loaded polymeric matrixes were dispersed in 10 mL of distilled water (pH ~5 for CS-*b*-PPEGMA@PPHs) or aqueous acetic acid solution (1% *v*/*v*) (pH ~4.5 for CS@PPHs) and then added to a dialysis tube (Spectra/Por® MWCO: 12–14 KDa, diameter 10 mm, Spectrum, Los Angeles, CA, USA). The dialysis tube was introduced into a 100 mL release medium, with mixture of 30% ethanol and 70% PBS inside an Erlenmeyer flask. The flask was placed in a shaking bath (Shel Lab, model SWBR17, Sheldon Manufacturing, Inc., Cornelius, OR, USA), operating at 37 °C and a shaking speed of 100 rpm. Medium aliquots of 2 mL were taken out at different times and replaced by 2 mL of fresh PBS at every sampling point. The released fraction of phenolic compounds was calculated from UV measurements at λ_{max} = 280 nm and 320 nm depending on the pH of the release medium and was then quantified using a calibration curve of phenolics compound in PBS.

2.11. In Vitro Gastrointestinal Digestion

A simulation of gastrointestinal digestion was performed according to the static in-vitro digestion method reported by Brodkorb, et al. [38]. This standardized procedure simulates the physiological conditions in the mouth, stomach, and small intestine, mimicking the chemical and pH conditions. Briefly, 1 mg of sample was mixed with simulated salivary fluids (SSF), then pH was adjusted to pH 7 with 6M NaOH; after that, the mixture was incubated for 5 min at 37 °C. Then, 1 mL of simulated gastric fluids (SGF), pH was adjusted to pH 3 and incubated for 2 h at 37 °C. Finally, 2 mL of simulated intestinal fluids (SIF) were added, pH was adjusted to pH 7, and the mixture was incubated for 2 h at 37 °C. In the final digestion step, the samples were centrifuged (9390× *g* at 4 °C for min), and the supernatant was collected and freeze-dried. After that, samples were resuspended in ethanol for antioxidant capacity assays.

3. Results and Discussion

3.1. Characterization of the Phenolic Compounds Present in L. graveolens

The results obtained from the nutraceutical characterization of the phenolic compounds in *L. graveolens* obtained by maceration in ethanol are found in Table 1, where the extracted compounds show antioxidant capacity. It can be seen that the extracted compounds have antioxidant activity against the different free-radical DPPH, AAPH, and ABTS. Comparing our results with the literature (TRC, 51.26 ± 2.36 mg EAG g^{-1}; TFC, 11.80 ± 0.12 mg QE g^{-1}; DPPH, 500.54 ± 9.63 µmol TE g^{-1}; ORAC, 812.31 ± 35.46 µmol TE g^{-1}; and ABTS, 350.07 ± 0.45 µmol TE g^{-1}) [9], it was observed that the TRC of both extracts is very similar, showing differences mainly in the TFC where a lower value was registered with the extraction in absolute ethanol. Cortes-Chitala, et al. [39], reported that the TRC of the *L. graveolens* was around 99.71 mg AGE g^{-1} dried weight; the higher reducing activity might be mainly because they used ethanol:water (58:42) as a solvent for extraction, plus the region where the sample was taken is different [39].

Table 1. Nutraceutical results of the ethanolic extract of oregano (*L. graveolens*).

TRC * (mg GAE g^{-1} Dried Oregano Leaf)	TFC ** (mg QE g^{-1} Dried Oregano Leaf)	DPPH ***	ORAC ***	ABTS ***
		(μmol TE g^{-1} Dried Oregano Leaf)		
50 ± 5.5	0.59 ± 0.019	339 ± 26.56	2639 ± 12.7	476 ± 1.27

* Total Reducing Capacity (TRC), ** Total Flavonoids Content (TFC) *** DPPH and ABTS are scavenging capacity, and ORAC is antioxidant capacity. Values represent the mean ± standard deviation (n = 3).

Characterization by UPLC-MS

The *L. graveolens* ethanolic extract was characterized by UPLC-MS, where it was possible to observe that the sample had a diversity of flavonoids and some phenolic acids (Table 2). Some of the identified compounds are flavones such as luteolin-glycoside, cosmoside, eriodictyol, and cirsimaritin; others are flavanones such as naringin, naringenin, and pinocembrin (Figure 2). The phenolic profile in this study is consistent with previous studies in *L. graveolens* extracts [9,39,40]. However, the distribution and content of phenolic content in our study could be different, owing to factors such as recollection time and the extraction method used for phenolic recovery. Moreover, in previous studies, the most abundant phenolics in methanolic extracts were naringenin, kaempferol-glucoside, kaempferide, caffeic acid, cirsimaritin, kaempferol, and taxifolin; most of these molecules were also found in our extracts. These metabolites have been associated with anti-inflammatory, antiapoptotic, and antimicrobial activity [4,39,41].

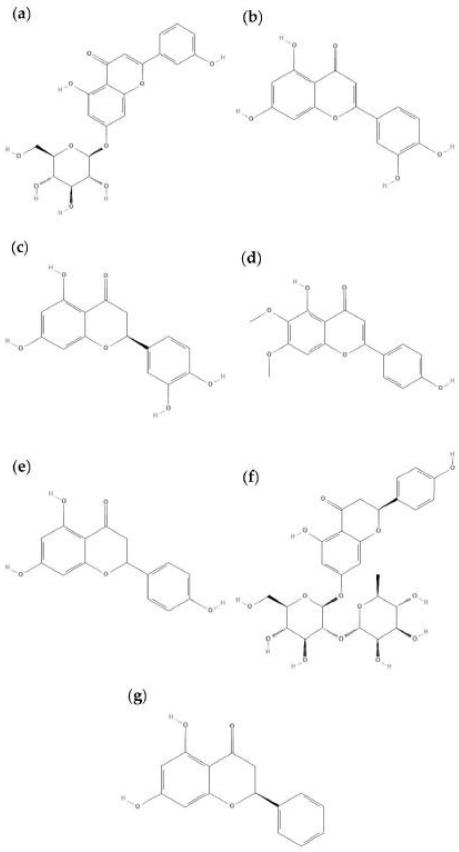

Figure 2. Chemical structures of some compounds contained in the phenolic extract characterized by UPLC-MS: (**a**) cosmoside, (**b**) luteolin, (**c**) eriodyctiol, (**d**) cirsimaritin, (**e**) naringenin, (**f**) naringin, (**g**) pinocembrin.

Table 2. Flavonoids from the ethanolic extract of *L. graveolens* characterized by UPLC-MS.

Compound	Compound Type	Molecular Mass [M-H]$^-$
Luteolin-glucoside	Flavone	447.1
Cosmoside	Flavone	431.1
Naringin	Flavanone	579.17
Quercetin	Flavonol	301.04
Kaempferol	Flavonol	285.04
Eriodictyol	Flavone	287.06
Naringenin	Flavanone	271.06
Pinocembrin	Flavanone	255.07
Taxifolin	Flavanonol	305.05
Cirsimaritin	Flavone	313.07

3.2. Synthesis and Characterization of Cationic Matrixes

3.2.1. Chitosan

After performing the purification of CS by precipitation in aqueous medium, it was characterized by ^{1}H-NMR (Figure 3). The assignment of the hydrogens corresponding to CS, which is a polysaccharide containing units of glucosamine (GlcN) and acetyl-glucosamine (GlcNAc), is the following: at 2.36 ppm, the signal corresponds to the hydrogens of the methyl group of the acetyl-glucosamine units (H_7); a signal with an intensity of around 2.67 ppm can also be observed, which corresponds to the signal of residual acetic acid (HAc), which comes from the purification of CS and was difficult to remove completely. Around 3.5 ppm, a multiplet is observed, and the signal is associated to the alpha hydrogen signal to the amino group of the repeating unit of GlcN (H_2); the signals located between 3.55 and 4.5 ppm correspond to the hydrogens from the polysaccharide ring (H_3-H_6); and the signal at 5.14 ppm corresponds to the H_1 of the repetitive unit of glucosamine [42].

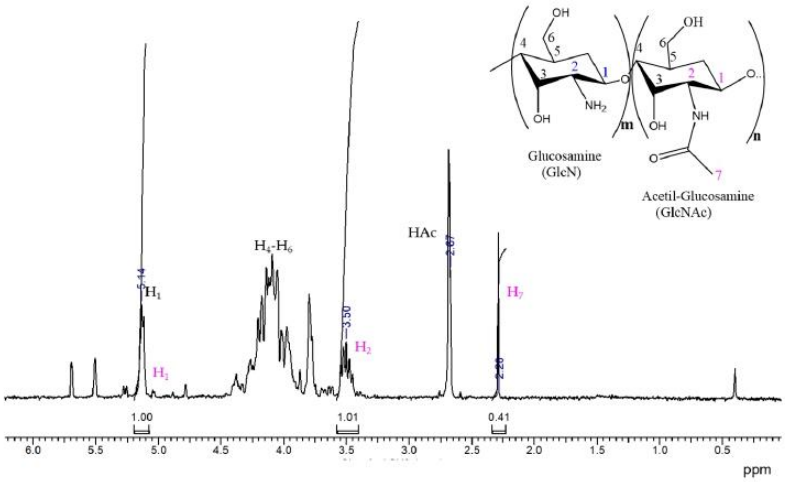

Figure 3. ^{1}H-NMR spectrum of chitosan in D_2O/DCl at 30 °C.

The degree of deacetylation (*DD*) of CS was calculated with Equation (3), using the integrations under the curve of the signal of H_1 (GlcN) and H_7 (GlcNAc), which gave us an 88% deacetylation degree of CS.

After obtaining the intrinsic viscosity, the viscosity-average molecular weight was calculated using the Mark–Houwink–Sakurada constants, with *K* and *a* being 2.14 × 10^{-3} mL g^{-1}

and 0.657, respectively [43]. As a result, the viscosimetric molecular weight obtained was 114 KDa, classified as relatively low molecular weight, which is suitable for using CS as a nanocarrier of different drugs.

$$DD = \left\{ \left(\frac{H_{1(GlcN)}}{H_{1(GlcN)} + \frac{H_{7(GlcNAc)}}{3}} \right) \times 100 \right\} \quad (3)$$

3.2.2. Chitosan-b-PPEGMA

The block copolymer based on CS and $PEGMA_{2000}$, was prepared following the methodology reported by Ganji and Abdekhodaie [35] applying some modifications. The product was characterized by ^{1}H-NMR (Figure 4). In the spectrum, the intense signal can be highlighted at 3.87 ppm that corresponds to the hydrogens (H_9 and H_{10}) of the repetitive ethoxy units in $PEGMA_{2000}$; and the signal of lower intensity at 3.55 ppm (H_{11}) corresponds to the hydrogen of methylene bound to oxygen at the end of the PPEGMA chain. Besides, the signals previously described for the chitosan backbone are also observed. This analysis indicated that the synthesis of chitosan-*b*-poly($PEGMA_{2000}$) was successfully accomplished.

The percentage of $PEGMA_{2000}$ present as poly$PEGMA_{2000}$ block was determined by ^{1}H-NMR. For that, the integration from 3.6 ppm to 4.4 ppm was related to the signal at 5.15 ppm, which turned out to be higher than 90%, which makes the copolymer very soluble in an aqueous medium. This is an important factor when using this type of biopolymer in different pharmacological applications because of its good reservoir capacity for loading different drugs. Furthermore, the average size of the CS backbone was shortened during the free-radical high-temperature synthesis; this was also determined by viscosimetry in an experiment without $PEGMA_{2000}$. The results showed that the size of the polysaccharide chains decreased by more than 90%, therefore it is not surprising that the CS content in the block copolymer is much lower than expected from the synthetic recipe [44].

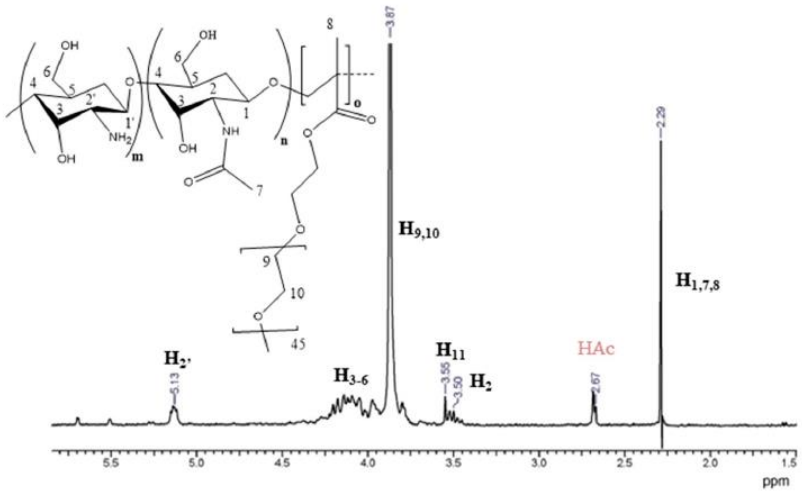

Figure 4. ^{1}H-NMR spectrum of chitosan-*b*-poly($PEGMA_{2000}$) in D_2O/DCl at 30 °C.

3.2.3. Thermal Characterization

A change in the structure of CS can be observed in the differential scanning calorimetry analysis (Figure 5); in the respective thermogram, only one thermal event can be observed at 303 °C, which is characteristic of the decomposition of glucosamine groups [45,46]. On the other hand, in the thermogram of the CS-*b*-PPEGMA blocks, two transition temperatures can be observed: the first at −12.5 °C, representing the glass transition temperature (T_g) of $PEGMA_{2000}$ (an expanded view is presented), and the second at 47 °C representing the melting point (T_m) also of $PEGMA_{2000}$ [35,47]; a third thermal event observed at

242 °C is related to the decomposition temperature of PEGMA and CS. The decrease in the decomposition temperature of CS could be attributed to the smaller size of the CS chain after the synthetic procedure.

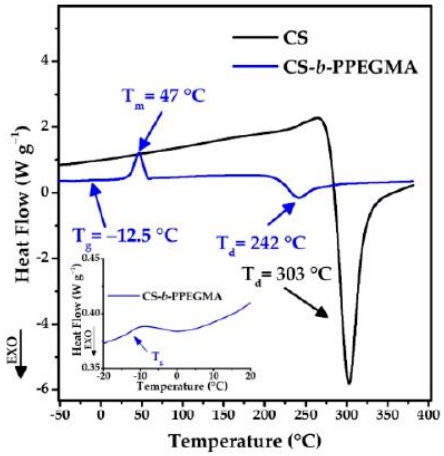

Figure 5. DSC thermograms of CS and CS-*b*-PPEGMA.

Thermogravimetric analysis shows differences between both compounds, highlighting that the decomposition temperatures of CS and the CS-*b*-PPEGMA block copolymer are similar (Figure 6a). Figure 6b shows the decomposition of these biopolymers; in the case of CS, a single decomposition around 300 °C is shown [48]. As for the CS-*b*-PPEGMA block copolymer, four decomposition steps can be observed: the first one at temperatures below 100 °C, which represents the loss of moisture from the sample; at 125 °C, this first decomposition step can be attributed to the low molecular weight chains of CS that formed after breaking the backbone, the next step at 227 °C corresponds to the first decomposition of $PEGMA_{2000}$, the third step at 334 °C corresponds to the decomposition of CS chains, and finally a weight loss at 456 °C, which would correspond to the second decomposition of $PEGMA_{2000}$ [49,50]. In both systems, a residue of around 40% is observed, being attributed to the formation of coke.

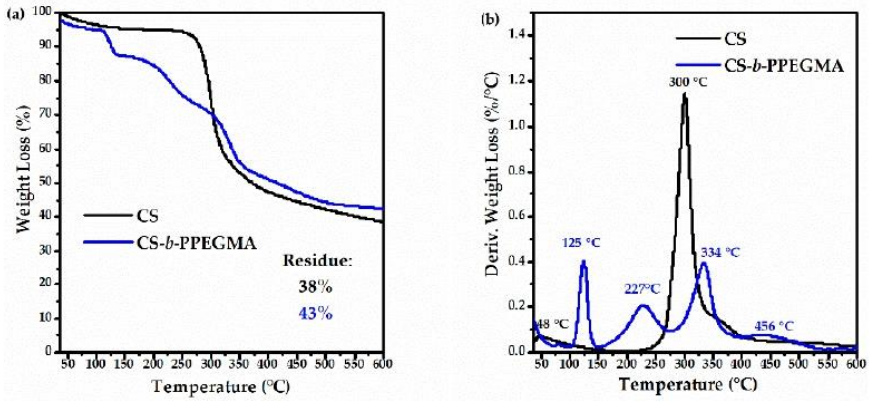

Figure 6. Thermograms of CS and CS-*b*-PPEGMA: (**a**) TG-thermogram and (**b**) DTG-thermogram.

3.3. Loading of Phenolic Compounds into Different Cationic Polymers

After loading the different matrixes, samples were analyzed by UV-vis spectroscopy to determine the content of phenolic compounds (Table 3). It was observed that CS had a loading efficiency between 90–99%, while for the blocks of CS-*b*-PPEGMA the

efficiency was lower from 50–60%; on the other hand, the loading content was 65% and 99%, respectively [51,52]. The pK_a of phenolic compounds varies around 6–9 [53–58], and the solubility of these is affected depending on the pH of the medium; considering that, their loading was carried out in an aqueous medium acidified with 1% v/v of acetic acid (pH = 4.5), it could be said that some of the compounds were partially soluble. An opposite case for CS with a pK_a around 6.17–6.51 [59–61], is completely soluble at acidic pH due to its protonated amines. When those amines are in contact with the hydroxyl groups (-OH) of the phenolic compounds (Figure 2) they can form hydrogen bonds or present electrostatic interactions (neutralization of charges) (Figure 7). Due to this molecular interaction in the case of CS, which has a higher content of free amines, it can encapsulate a higher concentration of the phenolic compounds; on the other hand, in the CS-*b*-PPEGMA blocks, the shorter CS chains and the fact that the ends are blocked with PPEGMA leads to less free amines per chain that can be available for interaction with the -OH of the phenolic compounds (Table 3). Moreover, a significant difference was registered in ζ change when a simple mixture of matrix and PPHs was prepared as compared with PPHs-loaded polymeric matrixes, so the stabilization and loading with the different matrixes can be inferred.

Table 3. Loading Efficiency (LE) and Loading Content (LC) of PPHs in polymer matrixes; zeta potential (ζ) and particle sizes of loaded (@PPHs) and unloaded (Matrix) polymer matrixes. Values represent the mean ± standard deviation (n = 3).

Polymer	LE (%)	LC (%)	ζ (mV)			D_h (nm)	
			Mixture	@PPHs	Matrix	@PPHs	Matrix
CS	90–99	65	10.2 ± 4.32	50.4 ± 3.27	55.4 ± 5.07	1106 ± 87	955 ± 75
CS-*b*-PPEGMA	50–60	99	7.91 ± 4.37	−15.5 ± 4.57	−9.07 ± 4.86	458 ± 0.01	190 ± 17
PPHs			−8.79 ± 4.29	-	-	-	-

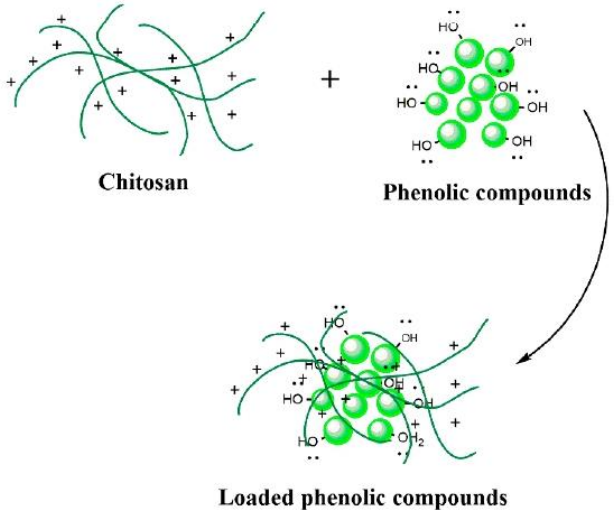

Figure 7. Scheme of the possible interaction between CS and the polyphenolic compounds.

To determine if these matrixes protected the phenolic compounds, the stability of these systems before and after loading was determined by zeta potential (Figure 8a) and particle size (Figure 8b) in measurements for about 15 days. From these experiments, the most stable system resulted to be the CS matrix, whilst the particle size of the CS-*b*-PPEGMA blocks increased with the time, although the latter presented good size stability for up to 5 days. On the other hand, the study of zeta potential for the two different systems and the unencapsulated polyphenols can be observed, and it was found that the zeta potential

(positive or negative) of the samples increased with the time. This effect may be because most of these compounds are not soluble in aqueous medium, so they precipitate, and those partially soluble compounds can be ionized [9,12].

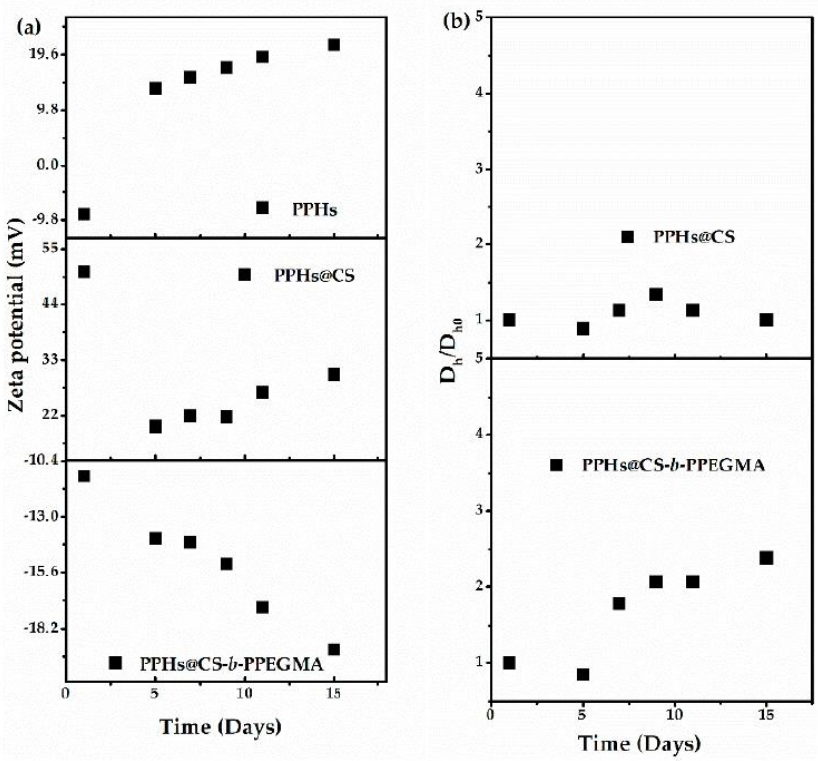

Figure 8. Stability study of systems loaded with phenolic compounds from *L. graveolens* zeta potential (**a**) and particle size (**b**).

On the other hand, in the case of CS systems, it can be observed how there was a drastic decrease in the surface charge after day 3 (compared with day 5), which could be caused by a decrease in the number of free amino groups improving the polymer-organic compounds interactions, maintaining similar particle size and colloidal stability along the days (Figure 8). In the case of the CS-PPHs system (PPHs@CS), the variations in the zeta potential did not significantly affect the size, and formation of more complex aggregates was not detected. In general, surface charge variations depend on free groups in their ionized form or forming hydrogen bonds, belonging to the polymer or the nutraceuticals. Figure 7 shows the possible interaction between CS and the polyphenolic compounds.

Thermal Characterization of Phenolic Compounds

The stability of the PPHs in the two different cationic matrixes was determined by thermogravimetric analysis, as is shown in Figure 9. It is shown that the decomposition signals of the single PPHs sample were not overlapped with the signals of the compounds loaded in the different cationic matrixes (CS@PPHs and CS-*b*-PPEGMA@PPHs). Also, a displacement of the decomposition temperatures of the PPHs can be observed, which would be associated with the cationic matrixes protecting these systems through different interactions, which could also impart on them higher thermal stability [62].

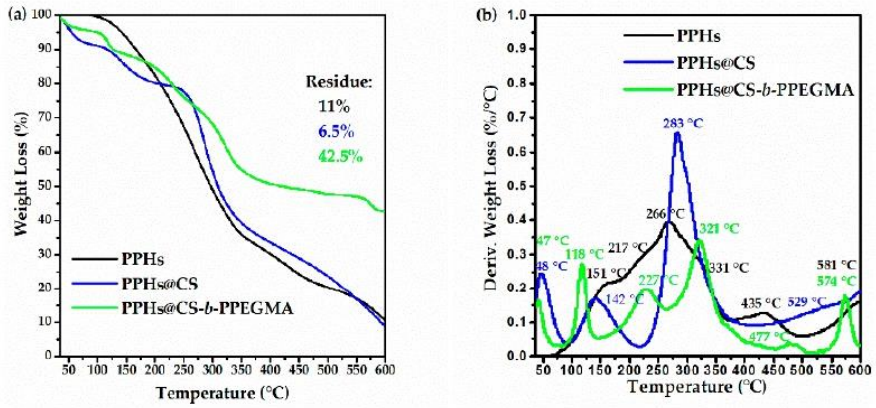

Figure 9. Thermal stability of loaded and unloaded PPHs: (**a**) TG-thermogram and (**b**) DTG-thermogram of Polyphenolics Compounds (PPHs), PPHs loaded in CS (CS@PPHs), and PPHs loaded in CS-*b*-PPEGMA (CS-*b*-PPEGMA@PPHs).

3.4. Release of Phenolic Compounds

The release profiles were performed by simulating pH conditions in the gastrointestinal tract using phosphate buffers with pH 7.4, 2, and 8 (Figure 10); each simulation was incubated for 24 h. Subsequently, a continuous release was also performed (pH 2, 6.8, 7.4 and 8); in the same way, the surface charge of both systems was determined at the different pH to study their behavior. In Figure 10a, it can be seen that the phenolic compounds show a higher percentage of release at pH 8, while at pH 7.4 a drop in their concentration is observed after 24 h of release; furthermore, the maximum release percentage of these compounds was 45%. It is relevant to specify that the rest of the PPHs precipitate as they are not completely soluble in an aqueous medium. According to the release profiles recorded from the two different matrixes, it can be seen that the CS-*b*-PPEGMA blocks provide a more controlled release of these compounds, releasing more than 80% of the PPHs after 24 h. On the other hand, CS only releases a maximum of around 40% of the guest compounds, and this is mainly due to the solubility of CS in the different pH values [63], observing that at pH 2, CS is completely soluble and releases a higher percentage of the phenolic compounds.

The release in all cases started quickly at the beginning and then a slower release of nutraceuticals compounds over time was recorded; this could result from a fraction of the molecules just being adsorbed onto the matrixes' surface, triggering an initial burst release [64].

In Figure 11, the continuous release profiles of the PPHs loaded in CS and CS-*b*-PPEGMA are shown—the systems presented different behavior when continuous release was performed, changing the pH and simulating the gastrointestinal tract passage as compared to individual pH values. It is observed that the maximum release for the CS-*b*-PPEGMA matrix was less than 20%, and in the case of CS a maximum of 8% was released; this shows a gap where more than 80% of these compounds are protected within the different matrixes [65]. The difference between the release of the different matrixes is mainly due to their solubility in the aqueous medium, as well as the solubility/stability of the phenolic compounds released in the medium; these tend to precipitate when they are in an aqueous medium. Nevertheless, there is still a possibility that the enzymes present in *in-vivo* systems can degrade these matrixes and release a higher percentage of these compounds [13].

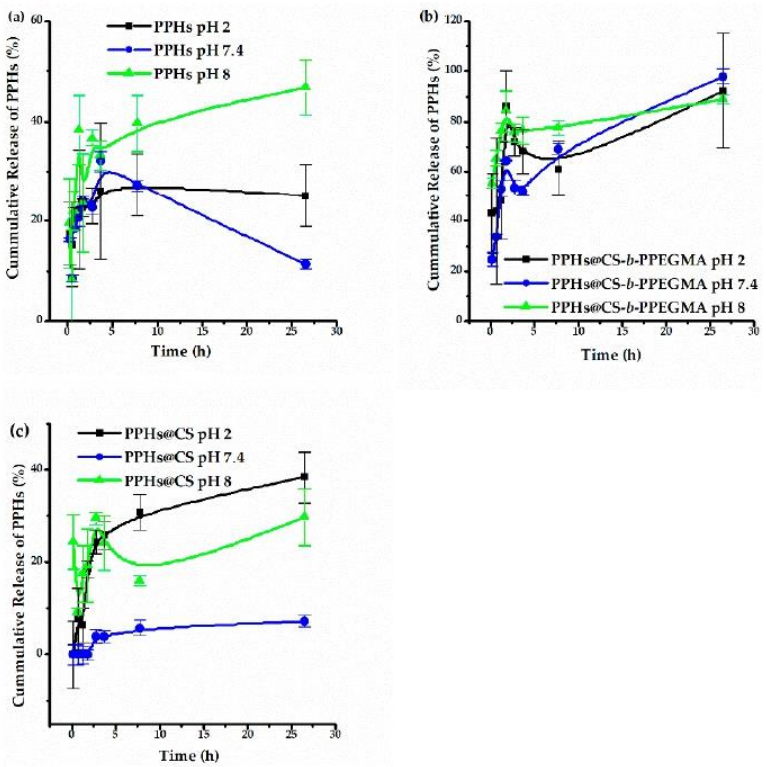

Figure 10. Release profiles of (**a**) PPHs, (**b**) PPHs@CS-*b*-PPEGMA, and (**c**) PPHs@CS. Values represent the mean ± standard deviation (n = 3).

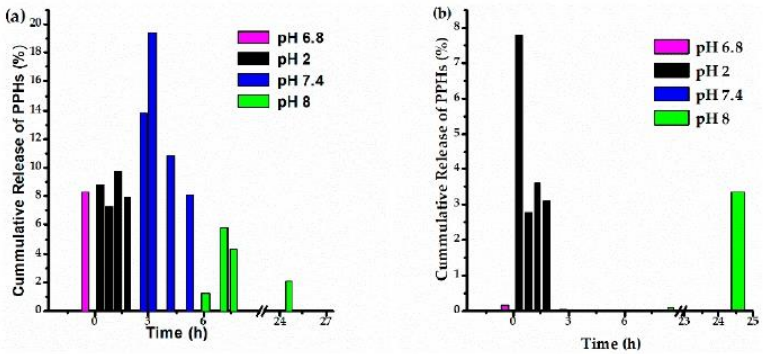

Figure 11. Cumulative release profiles of PPHs from CS-*b*-PPEGMA (**a**) and CS (**b**). Note: the cumulative release is only within a pH value; after every pH change, a new cumulative release is calculated.

3.5. In-Vitro Gastrointestinal Digestion

Encapsulation has been used both to enhance the bioaccessibility of phenolic compounds and to protect them from degradation [12]. In this sense, the properties of the charged and unloaded phenolic compounds were determined in both systems after the gastric and intestinal phase by the total reducing capacity and TEAC assays to evaluate if the compounds maintained their antioxidant properties.

Table 4 shows a summary of the results obtained, and it can be observed that both the total reducing capacity and the antioxidant capacity of the PPHs are diminished in the SGF phase. This may be mainly due to the ionization of the phenolic compounds present, which causes a decrease in their activity towards the free radical target; in the intestinal phase, a

decrease is seen mainly by the ABTS assay, which may have been because a large proportion of the released phenolic compounds could have been degraded or ionized in the gastric phase [9]. During in-vitro gastrointestinal digestion, encapsulated polyphenols can be partially released from the matrix; in this case, the matrix material can be affected by the pH changes during each digestive stage, CS matrix is most affected by this change in pH since it changes its solubility as it passes through the GI tract. At low pH, it is completely soluble, while at neutral-basic pH it is the opposite. The released polyphenols from the CS matrix are exposed to the different pH in the simulated gastrointestinal solutions, undergoing deprotonation of their chemical structures and partial hydrolysis, which has also been reported. Deprotonated polyphenols can affect the way they interact with the targeted free radicals in each antioxidant assay. The rate at which polyphenols are affected by the gastrointestinal environment is dependent on many factors, and one of the most reported is the matrix in which they are contained. In this work, we used the TEAC assay, which is based on the transfer method and depends on the reducing capacity of the evaluated substance [66,67].

Table 4. Results of the total reducing capacity (TRC) and Trolox equivalent antioxidant capacity (TEAC) of phenolic compounds loaded in chitosan (PPHs@CS), phenolic compounds loaded in CS-block-poly(PEGMA) (PPHs@CS-*b*-PPEGMA), and non-encapsulated phenolics (PPHs) after gastric and intestinal in-vitro digestion.

	TRC * (mg QE g^{-1} Dried Oregano)		TEAC ** (μmol TE g^{-1} Dried Oregano)	
	SGF	**SIF**	**SGS**	**SIF**
PPHs@CS	81.19 ± 4.18^{b}	111.70 ± 9.90^{a}	163.12 ± 79.11^{b}	446.56 ± 9.01^{a}
PPHs@CS-*b*-PEGMA	89.03 ± 2.39^{b}	135.50 ± 3.15^{a}	79.15 ± 23.15^{b}	415.79 ± 7.07^{a}
PPHs	16.68 ± 1.41^{b}	50.54 ± 2.90^{a}	104.19 ± 0.22^{a}	100.82 ± 7.99^{a}

* Total Reducing Capacity (TRC), ** Trolox equivalent antioxidant capacity (TEAC) is a scavenging capacity. Values represent the mean ± standard deviation (n = 3). ^{a,b} means are significantly ($\alpha > 0.05$) different according to the Tukey test.

In this approach, the encapsulated phenolic compounds have a higher activity than when they are not protected by one of the different matrixes [68]. In the same way, little difference can be observed between both matrix systems, and this may be mainly due to the effect of the surface charge that each system presents, causing the final TCR to be higher in the CS-*b*-PPEGMA matrix, having a negative partial charge because the amines are not protonated, and a higher concentration of these compounds remains inside; nonetheless, CS has a positive surface charge due to the number of amines that can be protonated, showing lower activity. The opposite is seen in the results obtained by TEAC, but in this case, it could be because the CS has a greater amount of compounds within the matrix; namely, there is a greater PPHs fraction compared to the block copolymers [52].

Moreover, it has been reported that CS-based polymers improve the disturbance in glucose metabolism in diabetic mice, such as reducing blood glucose, reversing insulin resistance, enhancement of the colonic epithelial integrity, and a modulatory effect on the gut microbiota. In addition, CS-based polymers loaded with phenolic compounds have been proposed as promising nanochemopreventive agents against cancer. Also, CS has been reported as a permeability enhancer, which must be addressed to evaluate if phenolic-loaded CS can increase the cell permeability of phenolics. Thus, CS and CS-based polymers loaded with phenolic compounds can result in multiple beneficial effects in the development of functional foods [11,41,69,70].

4. Conclusions

From the characterization, it can be concluded that the synthesis of block copolymers based on CS and PEGMA was successfully accomplished. The phenolic compounds were

efficiently encapsulated with the CS and CS-*b*-PPEGMA matrixes, which was verified by determining the surface charge (zeta potential) of the colloidal systems before and after the loading. This change is derived from the type of interaction taking place between the -OH groups of the phenolic compounds and the $-NH_2$ onto the CS backbone in the different aqueous medium. $PEGMA_{2000}$ led to the development of formulations having smaller particle size; however, CS plays a key role improving the matrix–guest compounds interactions and colloidal stability. The CS-*b*-PPEGMA matrix allowed a higher percentage of release, which can be attributed to the improved solubility of these platforms, as compared with single CS, and during cumulative release experiments only a maximum of 20% of active compounds were released from this platform; namely, 80% of the guest substances remained trapped in the polymeric matrix after the gastric and intestinal phases, indicating that the CS-*b*-PPEGMA may offer greater protection for the active compounds in the gastric phase. This could be related to the negative surface charge of this matrix undergoing delayed protonation, and an inverse effect was exhibited by CS. Thus, the results demonstrated that the encapsulation of nutraceuticals can improve their stability, solubility, and activity, and the CS-*b*-PPEGMA matrix can help improve the controlled release of compounds present in Mexican oregano (*Lippia graveolens*).

Author Contributions: Conceptualization, J.B.H. and A.L.-C.; Investigation, M.G.-C.; Resources, J.B.H. and A.L.-C.; Supervision, J.B.H. and A.L.-C.; Writing—original draft, M.G.-C.; Writing—review & editing, J.B.H., A.L.-C., E.P.G.-G., L.A.P.-C. and M.A.A.-E. All authors have read and agreed to the published version of the manuscript.

Funding: The APC was funded by CIAD, Mexico.

Institutional Review Board Statement: Not applicable.

Informed Consent Statement: Not applicable.

Data Availability Statement: The data that support the findings of this study are available from the corresponding author upon reasonable request.

Acknowledgments: We thank MC. L. Contreras (UPLC-MS measurements, CIAD-Culiacán) and V. Miranda (NMR measurements, ITT NMR facilities funded by CONACYT Grant: INFR-2011-3-173395). E.P.G.-G. thanks CONACYT for the Catedras Project #397.

Conflicts of Interest: The authors declare no conflict of interest.

References

1. Peanparkdee, M.; Iwamoto, S. Encapsulation for Improving In Vitro Gastrointestinal Digestion of Plant Polyphenols and Their Applications in Food Products. *Food Rev. Int.* **2020**, *38*, 335–353. [CrossRef]
2. Leyva-Lopez, N.; Gutierrez-Grijalva, E.P.; Vazquez-Olivo, G.; Heredia, J.B. Essential Oils of Oregano: Biological Activity beyond Their Antimicrobial Properties. *Molecules* **2017**, *22*, 989. [CrossRef] [PubMed]
3. Herrera-Rodriguez, S.E.; Lopez-Rivera, R.J.; Garcia-Marquez, E.; Estarron-Espinosa, M.; Espinosa-Andrews, H. Mexican oregano (*Lippia graveolens*) essential oil-in-water emulsions: Impact of emulsifier type on the antifungal activity of *Candida albicans*. *Food Sci. Biotechnol.* **2019**, *28*, 441–448. [CrossRef] [PubMed]
4. Subramanian, A.P.; Jaganathan, S.K.; Manikandan, A.; Pandiaraj, K.N.; Gomathi, N.; Supriyanto, E. Recent trends in nano-based drug delivery systems for efficient delivery of phytochemicals in chemotherapy. *RSC Adv.* **2016**, *6*, 48294–48314. [CrossRef]
5. Gutiérrez-Grijalva, E.P.; Picos-Salas, M.A.; Leyva-López, N.; Criollo-Mendoza, M.S.; Vazquez-Olivo, G.; Heredia, J.B. Flavonoids and Phenolic Acids from Oregano: Occurrence, Biological Activity and Health Benefits. *Plants* **2018**, *7*, 2. [CrossRef] [PubMed]
6. Gutiérrez-Grijalva, E.P.; Antunes-Ricardo, M.; Acosta-Estrada, B.A.; Gutiérrez-Uribe, J.A.; Basilio Heredia, J. Cellular antioxidant activity and in vitro inhibition of α-glucosidase, α-amylase and pancreatic lipase of oregano polyphenols under simulated gastrointestinal digestion. *Food Res. Int.* **2019**, *116*, 676–686. [CrossRef] [PubMed]
7. Gayoso, L.; Roxo, M.; Cavero, R.Y.; Calvo, M.I.; Ansorena, D.; Astiasarán, I.; Wink, M. Bioaccessibility and biological activity of Melissa officinalis, Lavandula latifolia and Origanum vulgare extracts: Influence of an in vitro gastrointestinal digestion. *J. Funct. Foods* **2018**, *44*, 146–154. [CrossRef]
8. Sęczyk, Ł.; Król, B.; Kołodziej, B. In vitro bioaccessibility and activity of Greek oregano (*Origanum vulgare* L. ssp. hirtum (link) Ietswaart) compounds as affected by nitrogen fertilization. *J. Sci. Food Agric.* **2020**, *100*, 2410–2417. [CrossRef]

9. Gutierrez-Grijalva, E.P.; Angulo-Escalante, M.A.; Leon-Felix, J.; Heredia, J.B. Effect of In Vitro Digestion on the Total Antioxidant Capacity and Phenolic Content of 3 Species of Oregano (*Hedeoma patens*, *Lippia graveolens*, *Lippia palmeri*). *J. Food Sci.* **2017**, *82*, 2832–2839. [CrossRef]
10. de Torre, M.P.; Vizmanos, J.L.; Cavero, R.Y.; Calvo, M.I. Improvement of antioxidant activity of oregano (*Origanum vulgare* L.) with an oral pharmaceutical form. *Biomed. Pharmacother.* **2020**, *129*, 110424. [CrossRef]
11. Martau, G.A.; Mihai, M.; Vodnar, D.C. The Use of Chitosan, Alginate, and Pectin in the Biomedical and Food Sector-Biocompatibility, Bioadhesiveness, and Biodegradability. *Polymers* **2019**, *11*, 1837. [CrossRef] [PubMed]
12. Grgic, J.; Selo, G.; Planinic, M.; Tisma, M.; Bucic-Kojic, A. Role of the Encapsulation in Bioavailability of Phenolic Compounds. *Antioxidants* **2020**, *9*, 923. [CrossRef] [PubMed]
13. Li, S.; Zhang, H.; Chen, K.; Jin, M.; Vu, S.H.; Jung, S.; He, N.; Zheng, Z.; Lee, M.S. Application of chitosan/alginate nanoparticle in oral drug delivery systems: Prospects and challenges. *Drug Deliv.* **2022**, *29*, 1142–1149. [CrossRef] [PubMed]
14. Rezagholizade-Shirvan, A.; Najafi, M.F.; Behmadi, H.; Masrournia, M. Design and Synthesis of Novel Curcumin/Chitosan-PVA-Alginate Nanocomposite to Improve Chemico-Biological and Pharmaceutical Curcumin Properties. *SSRN* **2022**, *24*, JDDST-D-22-00009. [CrossRef]
15. Sheorain, J.; Mehra, M.; Thakur, R.; Grewal, S.; Kumari, S. In vitro anti-inflammatory and antioxidant potential of thymol loaded bipolymeric (tragacanth gum/chitosan) nanocarrier. *Int. J. Biol. Macromol.* **2019**, *125*, 1069–1074. [CrossRef]
16. Niaz, T.; Imran, M.; Mackie, A. Improving carvacrol bioaccessibility using core-shell carrier-systems under simulated gastrointestinal digestion. *Food Chem.* **2021**, *353*, 129505. [CrossRef]
17. Bautista-Hernandez, I.; Aguilar, C.N.; Martinez-Avila, G.C.G.; Torres-Leon, C.; Ilina, A.; Flores-Gallegos, A.C.; Kumar Verma, D.; Chavez-Gonzalez, M.L. Mexican Oregano (*Lippia graveolens* Kunth) as Source of Bioactive Compounds: A Review. *Molecules* **2021**, *26*, 5156. [CrossRef] [PubMed]
18. Carrasco-Sandoval, J.; Aranda-Bustos, M.; Henríquez-Aedo, K.; López-Rubio, A.; Fabra, M.J. Bioaccessibility of different types of phenolic compounds co-encapsulated in alginate/chitosan-coated zein nanoparticles. *LWT* **2021**, *149*, 112024. [CrossRef]
19. Panda, P.K.; Yang, J.M.; Chang, Y.H. Preparation and characterization of ferulic acid-modified water soluble chitosan and poly (gamma-glutamic acid) polyelectrolyte films through layer-by-layer assembly towards protein adsorption. *Int. J. Biol. Macromol.* **2021**, *171*, 457–464. [CrossRef]
20. Panda, P.K.; Yang, J.M.; Chang, Y.H.; Su, W.W. Modification of different molecular weights of chitosan by p-Coumaric acid: Preparation, characterization and effect of molecular weight on its water solubility and antioxidant property. *Int. J. Biol. Macromol.* **2019**, *136*, 661–667. [CrossRef]
21. Silva, N.C.D.; Barros-Alexandrino, T.T.; Assis, O.B.G.; Martelli-Tosi, M. Extraction of phenolic compounds from acerola by-products using chitosan solution, encapsulation and application in extending the shelf-life of guava. *Food Chem.* **2021**, *354*, 129553. [CrossRef] [PubMed]
22. Hasan, K.M.F.; Wang, H.; Mahmud, S.; Jahid, M.A.; Islam, M.; Jin, W.; Genyang, C. Colorful and antibacterial nylon fabric via in-situ biosynthesis of chitosan mediated nanosilver. *J. Mater. Res. Technol.* **2020**, *9*, 16135–16145. [CrossRef]
23. Thomas, A.; Müller, S.S.; Frey, H. Beyond Poly(ethylene glycol): Linear Polyglycerol as a Multifunctional Polyether for Biomedical and Pharmaceutical Applications. *Biomacromolecules* **2014**, *15*, 1935–1954. [CrossRef] [PubMed]
24. Jun, H.W.; West, J.L. Endothelialization of microporous YIGSR/PEG-modified polyurethaneurea. *Tissue Eng.* **2005**, *11*, 8. [CrossRef]
25. Yu, H.; VandeVord, P.J.; Mao, L.; Matthew, H.; Wooley, P.H.; Yang, S.-Y. Improved tissue-engineered bone regeneration by endothelial cell mediated vascularization. *Biomaterials* **2009**, *30*, 508–517. [CrossRef]
26. Chiu, Y.-C.; Kocagöz, S.; Larson, J.C.; Brey, E.M. Evaluation of Physical and Mechanical Properties of Porous Poly (Ethylene Glycol)-co-(L-Lactic Acid) Hydrogels during Degradation. *PLoS ONE* **2013**, *8*, e60728. [CrossRef]
27. Martwong, E.; Tran, Y. Lower Critical Solution Temperature Phase Transition of Poly(PEGMA) Hydrogel Thin Films. *Langmuir* **2021**, *37*, 8585–8593. [CrossRef]
28. Zarei, B.; Tabrizi, M.H.; Rahmati, A. PEGylated Lecithin-Chitosan Nanoparticle-Encapsulated Alphα-Terpineol for In Vitro Anticancer Effects. *AAPS PharmSciTech* **2022**, *23*, 94. [CrossRef] [PubMed]
29. Cai, T.; Marquez, M.; Hu, Z. Monodisperse Thermoresponsive Microgels of Poly(ethylene glycol) Analogue-Based Biopolymers. *Langmuir* **2007**, *23*, 8663–8666. [CrossRef]
30. Matthes, R.; Frey, H. Polyethers Based on Short-Chain Alkyl Glycidyl Ethers: Thermoresponsive and Highly Biocompatible Materials. *Biomacromolecules* **2022**, *23*, 2219–2235. [CrossRef]
31. Swain, T.; Hillis, W.E. The phenolic constituents of Prunus domestica. I.—The quantitative analysis of phenolic constituents. *J. Sci. Food Agric.* **1959**, *10*, 63–68. [CrossRef]
32. Ghasemi, K.; Ghasemi, Y.; Ebrahimzadeh, M.A.; Ebrahimzadeh, M.A. Antioxidant activity, phenol and flavonoid contents of 13 citrus species peels and tissues. *Pak. J. Pharm Sci.* **2009**, *22*, 277–281. [PubMed]
33. Karadag, A.; Ozcelik, B.; Saner, S. Review of Methods to Determine Antioxidant Capacities. *Food Anal. Methods* **2009**, *2*, 41–60. [CrossRef]
34. Thaipong, K.; Boonprakob, U.; Crosby, K.; Cisneros-Zevallos, L.; Hawkins Byrne, D. Comparison of ABTS, DPPH, FRAP, and ORAC assays for estimating antioxidant activity from guava fruit extracts. *J. Food Compos. Anal.* **2006**, *19*, 669–675. [CrossRef]

35. Ganji, F.; Abdekhodaie, M.J. Synthesis and characterization of a new thermosensitive chitosan–PEG diblock copolymer. *Carbohydr. Polym.* **2008**, *74*, 435–441. [CrossRef]
36. Fang, Z.; Bhandari, B. Encapsulation of polyfenols-a review. *Trends Food Sci. Technol.* **2010**, *21*, 13. [CrossRef]
37. Picos-Corrales, L.A.; Garcia-Carrasco, M.; Licea-Claverie, A.; Chavez-Santoscoy, R.A.; Serna-Saldívar, S.O. NIPAAm-containing amphiphilic block copolymers with tailored LCST: Aggregation behavior, cytotoxicity and evaluation as carriers of indomethacin, tetracycline and doxorubicin. *J. Macromol. Sci.* **2019**, *56*, 759–772. [CrossRef]
38. Brodkorb, A.; Egger, L.; Alminger, M.; Alvito, P.; Assunção, R.; Ballance, S.; Bohn, T.; Bourlieu-Lacanal, C.; Boutrou, R.; Carrière, F.; et al. INFOGEST static in vitro simulation of gastrointestinal food digestion. *Nat. Protocols* **2019**, *14*, 991–1014. [CrossRef] [PubMed]
39. Cortes-Chitala, M.D.C.; Flores-Martinez, H.; Orozco-Avila, I.; Leon-Campos, C.; Suarez-Jacobo, A.; Estarron-Espinosa, M.; Lopez-Muraira, I. Identification and Quantification of Phenolic Compounds from Mexican Oregano (*Lippia graveolens* HBK) Hydroethanolic Extracts and Evaluation of Its Antioxidant Capacity. *Molecules* **2021**, *26*, 702. [CrossRef]
40. Lin, L.Z.; Mukhopadhyay, S.; Robbins, R.J.; Harnly, J.M. Identification and quantification of flavonoids of Mexican oregano (*Lippia graveolens*) by LC-DAD-ESI/MS analysis. *J. Food Compost Anal.* **2007**, *20*, 361–369. [CrossRef]
41. Paul, S.; Hmar, E.B.L.; Zothantluanga, J.H.; Sharma, H.K. Essential oils: A review on their salient biological activities and major delivery strategies. *Sci. Vis.* **2020**, *20*, 54–71. [CrossRef]
42. Hermosillo-Ochoa, E.; Picos-Corrales, L.A.; Licea-Claverie, A. Eco-friendly flocculants from chitosan grafted with PNVCL and PAAc: Hybrid materials with enhanced removal properties for water remediation. *Sep. Purif. Technol.* **2021**, *258*, 118052. [CrossRef]
43. Sabnis, S.; Block, L.H. Chitosan as an enabling excipient for drug delivery systems I. Molecular modifications. *Int. J. Biol. Macromol.* **2000**, *27*, 6. [CrossRef]
44. Kou, S.G.; Peters, L.; Mucalo, M. Chitosan: A review of molecular structure, bioactivities and interactions with the human body and micro-organisms. *Carbohydr. Polym.* **2022**, *282*, 119132. [CrossRef] [PubMed]
45. Nair, R.S.; Morris, A.; Billa, N.; Leong, C.O. An Evaluation of Curcumin-Encapsulated Chitosan Nanoparticles for Transdermal Delivery. *AAPS PharmSciTech* **2019**, *20*, 69. [CrossRef] [PubMed]
46. El-Sherbiny, I.M.; Smyth, H.D. Smart Magnetically Responsive Hydrogel Nanoparticles Prepared by a Novel Aerosol-Assisted Method for Biomedical and Drug Delivery Applications. *J. Nanomater* **2011**, *2011*, 910539. [CrossRef]
47. Paberit, R.; Rilby, E.; Göhl, J.; Swenson, J.; Refaa, Z.; Johansson, P.; Jansson, H. Cycling Stability of Poly(ethylene glycol) of Six Molecular Weights: Influence of Thermal Conditions for Energy Applications. *ACS Appl. Energy Mater.* **2020**, *3*, 10578–10589. [CrossRef]
48. Chuc-Gamboa, M.G.; Vargas-Coronado, R.F.; Cervantes-Uc, J.M.; Cauich-Rodriguez, J.V.; Escobar-Garcia, D.M.; Pozos-Guillen, A.; San Roman Del Barrio, J. The Effect of PEGDE Concentration and Temperature on Physicochemical and Biological Properties of Chitosan. *Polymers* **2019**, *11*, 1830. [CrossRef]
49. Hassani Najafabadi, A.; Abdouss, M.; Faghihi, S. Synthesis and evaluation of PEG-O-chitosan nanoparticles for delivery of poor water soluble drugs: Ibuprofen. *Mater. Sci. Eng. C Mater. Biol. Appl.* **2014**, *41*, 91–99. [CrossRef]
50. Li, R.; Wu, Y.; Bai, Z.; Guo, J.; Chen, X. Effect of molecular weight of polyethylene glycol on crystallization behaviors, thermal properties and tensile performance of polylactic acid stereocomplexes. *RSC Adv.* **2020**, *10*, 42120–42127. [CrossRef]
51. Kamel, K.M.; Khalil, I.A.; Rateb, M.E.; Elgendy, H.; Elhawary, S. Chitosan-Coated Cinnamon/Oregano-Loaded Solid Lipid Nanoparticles to Augment 5-Fluorouracil Cytotoxicity for Colorectal Cancer: Extract Standardization, Nanoparticle Optimization, and Cytotoxicity Evaluation. *J. Agric. Food Chem.* **2017**, *65*, 7966–7981. [CrossRef] [PubMed]
52. Espinosa-Sandoval, L.; Ochoa-Martinez, C.; Ayala-Aponte, A.; Pastrana, L.; Goncalves, C.; Cerqueira, M.A. Polysaccharide-Based Multilayer Nano-Emulsions Loaded with Oregano Oil: Production, Characterization, and In Vitro Digestion Assessment. *Nanomaterials* **2021**, *11*, 878. [CrossRef]
53. The Metabolomics Innovation Center. Quercetin. Available online: https://foodb.ca/compounds/FDB011904 (accessed on 15 June 2022).
54. The Metabolomics Innovation Center. Pinocembrin. Available online: https://foodb.ca/compounds/FDB002758 (accessed on 15 June 2022).
55. The Metabolomics Innovation Center. Naringin. Available online: https://foodb.ca/compounds/FDB011866 (accessed on 15 June 2022).
56. The Metabolomics Innovation Center. Cirsimaritin. Available online: https://foodb.ca/compounds/FDB001537 (accessed on 15 June 2022).
57. The Metabolomics Innovation Center. Luteolin. Available online: https://foodb.ca/compounds/FDB013255 (accessed on 15 June 2022).
58. The Metabolomics Innovation Center. Naringenin. Available online: https://hmdb.ca/metabolites/HMDB0002670 (accessed on 15 June 2022).
59. Wang, Q.Z.; Chen, X.G.; Liu, N.; Wang, S.X.; Liu, C.S.; Meng, X.H.; Liu, C.G. Protonation constants of chitosan with different molecular weight and degree of deacetylation. *Carbohydr. Polym.* **2006**, *65*, 194–201. [CrossRef]
60. Mazancová, P.; Némethová, V.; Treľová, D.; Kleščíková, L.; Lacík, I.; Rázga, F. Dissociation of chitosan/tripolyphosphate complexes into separate components upon pH elevation. *Carbohydr. Polym.* **2018**, *192*, 104–110. [CrossRef] [PubMed]

61. Ardean, C.; Davidescu, C.M.; Nemeş, N.S.; Negrea, A.; Ciopec, M.; Duteanu, N.; Negrea, P.; Duda-Seiman, D.; Musta, V. Factors Influencing the Antibacterial Activity of Chitosan and Chitosan Modified by Functionalization. *Int. J. Mol. Sci.* **2021**, *22*, 7449. [CrossRef] [PubMed]
62. Hussain, K.; Ali, I.; Ullah, S.; Imran, M.; Parveen, S.; Kanwal, T.; Shah, S.A.; Saifullah, S.; Shah, M.R. Enhanced Antibacterial Potential of Naringin Loaded β Cyclodextrin Nanoparticles. *J. Clust. Sci.* **2021**, *33*, 339–348. [CrossRef]
63. Hamdi, M.; Nasri, R.; Li, S.; Nasri, M. Design of blue crab chitosan responsive nanoparticles as controlled-release nanocarrier: Physicochemical features, thermal stability and in vitro pH-dependent delivery properties. *Int. J. Biol. Macromol.* **2020**, *145*, 1140–1154. [CrossRef]
64. Hosseini, S.F.; Zandi, M.; Rezaei, M.; Farahmandghavi, F. Two-step method for encapsulation of oregano essential oil in chitosan nanoparticles: Preparation, characterization and in vitro release study. *Carbohydr. Polym.* **2013**, *95*, 50–56. [CrossRef]
65. Maqsoudlou, A.; Assadpour, E.; Mohebodini, H.; Jafari, S.M. The influence of nanodelivery systems on the antioxidant activity of natural bioactive compounds. *Crit. Rev. Food Sci. Nutr.* **2022**, *62*, 24. [CrossRef]
66. Bermúdez-Soto, M.J.; Tomás-Barberán, F.A.; García-Conesa, M.T. Stability of polyphenols in chokeberry (*Aronia melanocarpa*) subjected to in vitro gastric and pancreatic digestion. *Food Chem.* **2007**, *102*, 865–874. [CrossRef]
67. Wootton-Beard, P.C.; Moran, A.; Ryan, L. Stability of the total antioxidant capacity and total polyphenol content of 23 commercially available vegetable juices before and after in vitro digestion measured by FRAP, DPPH, ABTS and Folin–Ciocalteu methods. *Food Res. Int.* **2011**, *44*, 217–224. [CrossRef]
68. Chew, S.-C.; Tan, C.-P.; Long, K.; Nyam, K.-L. In-vitro evaluation of kenaf seed oil in chitosan coated-high methoxyl pectin-alginate microcapsules. *Ind. Crops Prod.* **2015**, *76*, 230–236. [CrossRef]
69. Zheng, J.; Yuan, X.; Cheng, G.; Jiao, S.; Feng, C.; Zhao, X.; Yin, H.; Du, Y.; Liu, H. Chitosan oligosaccharides improve the disturbance in glucose metabolism and reverse the dysbiosis of gut microbiota in diabetic mice. *Carbohydr. Polym.* **2018**, *190*, 77–86. [CrossRef] [PubMed]
70. Terada, A.; Hara, H.; Sato, D.; Higashi, T.; Nakayama, S.; Tsuji, K.; Sakamoto, K.; Ishioka, E.; Maezaki, Y.; Tsugita, T.; et al. Effect of Dietary Chitosan on Faecal Microbiota and Faecal Metabolites of Humans. *Microb. Ecol. Health Dis.* **1995**, *8*, 15–21. [CrossRef]

3. LOADING AND RELEASE OF PHENOLIC COMPOUNDS FROM MEXICAN OREGANO (*Lippia graveolens*) IN DIFFERENT CATIONIC-PEGYLATED MATRIXES AND THEIR EFFECT ON CACO-2 AND CCD18-CO CELLS

Melissa Garcia-Carrasco[1], Lorenzo A. Picos-Corrales[2], Laura Contreras-Angulo[1], Erick P. Gutiérrez-Grijalva[3], Miguel A. Angulo-Escalante[1], Angel Licea-Claverie[4,*] and J. Basilio Heredia[1]

[1]Nutraceuticals and Functional Foods Laboratory, Centro de Investigación en Alimentación y Desarrollo, A.C., Carretera a Eldorado Km. 5.5, Col. Campo El Diez, Culiacán 80110, Sinaloa, México

[2]Facultad de Ingeniería Culiacán, Universidad Autónoma de Sinaloa, Ciudad Universitaria, Culiacán 80013, Sinaloa, México

[3]Cátedras CONACYT-Centro de Investigación en Alimentación y Desarrollo, A.C., Carretera a Eldorado Km. 5.5, Col. Campo El Diez, Culiacán 80110, Sinaloa, México

[4]Centro de Graduados e Investigación en Química, Tecnológico Nacional de México/Instituto Tecnológico de Tijuana, A.P. 1166, Tijuana 22000, Baja California, México

[*]aliceac@tectijuana.mx

Artículo Enviado:

Abril 2024

A la Revista:

Journal of Drug Delivery Science and Technology

Journal of Drug Delivery Science and Technology

Loading and release of Phenolic Compounds from Mexican Oregano (Lippia graveolens) in Different cationic-PEGylated Matrixes and their Effect on CACO-2 and CCD18-co Cells

--Manuscript Draft--

Manuscript Number:	
Article Type:	Research Paper
Keywords:	Phenolics Compounds; Oregano extract; Nanoemulsions; Caco-2 cells; cationic PEGylated matrixes; Chitosan
Corresponding Author:	Angel Licea Claverie, PHD Instituto Tecnologico de Tijuana, Centro de Graduados e Investigacion en Quimica MEXICO
First Author:	Melissa Garcia Carrasco
Order of Authors:	Melissa Garcia Carrasco
	Lorenzo Antonio Picos Corrales
	Laura Contreras-Angulo
	Erick P. Gutierrez Grijalva
	Miguel Angel Angulo Escalante
	Angel Licea Claverie, PHD
	J. Basilio Heredia
Abstract:	Phenolic compounds (PPHs) extracted from Mexican oregano (Lippia graveolens) have presented various biological activities, including their antioxidant, anti-inflammatory and anticancer properties. However, these compounds are unstable in aqueous medium and sensitive to changes in pH and temperature of the environment in which they are found. In this article, the encapsulation of this type of phenolic compounds in different poly(ethylene glycol) (PEG) functionalized cationic matrixes, based on poly(N,N'-diethylaminoethyl methacrylate) (PDEAEM) and Chitosan (CS), is reported. Particle sizes between 122-458 nm were obtained for the PDEAEM and CS platforms, and the loading content was around 62% for both systems, while the loading efficiency was higher than 90%. The identification of the loaded phenolic compounds by Ultra High-Resolution Liquid Chromatography/Mass Spectrometry (UPLC/MS) demonstrated that naringenin, phloridzin and cirsimaritin, predominated; being responsible for antitumor and inflammatory properties in in vitro cellular assays. As compared with the plain extract, the prepared formulation led to an increase in the extract stability and the antioxidant activity through TEAC and ORAC tests. It was also observed that concentrations of loaded extract lower than 500 µg mL-1 did not show cytotoxicity in CCD18 fibroblasts, while they exhibited substantial antiproliferative activity in CACO-2 cells. After 72 h, the activity of the loaded systems was very similar to that of the anticancer drug 5-fluorouracil (5FU), so these cationic systems loaded with phenolic compounds could act as a good coadjutant in the treatment of colon cancer.
Suggested Reviewers:	Carlos Peniche University of Havana peniche@fq.uh.cu Expert in Chitosan polymers for biomedical applications
	Carmen Alvarez Lorenzo University of Santiago de Compostela carmen.alvarez.lorenzo@usc.es Expert in Drug Delivery Systems
	Jayanta Kumar Patra Dongguk University - Seoul Campus jkpatra@dongguk.edu

Prof. Dr. Florence Siepmann, PhD
University of Lille, Faculty of Pharmacy, Lille, France
Editor-in-Chief
Journal of Drug Delivery Science and Technology

Dear editor:

Please find attached the manuscript entitled **Loading and Release of Phenolic Compounds from Mexican Oregano (Lippia graveolens) in Different Cationic-PEGylated Matrixes and their Effect on CACO-2 and CCD18-co Cells** by Garcia-Carrasco, Melissa, Picos-Corrales, Lorenzo A., Contreras-Angulo, Laura, Gutiérrez-Grijalva, Erick P., Angulo-Escalante, Miguel Angel, Licea-Claverie, Angel and Heredia, J. Basilio; for your kind consideration for publication in the Journal of Drug Delivery Science and Technology as a full-paper.

In this work we report, the loading of a mixture of phenolic compounds extracted from *Lippia graveolens* (oregano) in two different cationic matrixes with the aim to protect and maximize their biological properties for passage through the gastro-intestinal tract. A chitosan derived matrix and a fully synthetic micelle forming block copolymer were compared in their ability to encapsulate and protect the extract from the acid pH of stomach using two different models: a simple continuous release study at different pH values and a simulation of the passage through areas of different pH values with different resident times. Results demonstrate that both matrixes are able to protect the oregano extract but the block copolymer is more effective. At the end of the gastrointestinal passage up to 80% of the extract is still available for action when encapsulated in the cationic matrixes, while the non encapsulated extract is lost almost entirely. UPLC/MS studies demonstrated that after gastro-intestinal passage naringenin, phloridzin and cirsimaritin, predominated in the extract. As compared with the plain extract, the prepared encapsulated extracts led also to an increase in the antioxidant activity as demonstrated through TEAC and ORAC tests. Cell viability studies demonstrated that the encapsulated extract did not show cytotoxicity in healthy CCD18 fibroblast cells, while they exhibited substantial antiproliferative activity in CACO-2 colon cancer cells. After 72 h of contact, the activity of the loaded systems was very similar to that of the anticancer drug 5-fluorouracil, so these cationic systems loaded with the extract of phenolic compounds could act as a good coadjutant in the treatment of colon cancer.

We think that the presented work is of interest for the readers of the Journal of Drug Delivery Science and Technology for two reasons: First, it highlights the use of cationic matrixes for encapsulation, loading and release of natural extracts in one example: oregano extract. This methodology can be expanded to other types of extracts of plants. Second it shows that after a simulated intestinal passage the main components of the extract are keeped, and the antioxidant and antiproliferative activities of the cationic matrix loaded extract are demonstrated. In this case the encapsulated oregano extract has a great chance to be used as coadjutant in colon cancer treatment; while the investigation strategy can be

translated to test the potential use of other plant extracts in health related problems.

We confirm that this manuscript has not been published elsewhere and all authors have approved the manuscript, and they agree with its publication in the Journal of Drug Delivery Systems and Technology.

Best regards,

Prof. Dr. Angel Licea-Claverie
On behalf of all co-authors

Manuscript File

Highlights

- Extract from Oregano loaded in cationic polymers at 62% LC
- Chitosan-PEG and PEGylated tertiary amine block-copolymer used as cationic matrixes
- Loaded extracts show increased stability and antioxidant activity
- 80% of the extract remain after gastro-intestinal passage when loaded in matrixes
- Loaded extract show antiproliferative activity to colon cancer cells

Manuscript File

Click here to access/download;Graphical Abstract;graphical abstract JDDST3 final.tif

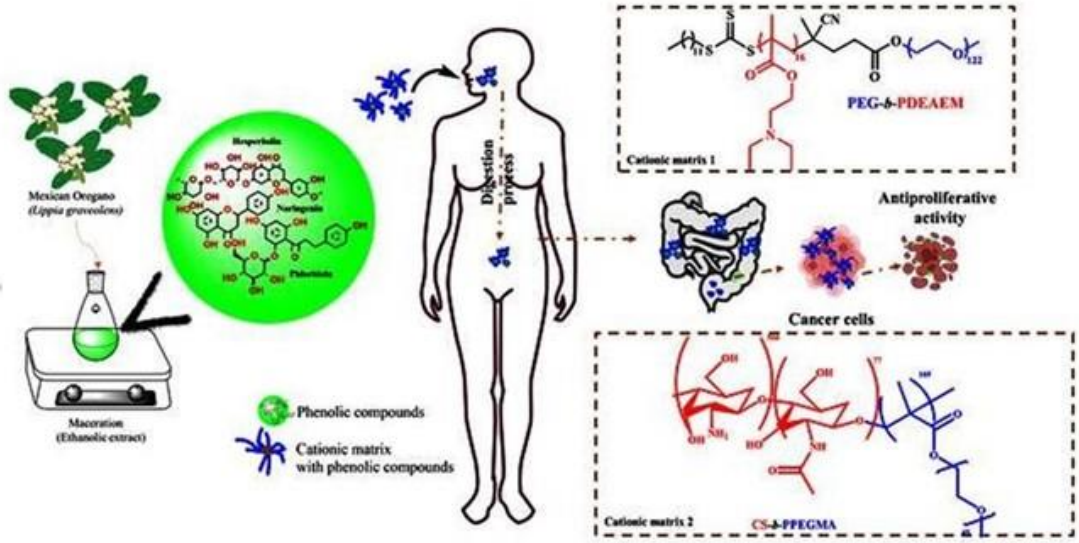

Loading and Release of Phenolic Compounds from Mexican Oregano (*Lippia graveolens*) in Different Cationic-PEGylated Matrixes and their Effect on CACO-2 and CCD18-co Cells.

Garcia-Carrasco, Melissa[1], Picos-Corrales, Lorenzo A.[2], Contreras-Angulo, Laura[1], Gutiérrez-Grijalva, Erick P.[3], Angulo-Escalante, Miguel Angel[1], Licea-Claverie, Angel[4*] and Heredia, J. Basilio.[1*]

[1]Nutraceuticals and Functional Foods Laboratory, Centro de Investigación en Alimentación y Desarrollo, A.C., Carretera a Eldorado Km. 5.5, Col. Campo El Diez, Culiacán 80110, Sinaloa, Mexico

[2]Facultad de Ingeniería Culiacán, Universidad Autónoma de Sinaloa, Ciudad Universitaria, Culiacán 80013, Sinaloa, Mexico

[3]Cátedras CONACYT-Centro de Investigación en Alimentación y Desarrollo, A.C., Carretera a Eldorado Km. 5.5, Col. Campo El Diez, Culiacán 80110, Sinaloa, Mexico

[4]Centro de Graduados e Investigación en Química, Tecnológico Nacional de Mexico/Instituto Tecnológico de Tijuana, A.P. 1166, Tijuana 22000, Baja California, Mexico

***Corresponding authors: *J. Basilio Heredia: Nutraceuticals and Functional Foods Laboratory, Centro de Investigación en Alimentación y Desarrollo, A.C., Carretera a Eldorado Km. 5.5, Col. Campo El Diez, Culiacán 80110, Sinaloa, Mexico. E-mail: jbheredia@ciad.mx**

***Angel Licea-Claverie: Centro de Graduados e Investigación en Química, Tecnológico Nacional de Mexico/Instituto Tecnológico de Tijuana, A.P. 1166, Tijuana 22000, Baja California, Mexico. E-mail: aliceac@tectijuana.mx Phone: +52-6646234043**

Abstract

Phenolic compounds (PPHs) extracted from Mexican oregano (*Lippia graveolens*) have presented various biological activities, including their antioxidant, anti-inflammatory and anticancer properties. However, these compounds are unstable in aqueous medium and sensitive to changes in pH and temperature of the environment in which they are found. In this article, the encapsulation of this type of phenolic compounds in different poly(ethylene glycol) (PEG) functionalized cationic matrixes, based on poly(*N,N'*-diethylaminoethyl methacrylate) (PDEAEM) and Chitosan (CS), is reported. Particle sizes between 122-458 nm were obtained for the PDEAEM and CS platforms, and the loading content was around 62% for both systems, while the loading efficiency was higher than 90%. The identification of the loaded phenolic compounds by Ultra High-Resolution Liquid Chromatography/Mass Spectrometry (UPLC/MS) demonstrated that naringenin, phloridzin and cirsimaritin, predominated; being responsible for antitumor and inflammatory properties in *in vitro* cellular assays. As compared with the plain extract, the prepared formulation led to an

increase in the extract stability and the antioxidant activity through TEAC and ORAC tests. It was also observed that concentrations of loaded extract lower than 500 μg mL^{-1} did not show cytotoxicity in CCD18 fibroblasts, while they exhibited substantial antiproliferative activity in CACO-2 cells. After 72 h, the activity of the loaded systems was very similar to that of the anticancer drug 5-fluorouracil (5FU), so these cationic systems loaded with phenolic compounds could act as a good coadjutant in the treatment of colon cancer.

Keywords: Phenolics Compounds, Nanoemulsions, Caco-2, CCD18-co, cationic PEGylated matrixes.

1. Introduction

The plant's secondary metabolites have many biological properties, including anti-inflammatory, antibacterial, and antifungal activities, among others [1, 2]. These properties are mainly related to antioxidant-type compounds such as phenolic compounds, since different studies have reported that the increase in the intake of these compounds results in a decrease in the appearance of various diseases related mainly to oxidative stress [3, 4], such as cancer [5, 6]. Since these compounds are primarily metabolized in the colon, their main action occurs more frequently in that area. However, because these compounds can lose their properties by digestion, or in other words, can be degraded when passing through the digestive tract, different approaches have been sought as alternatives to protect these properties. Among these approaches, the encapsulation of the compounds by different methodologies such as spray drying, and emulsions, among others, has been tested. For that, polymers obtained from animal or vegetable sources (e.g. chitosan) are the most widely used matrixes towards encapsulation of natural bioactive substances. Chitosan (CS) is a polyelectrolyte that can help to release phenolic compounds more effectively, but because CS is not soluble in plain water, different modifications have been made to increase its solubility. Poly(ethylene glycol) (PEG) is one of the most widely used synthetic polymers due to its high biocompatibility, simple way to bind to peptide sequences [7], growth factors

[8], and the ability to control mechanical properties regardless of polymerization conditions [9]. Another relevant factor for the characteristics of PEG is the length of chain; depending on that factor, this polymer is soluble in water and can also present a lower critical solution temperature (LCST) [10]. The latter can be modified by the terminal groups onto the PEG chain, whether they are of the acid, amino or hydroxyl type [11].

For this reason, poly (ethylene glycol) methyl ether methacrylate (PEGMA) has also been widely used. When it begins to degrade, some of its properties change, allowing a change in the size of the degraded by-products, which is highly favorable for medical application, since these by-products can be easily excreted by renal filtration [12]. Both PEG and PEGMA are hydrophilic polymers, and they can be copolymerized with hydrophobic monomers, which help to maintain a larger amount of the guest compounds to be transported to a specific site for a longer time. Another monomer that has been widely used in recent years in connection with controlled drug release systems is (*N,N'*-diethylamino ethyl methacrylate) (DEAEM); this monomer forms polymers that show changes in their conformation with variations in the pH of the medium, in other words, it forms polymers that are sensitive to changes in pH [13]. This polymer has also been confirmed to be pH sensitive with a pK_a close to 7 [14].

The combination of PEG with DEAEM results in copolymers that are sensitive to stimuli from the environment that surrounds them; in the structure of the designed macromolecule, DEAEM has a tertiary amine, which can be easily quaternized to produce a cationic polymer and may act as ligand for active compounds [15], while PEG helps stabilize the system. Hence, the main objective of this investigation was to encapsulate ethanolic extracts of *Lippia graveolens*, compare two PEGylated cationic polymer matrixes (CS-*b*-PPEGMA and PEG-*b*-PDEAEM) related to their encapsulation efficiency, and capacity to improve the antioxidant and antiproliferative properties of the single extract.

2. Materials and methodology

2.1 Materials

4-cyano-4-(dodecylsulfanylthiocarbonylsulfanyl)pentanoic acid (CTA) was kindly provided by Eduardo Marquez (TNM/Tijuana Tech). The following reagents were acquired from Sigma-Aldrich (Toluca-Mexico): methoxy polyethylene glycol (5000 g mol^{-1} MPEG), 4,4'-azobis(cyanovaleric acid) acid (ACVA, 98%,), 4-(dimethylamine)pyridine (DMAP, ≥99%) *N,N'*-diethylamino ethyl methacrylate (DEAEM, ≥99%), chitosan (Low molecular weight, 98%), deuterium chloride/deuterium oxide (D_2O/DCl 35% by weight, 99.9% deuterium), poly(ethylene glycol) methyl ether methacrylate (PEGMA2000) 2000 g mol^{-1}, ammonium persulfate (APS, 98%), *p*-Dioxane (≥99%), tetrahydrofuran (THF, ≥99%), deuterated chloroform ($CDCl_3$ 99.8% deuterium), Folin-Ciocalteu reagent (2N), aluminum chloride (99%), potassium acetate (≥99.0%), quercetin (≥95%), 2,2'-Azino-bis (3-ethylbenzothiazoline-6-sulfonic acid) diammonium salt radical cation (ABTS radical, ≥98%), potassium persulfate (≥99.0%), formic acid (≥95%), penicillin, streptomycin, 5-Fluorouracil (5FU), *In vitro* Toxicology Assay Kit based on the activity of lactate dehydrogenase enzyme (LDH) and *In vitro* Toxicology Assay Kit MTT. Dichloromethane (DCM, ≥99%), petroleum ether (≥99%) and glacial acetic acid (99.7%) were acquired from FERMONT. Acetone (≥99%), acetonitrile and HPLC grade water were purchased from JT Baker; methanol (MeOH, ≥99%) from MAYER, ethyl ether (≥99%) from FRAGA, Nitrogen (99.997% high purity) and Argon (99.998% high purity) from INFRA, Mexico. Fibroblast CCD18-co and Caco-2 cells lines were acquired from the American Type Culture Collection. Eagle's Minimum Essential Medium (EMEM) with L-glutamine, Dulbecco's Modified Eagle

Medium F12 (DMEM F12) and fetal bovine serum were purchased from Gibco Life Technologies.

2.2 Monomer and chitosan purification

The DEAEM monomer was purified by passing through an alumina column to remove the polymerization inhibitor. The PEGMA2000 monomer does not need purification; both monomers were refrigerated until use. Chitosan (CS) was dissolved in an aqueous acetic acid solution at 1% (v/v), up to a concentration of 1% (w/v); once dissolved, they were filtered under reduced pressure using a Büchner funnel. CS was precipitated from the acidic solution using 1M sodium hydroxide solution. The alkaline CS suspension was filtered under reduced pressure using a 5 µm pore size filter. The CS was washed with deionized water until its alkalinity was neutralized, frozen, and finally freeze dried using a Labconco Freeze Dry System Freezone 4.5 (Kansas City, MI, USA), with pre-cooling to -52 ◦C, and freeze-drying at a pressure of 0.02 mbar for 72 h.

2.3 Synthesis of block copolymers

2.3.1 Synthesis of PEG macro-CTA

The methodology proposed by García-Soria et al. [16] for the synthesis of a macro chain transfer agent for RAFT-polymerization containing poly(ethyleneglycol) (PEG) was followed but MPEG with a molecular weight of 5000 g mol^{-1} was used. The methodology is sketched below (Figure 1). In a 250 mL round-bottom flask equipped with a magnetic stirrer, 10.02 g (2 mmol) of 5000 g mol^{-1} poly(ethylene glycol) methyl ether in 50 mL of toluene was added. The solution was refluxed for 72 h. A Dean Stark system was adapted to the reflux system, in which molecular sieves (mesh #5) were added to remove water from the

PEG. The solution was cooled to room temperature and 1.6 g (0.644 mmol) of 4-cyano-4-(dodecylsulfanylthiocarbonylsulfanyl)pentanoic acid (CTA), 50 mL of dichloromethane (DCM), and 0.24 g (1.964 mmol) of dimethyl(aminopyridine) previously dissolved in 3 mL of DCM, were added. The flask with the reaction mixture was immersed in an ice bath and 0.82 g (3.9 mmol) of dicyclohexylcarbodiimide in 6 mL of DCM was added dropwise over 15 minutes. Once the dripping had finished, the solution was kept under stirring for 72 h. After the reaction time was completed, it was filtered off to remove the urea formed. The liquid was precipitated by adding diethyl ether, stirring for 20 min, and then 30 mL of petroleum ether was added. Finally, it was left to rest for 10 h at low temperature. The precipitate was dried under reduced pressure, and dissolved in DCM, the precipitation with ethyl ether was repeated in triplicate. At the end of the third purification cycle, the product was placed in a vacuum oven for 24 h. An ocher yellow product was obtained in 50% yield. The product was characterized by ^{1}H-NMR (Supplementary materials file Figure S1).

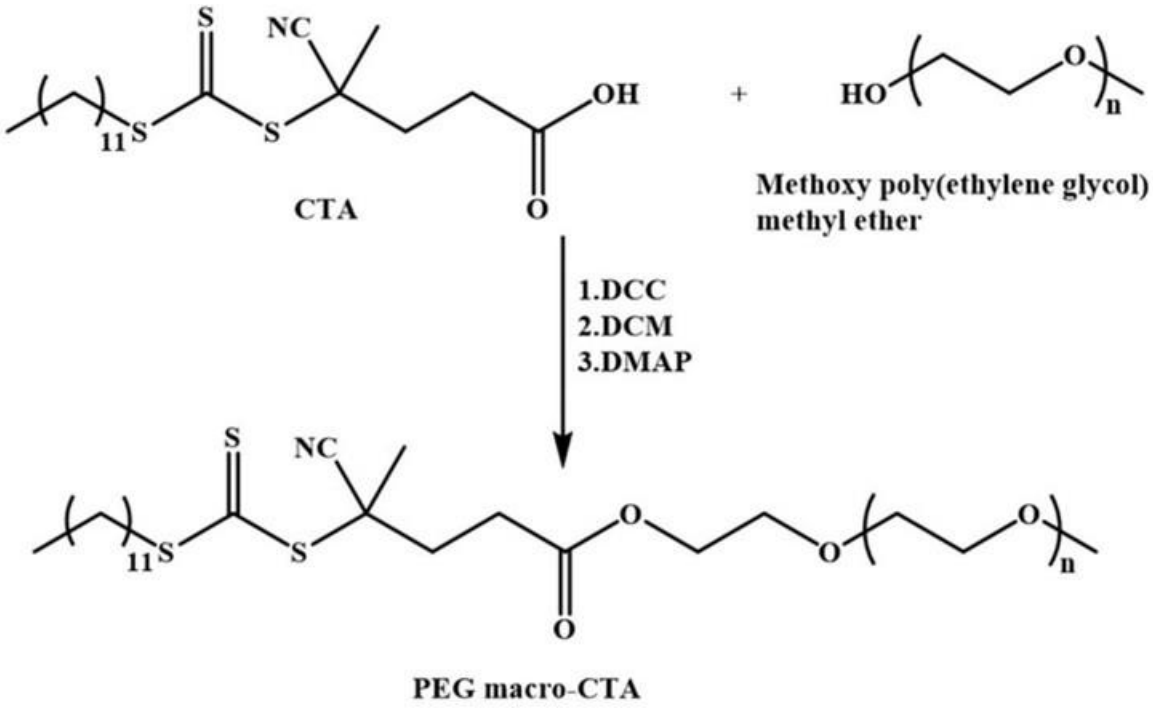

Figure 1. Scheme of the synthesis strategy for the PEG macroCTA.

2.3.2 Synthesis of PEG-*b*-PDEAEM block copolymers

The methodology of García-Soria et al. [16], was adapted to obtain the desired DEAEM concentration in the copolymer, an example is described below. In a 10 mL ampoule equipped with a magnetic stir bar, 1 g (5.4 mmol) of DEAEM, 0.4053 g (0.075 mmol) of the macro-CTA, 0.0035 g (0.0125 mmol) of initiator ACVA and 4 mL of *p*-dioxane were mixed (Figure 2). Oxygen was removed from the ampoule using three freeze (under argon) –thaw (under vacuum) evacuation cycles and was sealed with a propane torch flame under vacuum. The solution was heated to 70 °C in a mineral oil bath with magnetic stirring for 24 h. Once the polymerization time had elapsed, the content was poured into a 20 mL vial previously tared to proceed with its purification. The excess *p*-dioxane was concentrated under reduced pressure. Subsequently it was dissolved with a minimum amount of DCM and was

precipitated by adding an excess of 50/50% by volume solution of ethyl ether/petroleum ether. The solution was stirred for 2 h and was allowed to settle under refrigeration for 8-12 h until a yellow liquid phase and a white precipitate were observed. The liquid phase was removed, and the precipitate dissolved in DCM and dried under reduced pressure (this procedure was performed in triplicate). The obtained product was dissolved in 10 mL of acetone at 50 °C to eliminate the PEG residue, the supernatant was removed and dried under reduced pressure at 70 °C. The final product was placed in a vacuum oven at 35 °C for 24 h to eliminate traces of solvent. The polymerization yield was determined by gravimetry and characterized by ^{1}H-NMR

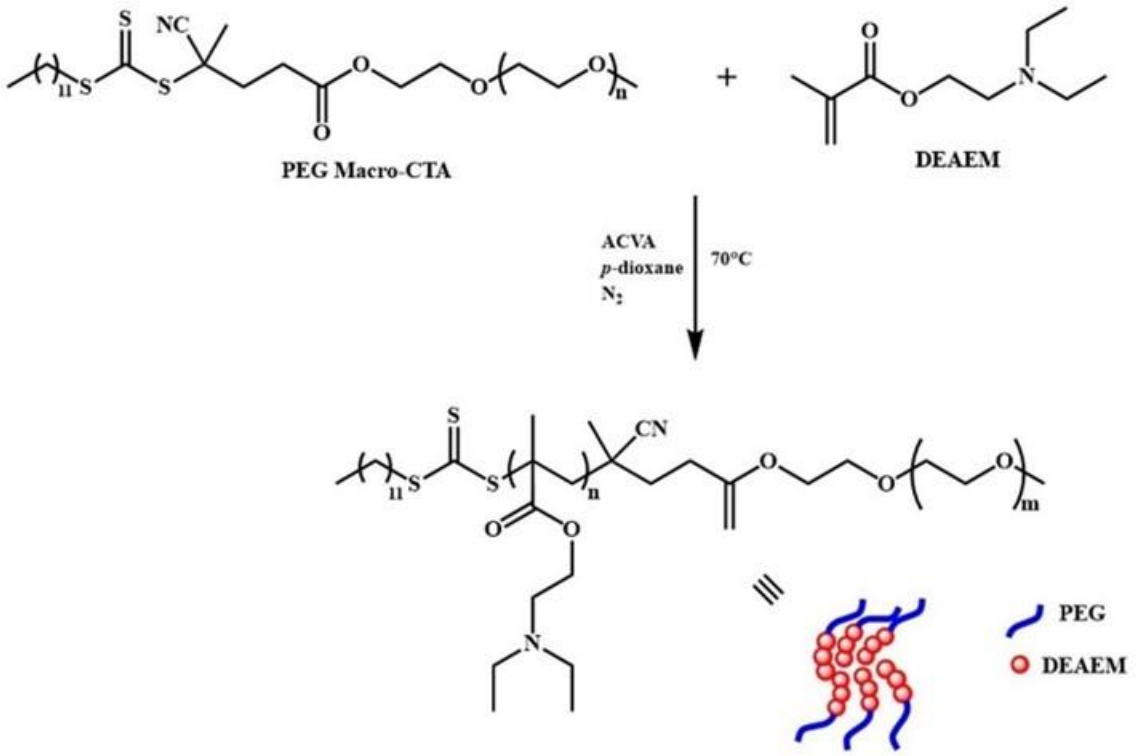

Figure 2. Synthesis scheme of PEG-*b*-PDEAEM copolymers.

2.3.3 Synthesis of Chitosan-block-poly(PEGMA)

The methodology for the synthesis of CS-*b*-PPEGMA blocks was carried out as published previously [17, 18]. First, the preparation was done using conventional free radical polymerization with a weight ratio of 50:50 CS:PEGMA adding 0.01M free radical initiator (KPS). CS (0.5 g) and KPS (0.135 g, 0.01M), were dissolved in 50 mL of water containing 1% (v/v) acetic acid in a three-necked round bottom flask equipped with a magnetic stir bar under an inert atmosphere (N_2). The flask was poured into an oil bath and heated to 60 °C for 30 min. After the time elapsed, PEGMA (0.46 mL, 0.5 g) was added dropwise, the reaction was left stirring (350 rpm) for 6 h. After the reaction time, the flask was removed from the oil and placed in a cold-water bath. For the purification of the product, NaOH 4M was first added to the solution to precipitate the CS that did not react; it was filtered off and subsequently washed with acetone to eliminate the residual PEGMA2000. Finally, the sample was dialyzed for 48 h, making changes of water periodically; after this, the recovered sample was freeze dried and weighed to determine the yield of the reaction, which was around 70%.

2.4 Characterization of block copolymers

2.4.1 Dynamic Light Scattering (DLS)

This technique allows for obtaining the hydrodynamic diameter (D_h). Samples for DLS were prepared with a concentration of 1 mg mL^{-1} and measured at 25 °C, in triplicate, using automatic measurement time and solvent viscosity. A Malvern ZetaSizer Nano ZS instrument (Malvern, Worcestershire, UK) was used for these measurements. The reported values of D_h correspond to the maximum of the size distribution by intensity.

2.11.2 Hydrogen Nuclear Magnetic Resonance (^{1}H-NMR).

The spectra were collected on a Bruker AMX-400 (Bruker Corporation, Billerica MA, USA) (400 MHz) spectrometer. This technique, was proposed to verify the incorporation of the main monomers and the determination of the real composition. All analyses were performed at room temperature using deuterated chloroform ($CDCl_3$) for PEG-*b*-PDEAEM and deuterium chloride (37%) (D_2O + DCl) for CS-*b*-PPEGMA spiked with tetramethyl silane (TMS). All samples were prepared by dissolving 10 to 20 mg of sample in 0.7 mL of $CDCl_3$ or D_2O + DCl. Measurements were made in precision Wilmad resonance tubes for 400 MHz. The chemical shift of the signals was calibrated using the TMS standard. The hydrogen spectra were processed with the ACD/D+H NMR Viewer 12.01 software package (Advanced Chemistry Development, 2008).

2.4.2 UV–Vis spectra of Phenolics Compounds (PPHs)

Optical spectra were acquired using a UV-Vis Varian Cary 100 spectrophotometer system (Agilent Technologies, Santa Clara, CA, USA) at room temperature from aqueous dispersions.

2.4.3 The Zeta potential (ζ)

The Zeta-potential of PPHs-loaded and not loaded in the polymeric matrixes in aqueous dispersions (1 mg mL^{-1}) was measured using a Malvern ZetaSizer Nano ZS instrument (Malvern, Worcestershire, UK). The measurements were the average of three runs performed at 25 °C in distilled water.

2.5 Nanometric Polymer Aggregates

2.5.1 Preparation of Aggregates

The copolymer aggregates were prepared through a direct dissolution consisting of the solubilization of the bulk copolymer CS-*b*-PPEGMA or PEG-*b*-PDEAEM (10 mg) in distilled water (10 mL) under magnetic stirring at room temperature for 24 h. The size of the aggregates was determined by dynamic light scattering (DLS) using a Malvern ZetaSizer Nano ZS instrument (Malvern, Worcestershire, UK) in the nanometer range.

9

2.6 Loading and release experiments of extracted phenolic compounds

2.6.1 Plant material and extraction of free polyphenols

Oregano (*L. graveolens*) was collected in Santa Gertrudis, Durango, México. Dried oregano leaves were ground using an Ika Werke M20 grinder (IKA, Germany) until a fine powder consistency was obtained. Oregano powder was stored at -4 °C until use. Garcia-Carrasco et al. [18] methodology was followed to get a stock of phenolic compounds extract.

2.6.2 Loading of Extracted Phenolic Compounds in Polymer Aggregates

The loading was performed based on a solvent evaporation method following the methodology reported by Picos-Corrales et al. [19], where 10 mg of block copolymers were dissolved in 10 mL of distilled water, and 20 mg of extracted phenolic compounds were dissolved in 5 mL of ethanol. The phenolic compounds solution was added dropwise into the polymer solution and left under magnetic stirring for 24 h. The phenolic compounds that

11

were not loaded were removed by centrifugation for 20 min. The purified material was filtered using a disc filter with a pore size of 1 μM and then frozen and freeze-dried. The mass of phenolic compounds loaded in block copolymers was determined by preparing a 0.3 mg mL^{-1} solution in PBS pH 6, measuring the absorbance by UV analysis at a maximum wavelength (λ_{max}) of 280 nm, and then quantified by using a calibration curve of phenolic compounds in PBS pH 6. The loading efficiency of phenolic compounds (LE) and the loading content (LC) of the cationic matrixes were calculated using equations 1 and 2.

LE(%) = (mass of PPHs in polymer/mass of PPHs in loading solution)x100 (1)

LC(%) = (mass of PPHs in polymers/(mass of PPHs in polymers + mass of dry polymer)x100 (2)

2.6.3 *In Vitro* Release Studies

For release profile studies, 0.3 mg mL^{-1} of PPHs-loaded polymeric matrixes were dispersed in 10 mL of distilled water and then added to a dialysis tube (Spectra/Por® MWCO: 12–14 KDa, diameter 10 mm, Spectrum, Los Angeles, CA, USA). The dialysis tube was introduced into a 100 mL release medium with a mixture of 30% ethanol and 70% PBS inside an Erlenmeyer flask. The flask was placed in a shaking bath (Shel Lab, model SWBR17, Sheldon Manufacturing, Inc., Cornelius, OR, USA), operating at 37 °C and a shaking speed of 100 rpm. Medium aliquots of 2 mL were taken out at different times and replaced by 2 mL of fresh PBS at every sampling point. The released fraction of phenolic compounds was calculated from UV measurements at λ_{max} = 280 nm and 320 nm for basic pH (7.4 and 8) and

acid pH (2 and 6.8), respectively, and was then quantified using a calibration curve of phenolic compounds in PBS (Supplementary materials file Figure S2).

2.6.3.1 *In vitro* Continuous Release Studies

For the continuous release studies, the methodology used is the same as that mentioned above, with the difference that the same dialysis tube was changed to a different release medium, simulating gastrointestinal tract passage following the pH of the mouth, stomach, duodenum and colon, and the time that liquids are in each area. Aliquots and measurements were measured as mentioned above.

2.6.4 Stability of PPHs loaded in block copolymer aggregates

A study of the stability of aggregates given by the different copolymer matrixes based on chitosan and PDEAEM was carried out for 17 weeks. The stability was determined by turbidimetry using a Hach 2100P portable turbidimeter (Loveland, CO. USA), and the results were expressed in NTU.

2.6.5 *In Vitro* Gastrointestinal Digestion

A simulation of gastrointestinal digestion was performed according to the static in-vitro digestion method reported by Brodkorb et al. [20]. This standardized procedure simulates the physiological conditions in the mouth, stomach, and small intestine, mimicking the chemical and pH conditions. Briefly, 1 mg of sample was mixed with simulated salivary fluids (SSF), then pH was adjusted to pH 7 with 6M NaOH; after that, the mixture was incubated for 5 min at 37 °C. Then, 1 mL of simulated gastric fluids (SGF), was adjusted to pH 3 and incubated for 2 h at 37 °C. Finally, 2 mL of simulated intestinal fluids (SIF) were added, pH was adjusted to pH 7, and the mixture was incubated for 2 h at 37 °C. In the final digestion step, the samples were centrifuged (9390×*g* at 4 °C for min), and the supernatant was

collected and freeze-dried. After that, samples were resuspended in ethanol for antioxidant capacity assays.

7

2.7 Characterization of the free and encapsulated L. graveolens extract (PPHs)

2.7.1 Antioxidant Capacity Method

2.7.1.1 Trolox equivalence antioxidant capacity (TEAC).

The antioxidant capacity by the TEAC assay of the encapsulated sample was determined as described by Thaipong et al. [21]. The interaction between the antioxidant and the ABTS•+ radical degrades the coloration of the solution. ABTS was dissolved in distilled water at a concentration of 7.4 mM (stock solution). The ABTS•+ radical was produced by mixing the ABTS stock solution with 2.6 mM potassium persulfate (1:1 v/v) and incubating the mixture in the dark at 25 °C for 12-16 h before use. Subsequently, the reaction solution was prepared by taking 100 µL of the radical and dissolved in 2900 µL of solvent to adjust the absorbance. For the assay, aliquots of 15 µL of extract and 285 µL of the reaction solution were added and homogenized using a vortex. Subsequently, it was incubated in the dark for 2 h. After the time elapsed, the absorbance at 734 nm was read in a Synergy HT microplate using transparent 96-well flat-bottom plates. The reaction solution was taken as a blank. A Trolox curve from 0.1 to 1 mmol TE g^{-1} was used to calculate the results, which are expressed as mmol Trolox equivalent per gram of powder (mmol TE g^{-1}). Each sample was measured in triplicate (n = 3).

5

6

2.7.1.2 Oxygen Radical Absorbance Capacity (ORAC)

ORAC Assay is a standardized method for determining the antioxidant capacity of a substance. This method measures a fluorescent signal from fluorescein in the presence of radicals such as AAPH (2,2'-Azobis 2-methylpropionamidine dihydrochloride) that was used as a peroxyl radical generator. This assay was performed on a 96-well microplate with dark background. Aliquots of 25 µL of extract/nanoemulsion, blanks (75 mM phosphate buffer, pH 7.4), and a standard Trolox curve were added for the assay. After, the plate was placed in a Synergy HT microplate reader (Bio-Tek Instruments, Winooski, VT, USA) and preincubated at 37 °C. The equipment dispenses the fluorescein and AAPH. The fluorescent was measured every 60 s for 60 min with a 485 nm excitation filter and a 580 nm emission. A Trolox curve from 12.5 to 125 µmol TE g^{-1} was used to calculate the results, which are expressed as µmol Trolox equivalent per gram of sample (µmol TE g^{-1}). Each sample was measured in triplicate (n = 3).

0

2.7.2 Identification of PPHs in the extract by Ultra Performance Liquid Chromatography/Mass Spectrometry (UPLC/MS)

Mass-liquid chromatography was used to carry out the separation to identify individual phenolic compounds from the oregano extract. The analysis was performed in a class H UPLC unit (Waters Corporation, USA) coupled to a G2-XS QT of mass analyzer (quadrupole and time of flight). The separation of flavonoids was performed with a different set of conditions, including a UPLC BEH C18 column (1.7 µm × 2.1 mm × 100 mm) at 30 °C, with gradient elution solution A (water-0.05% formic acid) and solution B (acetonitrile), which is

supplied at a flow rate of 0.3 ml min^{-1}. The ionization of the compounds was performed by electrospray (ESI), and the parameters used consisted of a capillary voltage of 1.5 kV, sampling cone: 30 V, desolvation gas of 800 (L h^{-1}), and a temperature of 500 °C. A collision ramp of 0-30 V was used. The Massbank of North America (MoNA) database was used for compound identification. The identification of phenolic compounds by UPLC was performed in triplicate (n = 3).

5

2.8 Cytotoxicity and antiproliferative Assays

2.8.1 Cell lines

All cell lines (CCD18 and Caco-2), were acquired from the American Type Culture Collection (ATCC, Manassas, VA, USA). The cell lines were cultured as recommended by the suppliers in an incubator at 37 °C with 5% of CO_2 until reaching the appropriate density for the test.

2.8.2 Assays

The cytotoxicity of the free phenolic compounds (ethanolic extract from Oregano=PPHs) and nanoemulsions of PPHs encapsulated in the cationic polymer matrixes studied=encapsulated PPHs was evaluated by the *in vitro* Toxicology Assay kit based on the activity of lactate dehydrogenase enzyme (LDH) following the supplier's recommendations. In a 96-well sterile plate, $10X10^3$ CCD18 Fibroblast cells/well were seeded, and the treatments were evaluated at concentrations of 100, 150, 250, 500, and 1000 µg mL^{-1} of free PPHs, encapsulated PPHs and polymer matrixes without PPHs. DMSO was used as positive control

(lysis), and untreated cells were used as negative control (-). The antiproliferative activity was assessed by *in vitro* Toxicology Assay Kit MTT. Caco-2 cells were seeded in 96-well sterile plates at $10X10^3$ cells/well density. The concentrations of free PPHs and encapsulated PPHs evaluated were 500 and 150 μg mL^{-1} and were incubated for 24, 48, and 72 h at 37 °C with 5% CO_2. 5FU (250 μM) was used as the reference drug to compare the effect on the treated cells. DMSO was used as positive control (lysis), and untreated cells were used as negative control (-). The percentage of cell viability was calculated by equation (3):

% Cell viability: ((Absorbance control-Absorbance sample)/Absorbance control)*100 (3)

2.8.3 Statistical Analysis

All tests were performed in triplicate (n=3), and the results are presented as mean ± standard deviation (SD). The ANOVA was evaluated with the Tukey or Dunnett test to determine significant differences using the Minitab 19 software.

3 Results

3.1 Characterization of PEG-b-PDEAEM and CS-b-PPEGMA cationic matrixes

3.1.1 ^{1}H-RMN

Figure 3a shows the ^{1}H-NMR spectrum of the PEG-*b*-PDEAEM block copolymer. No signal is observed between 5 and 6 ppm, which indicates the absence of residual monomer. The composition of the PEG-*b*-PDEAEM was calculated by integrating the **d** and **a** signals in the ^{1}H-NMR spectrum, corresponding to two methylene hydrogens bound to oxygen of the

PDEAEM (≈4.2 ppm), and to the three terminal methoxy hydrogens of the PEG (≈ 3.4 ppm). The weight composition was: 36:64 DEAEM:PEG, respectively. The calculated molecular weight was 8400 g mol^{-1} by ^{1}H-RMN, considering that the PEG unit has a real molecular weight of 5400 g mol^{-1}. Figure 3b shows the spectrum of CS-*b*-PPEGMA block copolymer. The characteristic signals of CS can be observed, and in addition the signals of PPEGMA at 3.55 ppm for the methoxy group hydrogens and 3.8 ppm for the methylene hydrogens in the PEG chain repetitive units. The slight displacement in the chemical shift of these signals compared to those in the PEG-*b*-PDEAEM spectrum is due to the use of different deuterated solvents for the spectrum acquisition of each block. The molecular weight for the CS-*b*-PPEGMA was calculated by ^{1}H-RMN, considering that the CS molecular weight remains 114 000 g mol^{-1} after the reaction. The PEGMA block units are incorporated randomly in the CS polymer chain and the total molecular weight of the block copolymer was calculated to be 323 800 g mol^{-1}, 65.8 wt% of PEGMA and 34.2 wt% of CS.

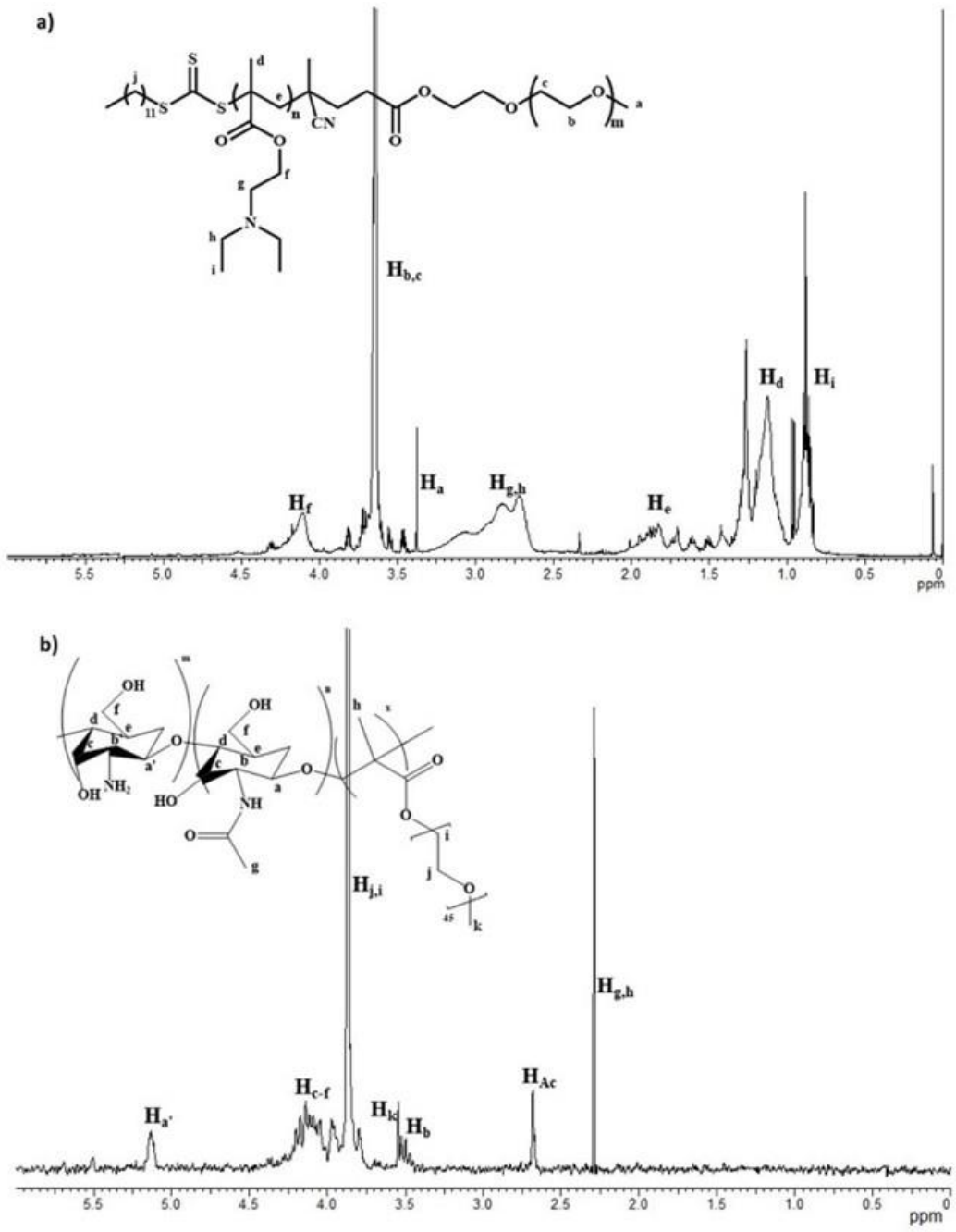

Figure 3. ^{1}H-NMR Spectra: a) PEG-*b*-PDEAEM copolymer in $CDCl_3$; b) CS-*b*-PPEGMA in DCl/D_2O 35wt%.

3.1.2 Thermogravimetric analysis (TGA) of PPHs loaded in cationic matrixes

The characterization by thermogravimetric analysis of the synthesized block copolymers was carried out, in which a comparative analysis of the weight derivate is shown when the temperature increases. In the thermogram (Figure 4, black curves) three well marked decomposition steps can be observed for the PEG-*b*-PDEAEM copolymers. The first decomposition step is at around 247 °C, corresponding to the first decomposition stage of DEAEM units. The second decomposition step is shown around 357 °C, which would correspond to the decomposition of PEG2000 and the second stage of decomposition of PDEAEM. Finally, a third decomposition step is presented around 515 °C, which could be the carbonization of the residual polymer chains; 6% organic residue is also shown. Similar to the CS-*b*-PPEGMA copolymer decomposition (Figure S3 in Supplementary material), overlapping decomposition stages are observed, which indicates that the decomposition temperatures of the other components are very close to each other and that this overlap exists [18]. The extract of phenolic compounds decomposes over a wide temperature range from 110 to 350 °C while a second step is located at a higher temperature (Figure 4 blue line). The PPHs-loaded block copolymer (PEG-*b*-PDEAEM) show a maximum of decomposition at 404 °C which is at a higher temperature than the single block copolymer and free PPHs (Figure 4 red line), suggesting that there are strong interactions between the PPHs and the block copolymer. A similar behavior was reported previously for PPHs loaded in CS-*b*-PPEGMA [18].

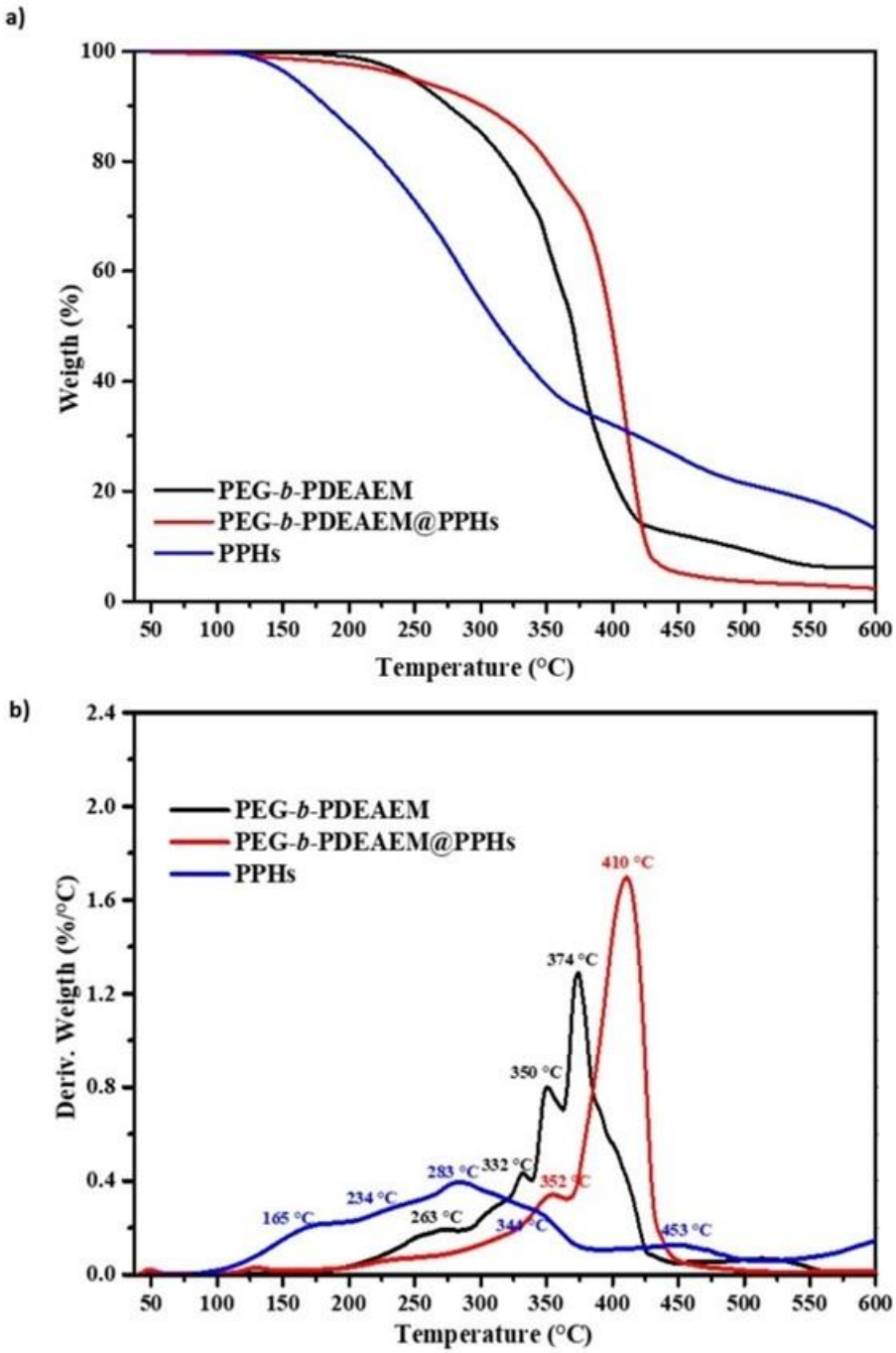

Figure 4. TGA thermogram of PPHs and PPHs loaded in PEG-*b*-PDEAEM copolymer aggregates: a) Weight loss; b) Derivative of weight loss.

2

3.1.3 Stability of Phenolic compounds loaded in cationic matrixes

The stability of the free Oregano extract (PPHs) and the loaded extract in the different cationic matrixes was studied for around four months through turbidity tests, where it was observed that the block copolymers used as cationic matrixes provided greater stability based on time compared to the free PPHs that tended to precipitate in the long run (Figure 5).

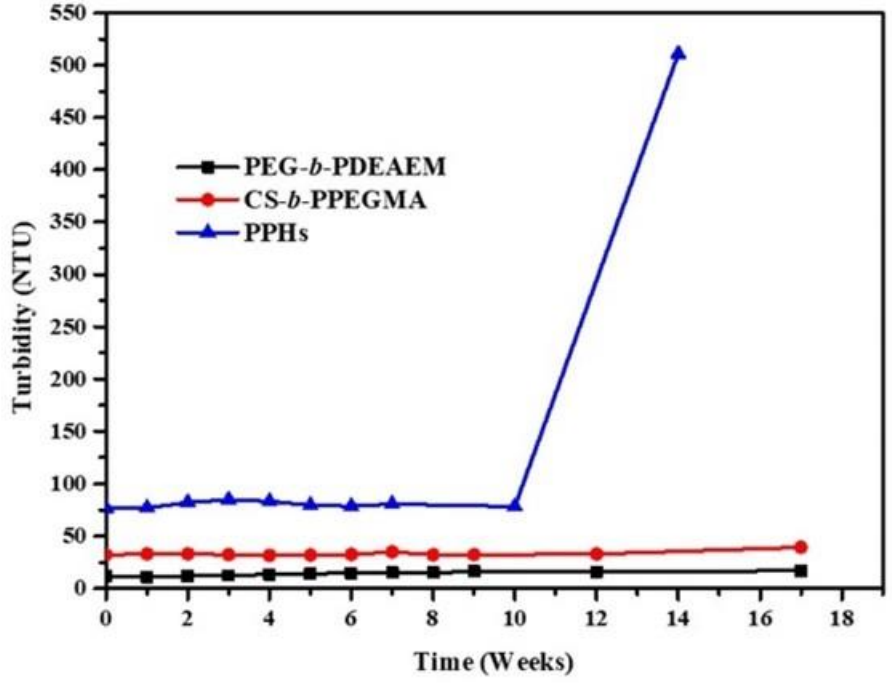

Figure 5. Stability of the phenolic compounds in water as studied by turbidimetry.

3.2 Loading and release of phenolic compounds from L. graveolens

The *L. graveolens* extract and CS-*b*-PPEGMA were characterized in a previously published work [18]. Table 1 shows the loading efficiency and content of PPHs in the copolymers. The LE is high, between 83.5 and 92%, and the loading content is also high (>60%), showing

only slight differences among both matrixes (PEG-*b*-PDEAEM slightly better). The size of the aggregates is doubled when the PPHs are inside the matrix, this is accompanied by a decrease of the surface charge (Zeta potential) of the aggregates when the PPHs are loaded in the different matrixes.

Table 1. Characterization parameters of polyphenols and encapsulated polyphenols: Loading Efficiency (LE), Loading content (LC), Zeta potential (ζ), and hydrodynamic diameter (D_h).

	LE (%)	**LC (%)**	**ζ (mV)**			**D_h (nm)**	
	By UV-Vis		Mixture	W PPHs	W/O PPHs	W PPHs	W/O PPHs
CS-*b*-PPEGMA	83.5	62.6	7.91 ± 4.37	-15.5 ± 4.57	-9.07 ± 4.86	458 ± 0.01	190 ± 17
PEG-*b*-PDEAEM	92.1	64.8	10.93 ± 2.21	16.8 ±1.99	21.66 ± 1.88	122.4 ± 0	64.94 ± 5.34
PPHs	-	-	- 8.79 ± 4.29	-	-	-	-

mV: Milivolts, nm: nanometers: W PPHs: with Polyphenols Loaded, W/O PPHs: without Polyphenols. Values for ζ and D_h are for three samples ± standard deviation. The ANOVA was evaluated with Tukey's comparison ($p<0.05$) for ζ showing significance in all cases.

The PPHs release studies showed that when the extract is encapsulated in the PEG-*b*-PDEAEM blocks there is a clear difference in the release rate as a function of pH, releasing a greater amount of PPHs at an acidic pH=2 after 8 h, 40% (Figure 6a); almost three times the release rate as compared to pH=8. This is unsurprising since the PDEAEM aggregates may disintegrate when subjected to acidic pH for a long time. On the other hand, in the continuous release study (Figurer 6b), in which the times of the gastrointestinal process were simulated, it can be observed that the release percentage is much lower at pH 2, with the same behavior occurring at every change in pH; nevertheless, the fact that at pH 8 the release rate is one third of that at pH 2 remains the same. The big change is the total release rate after the gastrointestinal process, where 76% of PPHs were still not released. For the PPHs loaded

in CS-*b*-PPEGMA blocks, the abrupt change of release rate with pH-changes is not observed, but a higher percentage of total released PPHs (close to 80%) is observed (Figure S4 in Supporting information); this can be attributed to the high solubility that these copolymers have in aqueous medium due to the large amount of PEGMA units.

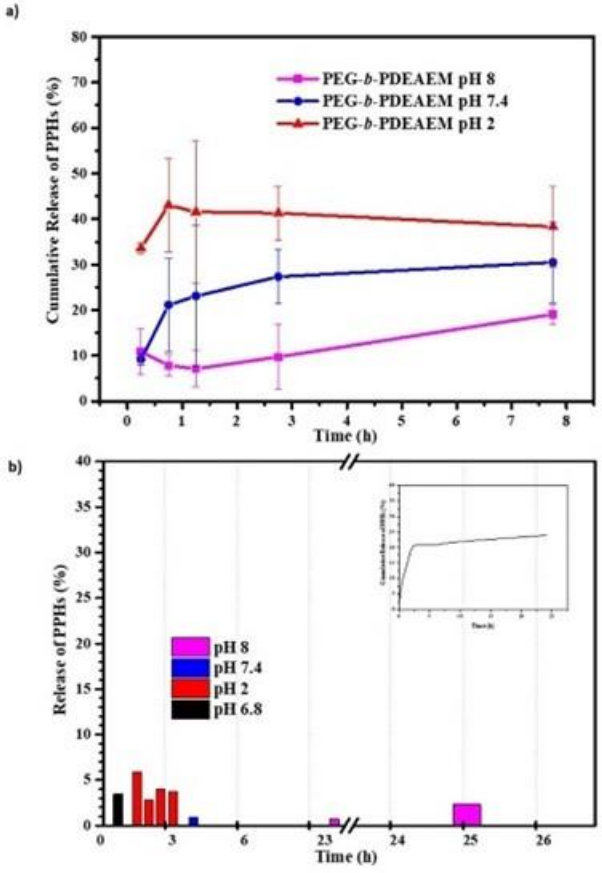

Figure 6. Release profiles of PPHs from PEG-*b*-PDEAEM: a) At different pH values; and b) by sequential change of pH: 6.8, 2, 7.4 and 8, simulating gastrointestinal tract passage and cumulative release.

Comparing the profiles of the copolymers with that of the non-encapsulated PPHs, a higher release percentage of the compounds at pH 2 and pH 7.4 can be observed when they are

encapsulated, especially in the CS-*b*-PPEGMA matrix (Figure S4a in Supporting information).

The study by UPLC/MS, has provided significant insights into the content of phenolic compounds during the gastric and intestinal phases. The results show that the release of these compounds from the cationic matrixes is significantly lower during the gastric phase compared to the release at pH 2 for 8 h. When no matrix is used and the PPHs are subjected to the simulated gastrointestinal phase, only 2% of them remain intact after this passage; however, the use of PEG-*b*-PDEAEM and CS-*b*-PPEGMA matrixes has proved to be highly effective in protecting about 80% of the phenolic compounds after the passage of the gastrointestinal phase. These findings provide a great opportunity to improve the efficacy of phenolic compounds for various applications (details in section 3.4).

6

3.3 Gastro-intestinal in vitro assay

The antioxidant activity and reducing capacity were determined by the gastrointestinal test after passing through the intestinal phases, finding that for the total reducing capacity (Table 2) the matrixes by themselves provide joint activity with the polyphenolic extract, contrary to the antioxidant activity (AOX) where said activity is not observed for the matrixes. This may be due to the mechanisms of the radicals present in each of the tests, since while in the reducing capacity test electron exchange is needed in the others hydrogen exchange is necessary. Therefore, due to the nature of the groups (quaternary amines), the exchange of electrons is facilitated over the exchange of hydrogen.

Table 2. AOX capability of PPHs loaded in matrixes by ORAC and TEAC methods after gastrointestinal assays.

Matrix	AOX Free	AOX Loaded	Gastro-intestinal assay			
			ORAC		TEAC	
	µmol TE g^{-1} Dried Oregano Leaf		µmol TE g^{-1} Dried Oregano Leaf			
			Gastric	Intestinal	Gastric	Intestinal
None	18.68 ± 2.79	-	10.09 ± 1.39	2.74 ± 0.34	125 ± 40.53	310 ± 77.78
CS-*b*-PPEGMA	NA	7.30 ± 0.60	47.56 ± 4.96	32.34 ± 1.52	205 ± 59.62	416.25 ± 30.05
PEG-*b*-PDEAEM	NA	7.87 ± 1.99	39.36 ± 8.46	31.63 ± 0.92	206.25 ± 28.28	551.25 ± 1.76

The tests were performed in triplicate, and results were presented as mean ± standard deviation all showing a significance of $p<0.05$ between each of the samples by the Tukey test.
NA: No activity.

3.4 Quantification of the content of phenolic compounds by UPLC/MS

The content of some flavonoids previously detected in the *L. graveolens* extract was determined by UPLC/MS. Table 3 shows the quantities of these compounds in mg mL^{-1} of the dissolved sample, finding that the maceration method used, followed by ethanolic extraction resulted in the highest concentration of hesperidin, followed by naringenin and phloridzin. After the simulated gastro-intestinal passage (Table 4) it can be seen that most of the compounds are lost when they are not encapsulated, while around 80% of these remain encapsulated in the PEG-*b*-PDEAEM and CS-*b*-PPEGMA blocks after the gastro-intestinal passage, with naringenin, phloridzin and cirsimaritin predominating.

Table 3. Flavonoid content was determined by UPLC/MS in 1 mg mL^{-1} of PPHs, and PPHs loaded in PEG-*b*-PDEAEM and in CS-*b*-PPEGMA. The tests were performed in triplicate and the results were presented as mean ± standard deviation. All values show significance of $p<0.05$ between each of the samples by the Tukey test.

	PPHs	**PEG-*b*-PDEAEM**	**CS-*b*-PPEGMA**
	(mg mL^{-1})		
Api	4.057 ± 0.357	2.865 ± 0.059	0.421 ± 0.39
QuerOrham	0.259 ± 0.081	0.443 ± 0.08	0.682 ± 0.127
Lu	5.128 ± 0.94	0.864 ± 0.042	0.904 ± 0.588
Lu7gli	12.88 ± 0.68	8.237 ± 0.189	13.679 ± 2.422
Narin	144.926 ± 2.68	46.102 ± 0.7	71.262 ± 0.88
Ru	0.143 ± 0.037	0.363 ± 0.041	0.403 ± 0.106
Hesp	155.903 ± 13.74	65.661 ± 7.522	114.12 ± 17.347
Kaem	3.505 ± 0.508	1.684 ± 0.018	1.286 ± 0.812
Phlo	38.157 ± 1.141	26.561 ± 1.64	45.546 ± 2.935
Cir	18.243 ± 0.46	7.977 ± 0.642	4.312 ± 1.86
Quer	0.606 ± 0.006	-	-
TOTAL	383.807	160.747	252.615

Api: Apigenine; QuerOrham: Quercetin-O-Rhamnosido; Lu: Luteoline; Lu7gli: Luteolin-7-glicoside; Narin: Naringenin; Ru: Rutin; Hesp: Hesperidin; Kaem: Kaempherol; Phlo: Phloridzin; Cir: Cirsimaritin; Quer: Quercetin

Table 4. Flavonoid content determined by UPLC/MS in 1 mg mL^{-1} of PPHs, and PPHs loaded in PEG-*b*-PDEAEM and in CS-*b*-PPEGMA after gastrointestinal *in vitro* assay (intestinal phase). The tests were performed in triplicate, and the results were presented as mean ± standard deviation. All values show significance of $p<0.05$ between each of the samples by the Tukey test.

	PPHs	PEG-*b*-PDEAEM	CS-*b*-PPEGMA
	(mg mL^{-1})		
Api	0.035 ± 0.003^{C}	2.076 ± 0.273^{A}	1.729 ± 0.795^{B}
QuerOrham	-	0.201 ± 0.033^{A}	0.195 ± 0.059^{B}
Lu	$0.044 \pm 0.0.004^{C}$	1.371 ± 0.653^{B}	2.093 ± 1.056^{A}
Lu7gli	0.077 ± 0.006^{C}	5.266 ± 0.581^{B}	29.568 ± 1.460^{A}
Narin	0.991 ± 0.086^{C}	83.690 ± 0.379^{B}	132.575 ± 5.570^{A}
Ru	-	0.190 ± 0.011^{A}	0.039 ± 0.035^{B}
Hesp	0.037 ± 0.004^{C}	0.817 ± 0.403^{B}	17.753 ± 2.220^{A}
Kaem	0.023 ± 0.002^{C}	0.839 ± 0.106^{B}	1.0466 ± 0.510^{A}
Phlo	0.325 ± 0.028^{C}	36.665 ± 1.947^{B}	49.969 ± 4.361^{A}
Cir	0.637 ± 0.090^{C}	18.968 ± 2.472^{A}	12.604 ± 1.566^{B}
Quer	-	0.246 ± 0.023^{A}	0.167 ± 0.011^{B}
TOTAL	2.169	150.329	247.7386

Api: Apigenine; QuerOrham: Quercetin-O-Rhamnosido; Lu: Luteoline; Lu7gli: Luteolin-7-glicoside; Narin: Naringenin; Ru: Rutin; Hesp: Hesperidin; Kaem: Kaempherol; Phlo: Phloridzin; Cir: Cirsimaritin; Quer: Quercetin

3.5 Cytotoxicity Assay

To determine the cytotoxicity of the cationic matrixes (block copolymers) and the ethanolic extract from Oregano (PPHs), a range of concentrations were tested in a colon fibroblasts cell-line (CCD18) by means of a colorimetric assay. The concentration of LDH (Figure 7) was determined, which indicates the percentage of dead cells; among the concentration of tested compounds, the highest was 1000 μg mL^{-1} and the lowest was 100 μg mL^{-1}, in which it was possible to observe that the extract does not show cytotoxicity (Figure 7a) at the high

concentration of 500 μg mL^{-1} and slightly exceeding 20% at the highest concentration used (1000 μg mL^{-1}); while the PEG-*b*-PDEAEM (Figure 7b) cationic block without PPHs (PPB, blue columns) show cell death exceeding 70% at the highest concentrations (1000 and 500 μg mL^{-1}). In the case of PDEAEM, it is known that this polymer is cytotoxic, so it is normally used in low concentrations and copolymerized with non-cytotoxic polymers [15]. In the same way, it can be observed that the cytotoxicity of this block copolymer decreases attenuated when the polyphenolic compounds are encapsulated (PP, red columns); this could be because the quaternary amines are not fully exposed, masked by interactions with the PPHs. In the case of the CS-*b*-PPEGMA cationic block (Figure 7c) without PPHs (CPB, blue columns), the percentage of cell death was around 30% at the highest concentration (1000 μg mL^{-1}), and also the cell death diminished after loading with PPHs (CP, red columns). In both cases, the PPHs loaded in block copolymers up to a concentration of 1000 μg mL^{-1} are not cytotoxic to the non-cancerous fibroblast cell line. The microscopic images of cells corresponding to this test can be seen in the supplementary material (Figures S5-S7 in Supplementary material).

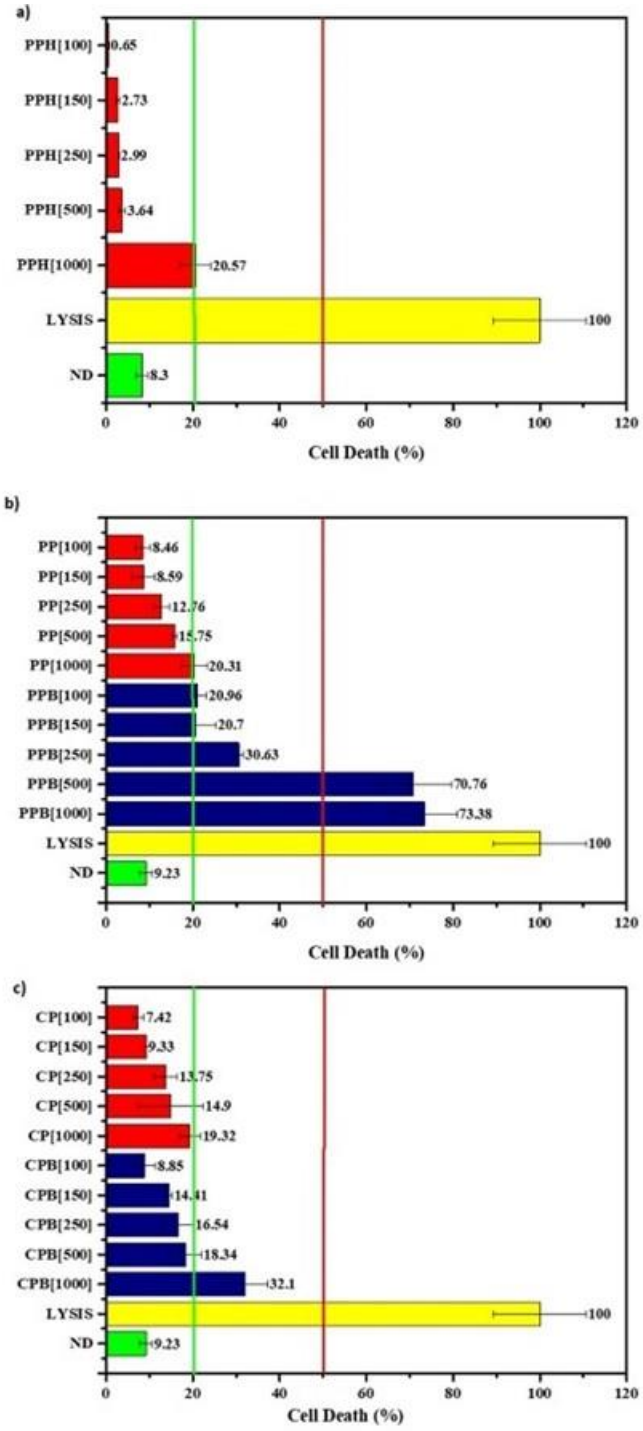

Figure 7. Cell death by LDH test for non-cancerous colon cell line (CCD18): a) PPHs, b) PEG-*b*-PDEAEM with PPHs (PP) and without (PPB) and c) CS-*b*-PPEGMA with PPHs (CP)

and without (CPB) at a concentration of 100 to 1000 μg mL^{-1}. The tests were performed in triplicate and the results were presented as mean ± standard deviation.

3.6 Antiproliferative Assay

After determining the concentration at which the cationic matrixes (CS-*b*-PPEGMA and PEG-*b*-PDEAEM) and the extract (PPHs) did not show cytotoxicity to the CCD18-colon fibroblasts cell line, the antiproliferative capacity was determined by the MTT colorimetric assay on colon cancer Caco-2 cells at concentrations of 500 and 150 μg mL^{-1} for each PPHs and PPHs loaded cationic matrixes, having 5-fluorouracil (5FU), a common colon-cancer chemotherapeutic agent, as positive control after 24, 48 and 72 h of contact (Figure 8a). At 24 h, cell viability decreased to 15% with the PPHs (500 μg mL^{-1}), while encapsulated in both matrixes, PPHs decreased cell viability only to 73-83% at the same concentration suggesting that the encapsulated PPHs were not released; while it could be observed that no significant difference was observed to the anticancer drug 5FU at the concentration used. After 48 and 72 h (Figure 8b and c), it can be seen that the treatments decreased the cell viability, while free PPHs at 500 μg mL^{-1} after 72 h almost completely inhibited the growth of Caco-2 cells. On the other hand, PPHs loaded on both cationic matrixes after 72 h of treatment at the same concentration (500 μg mL^{-1}) reached the half-maximal inhibitory concentration (IC_{50}) for Caco-2 cells, similar to the 5FU positive control. In general terms, the 150 μg mL^{-1} treatments decreased the cell viability of Caco-2 cells slightly (74%), and this effect increased after 72 h of contact (Figure 8c): 65% for PEG-*b*-PDEAEM (PP) and 69% for CS-*b*-PPEGMA (CP) suggesting a slow release of the PPHs from the cationic matrixes.

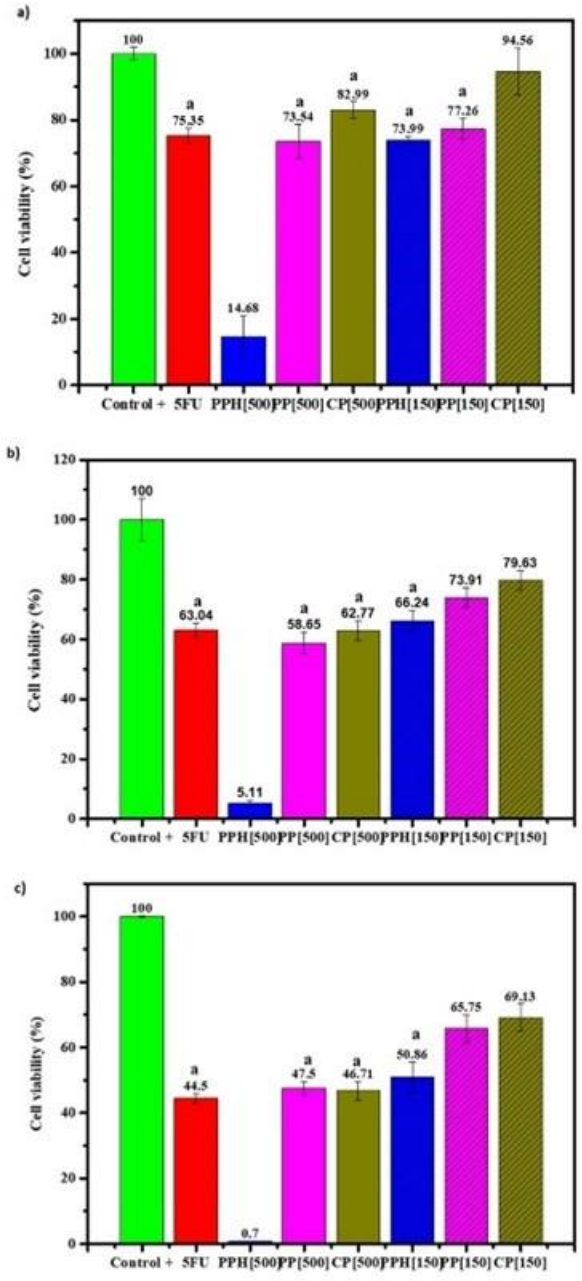

Figure 8. Cell viability (antiproliferative assay) for Caco-2 colon cancer cells treated with free PPHs and PPHs loaded on CS-*b*-PPEGMA (CP), and loaded on PEG-*b*-PDEAEM (PP) at concentrations of 150 and 500 μg mL^{-1} for a) 24 h, b) 48 h and c) 72 h. The tests were performed in triplicate, and the results were presented as mean ± standard deviation. The ANOVA was evaluated with the Dunnett test taking 5FU as a control.

The microscopic images of the cells corresponding to the activity of antiproliferative assay can be seen in the supplementary material (Figures S8-S10 in Supplementary material).

4 Discussion

The use of polymeric systems with cationic monomers has been widely used in recent years since the transport of active compounds is facilitated by electrostatic interactions with them, as is the case of PDEAEM and CS [16, 22-24]. These polymers are coupled with other hydrophilic polymers such as PEG or PEGMA, which help in the formation of more stable and well-dispersable nanoparticles in aqueous medium, thus improving the solubility of active ingredients that are poorly soluble in aqueous medium, as is the case of phenolic compounds [25, 26]. In addition, using PEG and PEG-derivatives results in having less adhesion to molecules present in physiological media so that they may travel without being detected [27]. The results show that both tested systems, CS-*b*-PPEGMA and PEG-*b*-PDEAEM, can provide thermal protection to the loaded Oregano extract (Figure 4) and stability in the aqueous medium (Figure 5). In both tested systems, the protection may be due to the interaction of the amino and tertiary amine groups of the polymers with the OH groups of the polyphenols, which would cause the displacement of decomposition temperatures and high stability in aqueous medium [25], as shown in the results obtained. Regarding the stability studied by turbidity measurements, it can be assumed that a similar turbidity indicates that there were no marked variations in the intensity of scattered light during the monitoring of a sample, that is, there was no marked variation in the sizes and number of suspended particles. However, for free PPHs, the agglomeration phenomenon increased the

586 intensity of scattered light, resulting in higher turbidity. On the other hand, the loading of
587 phenolic compounds in different systems has been carried out using different methodologies;
588 however, the loading efficiency is maximized in cases where solvent evaporation is used, in
589 addition to obtaining much smaller particle sizes [28]. In the current report, the used strategy
590 was good enough to obtain LE higher than 90%. The methodology used for the synthesis of
591 each of the blocks may contribute to the difference in the size of the same particles, while for
592 the PDEAEM blocks controlled synthesis (RAFT) was used. For the CS blocks, synthesis by
593 conventional free radical polymerization was used, so the size of both CS and PEGMA chains
594 can vary. The sizes were smaller for PDEAEM block aggregates. On the other hand, a
595 decrease in Zeta potential was observed after encapsulating the compounds and this is
596 because the interaction of the phenolic compounds with the amino groups that are previously
597 protonated is taking place. Regarding the release profiles of phenolic compounds from PEG-
598 *b*-PDEAEM compared to the CS-*b*-PPEGMA and PPHs reported previously by Garcia-
599Carrasco et al. [18], it can be observed that changes in pH significantly affect the release of 600
these systems and this may be due to the type of amine groups, contained in PEG-*b*- 601
PDEAEM as well as how free or impeded they are to be able to protonate/deprotonate when 602
the pH of the medium changes [29, 30]. In the same way, it was observed a maximum release 603 of
80% of PPHs from the CS-*b*-PPEGMA matrix, and an increase in the PPHs solubility and 604
apparently their bioavailability is suggested [31]. Comparing both cationic systems, it can be 605
said that the one that provides greater protection for phenolic compounds in the stomach is 606
the PEG-*b*-PDEAEM matrix. Results of release in individual pH values compared to 607
continuous release profiles changing the pH simulating a gastro-intestinal passage, showed a 608
clear difference in the release percentage. The changes in medium's pH that occur when 609
passing from one phase of the gastrointestinal system to another, resulted in a lower release

of phenolic compounds for the PEG-*b*-PDEAEM matrix as compared to the CS-b-PPEGMA system which is because the matrixes take different times to solvate in the new medium. As a result, the PEG-*b*-PDEAEM matrix protects better the phenolic compounds in the gastrointestinal process. The protection of PPHs after intestinal passage is more clearly observed in the gastrointestinal *in vitro* assay for antioxidant activity in which by TEAC and ORAC (Table 2), greater antioxidant activity can be observed in the intestinal phase, which infers the protection and release of compounds in the gastric phase when the cationic matrixes were used. The amount of some phenolic compounds of the flavonoid type was determined by UPLC/MS. It can be observed that naringenin, phloridzin and cirsimaritin predominated in the loaded cationic matrixes; the larger proportion of these encapsulated compounds has to do with the presence of many OHs groups and their interaction with the tertiary amino groups of PDEAEM and amino groups of CS. On the other hand, hydrogen bonds could also be forming with the ethyleneglycol units of PEG/PEGMA chains due to its hydrophilicity, which is reflected in the decrease of Zeta potential of the CS blocks, since having a greater amount of PEGMA has a greater probability of carrying out this type of interaction with phenolic compounds [32, 33]. In the same way, it was possible to determine the percentage of loading of flavonoids in the cationic matrixes by UPLC/MS, where the loading content in the cationic blocks of PEG-*b*-PDEAEM and CS-*b*-PPEGMA was 47 and 81%, respectively as compared to the content of flavonoids in the extract. There is no difference to the loading efficiency of the whole extract as determined by UV-vis (Table 1) in the case of the PEG-*b*-PDEAEM matrix, but in the case of the CS-*b*-PPEGMA there seems to be a preference to load of the flavonoids. Of course, this is a rough estimate since, by UV-vis, the loaded content on PPHs was estimated at a single wavelength. Likewise, the bioavailability of these compounds was determined after passing through the gastrointestinal phase (Table 4), where

it can be seen that the phenolic compounds were almost completely lost when they were not encapsulated, otherwise by the use of PEG-*b*-PDEAEM and CS-*b*-PPEGMA around 84 and 79%, respectively of the compounds are still conserved. On the other hand, different investigations have determined that the compounds present in a greater proportion, in this case naringenin, phloridzin and cirsimaritin, have anti-inflammatory and antiproliferative properties [34-37]. This was reflected clearly in the antiproliferative capacity test (Figure 8), in which it can be observed that the bare phenolic compounds inhibit the proliferation of Caco-2 cells almost entirely after 72 h. Still, when they were loaded in the different cationic matrixes, it was observed that they showed a lower, nevertheless similar activity to that of 5FU, without presenting cytotoxicity to healthy cells at the same concentration. Tian et al. [38] demonstrated that PEG-*b*-PDEAEM blocks did not show cytotoxicity in HeLa cells. On the other hand Manzanares-Guevara et al [15], determined that PDEAEM-*net*-PEGMA nanogels presented cytotoxicity to HCT29 cells, when the PDEAEM content was greater than 20% in the nanogels, so the morphology of the matrixes can determine whether they will present greater or lesser cytotoxicity depending on the cell line; and also, how exposed the quaternary amino groups of PDEAEM are, which have been shown to cause this cytotoxicity. This can be verified with the cytotoxicity test performed in the current study; when the cationic blocks were not loaded with PPHs, they presented greater cytotoxicity than when loaded. Moreover, they are safe up to concentrations of 1000 $\mu g\ mL^{-1}$. It is also important to note that the bare PPHs are non-cytotoxic to the tested healthy colon cell line but are highly cytotoxic to the colon cancer cell line.

5 *Conclusion*

The phenolic compounds extracted from Mexican Oregano (*Lippia graveolens*) increased their solubility, as well as their antioxidant activity after being loaded in cationic polymer matrixes. It was demonstrated that both the PDEAEM-based and CS-based cationic matrixes provide the phenolic compounds with stability in an aqueous medium for a little over 4 months. On the other hand, results suggest that in addition to the interactions with the amino groups, phenolic compounds can create hydrogen bonds with hydrophilic ethoxy compounds such as PEG/PEGMA. These systems protect a good part of the phenolic compounds when passing through the gastric phase, thus increasing their antioxidant (TEAC and ORAC) activity, after passing the intestinal phase, protecting more than 80% of the phenolic compounds encapsulated in the different systems. UPLC/MS test showed that in the better protected Oregano extracts, predominate the flavonoid type compounds such as naringenin, phloridzin and cirsimaritin, to which anti-inflammatory and anticancer properties have been attributed. It was also observed that these extracts do not show cytotoxicity to colon fibroblasts (CCD18), at concentrations lower than 500 $\mu g\ mL^{-1}$, while they do show antiproliferative activity in CACO-2 cells (cancerous cells) similar to that of the well-known anticancer drug 5FU used in colon cancer chemotherapy. Therefore, it is inferred that the cationic matrix loaded Oregano extract could be used in the future as an adjuvant drug in the treatment of colon cancer by oral administration since the PPhs are well protected with the cationic matrixes after digestive tract passage and the active compounds are much more active against colon cancer cells than healthy cells.

Funding disclosure

This investigation was supported by internal funds of the participating Institutions of the authors: Tecnológico Nacional de México/Instituto Tecnológico de Tijuana (TNM/ITT) and the Centro de Investigación en Alimentación y Desarrollo, A.C. (CIAD).

Authorship contribution statement

Conceptualization, J.B.H., A.L.-C. and M.G-C; Investigation, M.G.-C. and L.C.A; Resources, J.B.H. and A.L.-C.; Supervision, J.B.H. and A.L.-C.; Writing—original draft, M.G.-C.; Writing—review & editing, J.B.H., A.L.-C. and M.G-C. All authors have read and agreed to the published version of the manuscript.

Declaration of competing interest

The authors declare that they have no known competing financial interests or personal relationships that could have appeared to influence the work reported in this paper.

Data availability

The data that support the findings of this study are available from the corresponding author upon reasonable request.

Acknowledgments

We thank Dr. L. Contreras and Dr. N. Leyva (UPLC-MS measurements, CIAD-Culiacán) and V. Miranda (NMR measurements, ITT NMR facilities funded by CONACYT Grant: INFR-2011-3-173395). E.P.G.-G. thanks CONACYT for the Catedras Project #397.

References

[1] D. Tungmunnithum, A. Thongboonyou, A. Pholboon, A. Yangsabai, Flavonoids and Other Phenolic Compounds from Medicinal Plants for Pharmaceutical and Medical Aspects: An Overview, Medicines 5(3) (2018) 93. https://doi.org/10.3390/medicines5030093

[2] D.L. Ambriz-Pérez, N. Leyva-López, E.P. Gutierrez-Grijalva, J.B. Heredia, Phenolic compounds: Natural alternative in inflammation treatment. A Review, Cogent Food & Agriculture 2(1) (2016) 1131-412.https://doi.org/10.1080/23311932.2015.1131412

[3] H. Rasouli, M.H. Farzaei, K. Mansouri, S. Mohammadzadeh, R. Khodarahmi, Plant Cell Cancer: May Natural Phenolic Compounds Prevent Onset and Development of Plant Cell Malignancy? A Literature Review, Molecules 21(9) (2016) 1104. https://doi.org/10.3390/molecules21091104

[4] M.A. Soobrattee, T. Bahorun, O.I. Aruoma, Chemopreventive actions of polyphenolic compounds in cancer, BioFactors 27 (2006) 19-35.https://doi.org/10.1002/biof.5520270103

[5] A.G. Muller, S.D. Sarker, I.Y. Saleem, G.A. Hutcheon, Delivery of natural phenolic compounds for the potential treatment of lung cancer, DARU Journal of Pharmaceutical Sciences 27(1) (2019) 433-449.https://doi.org/10.1007/s40199-019-00267-2

[6] M.-T. Huang, T. Ferraro, Phenolic Compounds in Food and Cancer Prevention, Phenolic Compounds in Food and Their Effects on Health II, American Chemical Society, 1992, pp. 8-34. https://doi.org/10.1021/bk-1992-0507.ch002

[7] H.W. Jun, J.L. West, Endothelialization of microporous YIGSR/PEG-modified polyurethaneurea, Tissue Engineering 11(1076-3279 (Print)) (2005).https://doi.org/10.1089/ten.2005.11.1133

[8] H. Yu, V.P. J., M.L. ., M.H. W., W.P. H., S.-Y. Yang, Improved tissue-engineered bone regeneration by endothelial cell mediated vascularization, Biomaterials 30(4) (2009) 508-517. https://doi.org/10.1016/j.biomaterials.2008.09.047

[9] Y.-C. Chiu, S. Kocagöz, J.C. Larson, E.M. Brey, Evaluation of Physical and Mechanical Properties of Porous Poly (Ethylene Glycol)-co-(L-Lactic Acid) Hydrogels during Degradation, PLOS ONE 8(4) (2013).https://doi.org/10.1371/journal.pone.0060728

[10] J.B. Maria Molina, Ana Sousa-Hervés, Marcelo Calderón, APLICACIONES BIOMÉDICAS DE NANOGELES DENDRÍTICOS TERMOSENSIBLES, Revista Iberoamericana de Polímeros 16 (2015) 9

[11] H. Otsuka, N. Y., K. Kataoka, PEGylated nanoparticles for biological and pharmaceutical applications, Advanced Drug Delivery Reviews 64 (2012) 246-255.https://doi.org/0.1016/s0169-409x(02)00226-0

[12] Q. Chen, S. Li, Z. Feng, M. Wang, C. Cai, J. Wang, L. Zhang, Poly(2-(diethylamino)ethyl methacrylate)-based, pH-responsive, copolymeric mixed micelles for targeting anticancer drug control release, International Journal of Nanomedicine 12 (2017) 6857-6870. https://doi.org/10.2147/IJN.S143927

[13] C.C. Lin, K.S. Anseth, PEG hydrogels for the controlled release of biomolecules in regenerative medicine, Pharmaceutical Research 26 (2009) 631-643. https://doi.org/10.1007/s11095-008-9801-2

[14] J.I. Amalvy, E.J. Wanless, Y. Li, V. Michailidou, S.P. Armes, Y. Duccini, Synthesis and Characterization of Novel pH-Responsive Microgels Based on Tertiary Amine Methacrylates, Langmuir 20(21) (2004) 8992-8999.https://doi.org/10.1021/la049156t

[15] L.A. Manzanares-Guevara, A. Licea-Claverie, F. Paraguay-Delgado, Preparation of stimuli-responsive nanogels based on poly(N,N-diethylaminoethyl methacrylate) by a simple "surfactant-free" methodology, Soft Materials 16(1) (2018) 37-50. https://doi.org/10.1080/1539445X.2017.1391845

[16] N.A. Cortez-Lemus, S.V. García-Soria, F. Paraguay-Delgado, A. Licea-Claveríe, Synthesis of gold nanoparticles using poly(ethyleneglycol)-b-poly(N,N-diethylaminoethylmethacrylate) as nanoreactors, Polymer Bulletin 74(9) (2017) 3527-3544.https://doi.org/10.1007/s00289-017-1906-5

[17] F. Ganji, M.J. Abdekhodaie, Synthesis and characterization of a new thermosensitive chitosan–PEG diblock copolymer, Carbohydrate Polymers 74(3) (2008) 435-441. https://doi.org/10.1016/j.carbpol.2008.03.017

[18] M. Garcia-Carrasco, L.A. Picos-Corrales, E.P. Gutiérrez-Grijalva, M.A. Angulo-Escalante, A. Licea-Claverie, J.B. Heredia, Loading and Release of Phenolic Compounds Present in Mexican Oregano (Lippia graveolens) in Different Chitosan Bio-Polymeric Cationic Matrixes, Polymers 14(17) (2022) 3609. https://doi.org/10.3390/polym14173609

[19] L.A. Picos-Corrales, M. Garcia-Carrasco, A. Licea-Claverie, R.A. Chavez-Santoscoy, S.O. Serna-Saldívar, NIPAAm-containing amphiphilic block copolymers with tailored LCST: Aggregation behavior, cytotoxicity and evaluation as carriers of indomethacin, tetracycline and doxorubicin, Journal of Macromolecular Science, Part A 56(8) (2019) 759-772. https://doi.org/10.1080/10601325.2019.1586440

[20] A. Brodkorb, L. Egger, M. Alminger, P. Alvito, R. Assunção, S. Ballance, T. Bohn, C. Bourlieu-Lacanal, R. Boutrou, F. Carrière, A. Clemente, M. Corredig, D. Dupont, C. Dufour, C. Edwards, M. Golding, S. Karakaya, B. Kirkhus, S. Le Feunteun, U. Lesmes, A. Macierzanka, A.R. Mackie, C. Martins, S. Marze, D.J. McClements, O. Ménard, M. Minekus, R. Portmann, C.N. Santos, I. Souchon, R.P. Singh, G.E. Vegarud, M.S.J. Wickham, W. Weitschies, I. Recio, INFOGEST static *in vitro* simulation of gastrointestinal food digestion, Nature Protocols 14(4) (2019) 991-1014. https://doi.org/10.1038/s41596-018-0119-1

[21] K. Thaipong, U. Boonprakob, K. Crosby, L. Cisneros-Zevallos, D. Hawkins Byrne, Comparison of ABTS, DPPH, FRAP, and ORAC assays for estimating antioxidant activity from guava fruit extracts, Journal of Food Composition and Analysis 19(6) (2006) 669-675. https://doi.org/10.1016/j.jfca.2006.01.003

[22] M. Hasannia, A. Aliabadi, K. Abnous, S.M. Taghdisi, M. Ramezani, M. Alibolandi, Synthesis of block copolymers used in polymersome fabrication: Application in drug delivery, Journal of Controlled Release 341 (2022) 95-117. https://doi.org/10.1016/j.jconrel.2021.11.010

[23] H. Wang, C. Wang, Y. Zou, J. Hu, Y. Li, Y. Cheng, Natural polyphenols in drug delivery systems: Current status and future challenges, Giant 3 (2020) 100022. https://doi.org/10.1016/j.giant.2020.100022

[24] M.J. Manganiello, C. Cheng, A.J. Convertine, J.D. Bryers, P.S. Stayton, Diblock copolymers with tunable pH transitions for gene delivery, Biomaterials 33(7) (2012) 2301-2309. https://doi.org/10.1016/j.biomaterials.2011.11.019

[25] S. Rahaiee, E. Assadpour, A. Faridi Esfanjani, A.S. Silva, S.M. Jafari, Application of nano/microencapsulated phenolic compounds against cancer, Advances in Colloid and Interface Science 279 (2020) 102153. https://doi.org/10.1016/j.cis.2020.102153

[26] D. Shukla, N.K. Nandi, B. Singh, A. Singh, B. Kumar, R.K. Narang, C. Singh, Ferulic acid-loaded drug delivery systems for biomedical applications, Journal of Drug Delivery Science and Technology 75 (2022) 103621. https://doi.org/10.1016/j.jddst.2022.103621

[27] S.K. Mann, A. Dufour, J.J. Glass, R. De Rose, S.J. Kent, G.K. Such, A.P.R. Johnston, Tuning the properties of pH responsive nanoparticles to control cellular interactions *in vitro* and ex vivo, Polymer Chemistry 7(38) (2016) 6015-6024. https://doi.org/10.1039/C6PY01332E

[28] A. Borges, V. de Freitas, N. Mateus, I. Fernandes, J. Oliveira, Solid Lipid Nanoparticles as Carriers of Natural Phenolic Compounds, Antioxidants 9(10) (2020) 998. https://doi.org/10.3390/antiox9100998

795 [29] G. Aguirre, E. Villar-Alvarez, A. González, J. Ramos, P. Taboada, J. Forcada, Biocompatible 796 stimuli-responsive nanogels for controlled antitumor drug delivery, Journal of Polymer Science Part 797 A: Polymer Chemistry 54(12) (2016) 1694-1705. https://doi.org/10.1002/pola.28025
798 [30] A. Pikabea, E. Villar-Álvarez, J. Forcada, P. Taboada, pH-controlled doxorubicin delivery from 799 PDEAEMA-based nanogels, Journal of Molecular Liquids 266 (2018) 321-329.
800 https://doi.org/10.1016/j.molliq.2018.06.068
801 [31] J.R. Costa, M. Xavier, I.R. Amado, C. Gonçalves, P.M. Castro, R.V. Tonon, L.M.C. Cabral, L. 802 Pastrana, M.E. Pintado, Polymeric nanoparticles as oral delivery systems for a grape pomace extract 803 towards the improvement of biological activities, Materials Science and Engineering: C 119 (2021) 804 111551.https://doi.org/10.1016/j.msec.2020.111551
805 [32] L. Xavier, M.S. Freire, I. Vidal-Tato, J. González-Álvarez, Recovery of Phenolic Compounds from 806 Eucalyptus globulus Wood Wastes using PEG/phosphate Aqueous Two-Phase Systems, Waste and 807 Biomass Valorization 8(2) (2017) 443-452. https://doi.org/10.1007/s12649-016-9579-0
808 [33] N. Rodríguez-Salazar, S. Valle-Guadarrama, Separation of phenolic compounds from roselle 809 (Hibiscus sabdariffa) calyces with aqueous two-phase extraction based on sodium citrate and 810 polyethylene glycol or acetone, Separation Science and Technology 55(13) (2020) 2313-2324.
811 https://doi.org/10.1080/01496395.2019.1634730
812 [34] V. Crespy, O. Aprikian, C. Morand, C. Besson, C. Manach, C. Demigné, C. Rémésy, Bioavailability 813 of Phloretin and Phloridzin in Rats, The Journal of Nutrition 131(12) (2001) 3227-3230. 814 https://doi.org/10.1093/jn/131.12.3227
815 [35] L.V. Gromova, Effect of phloretin and phloridzin on properties of digestion and absorption in 816 the rat small intestine, Journal of Evolutionary Biochemistry and Physiology 42(4) (2006) 454-460. 817 https://doi.org/10.1134/S0022093006040119
818 [36] J. Stabrauskiene, D.M. Kopustinskiene, R. Lazauskas, J. Bernatoniene, Naringin and Naringenin: 819 Their Mechanisms of Action and the Potential Anticancer Activities, Biomedicines 10 (17) (2022) 820 1686. https://doi.org/10.3390/biomedicines10071686
821 [37] H. Parhiz, A. Roohbakhsh, F. Soltani, R. Rezaee, M. Iranshahi, Antioxidant and Anti-Inflammatory 822 Properties of the Citrus Flavonoids Hesperidin and Hesperetin: An Updated Review of their 823 Molecular Mechanisms and Experimental Models, Phytotherapy Research 29(3) (2015) 323-331.
824 https://doi.org/10.1002/ptr.5256
825 [38] J. Tian, C. Xiao, B. Huang, X. Jiang, H. Cao, F. Liu, W. Zhang, Combating Multidrug Resistance 826 through an NIR-Triggered Cyanine-Containing Amphiphilic Block Copolymer, ACS Applied Bio 827 Materials 2(5) (2019) 1862-1874. https://doi.org/10.1021/acsabm.8b00793

828

829

4. CONCLUSIONES GENERALES

Los sistemas poliméricos utilizados para la encapsulación del extracto etanólico de orégano mexicano (*Lippia graveolens*) comprobaron mantener la actividad y en algunos casos aumentar la capacidad antioxidante del mismo, cuando se encontraban encapsulados. Así mismo se observó que al finalizar el ensayo de la simulación gastrointestinal *in vitro* los sistemas a base de PEG con los polímeros catiónicos (Quitosano y PDEAEM), desmostaron proteger al extracto de la fase gástrica, después de pasar por la fase intestinal se determinó que quedó más del 70% del contenido del extracto inicial. En las células CCD18-co se observó que los bloques sin cargar a base de quitosano no presentaron una alta citotoxicidad comparada a los bloques de PDEAEM, cuando el extracto polifenólico se encontraba encapsulado estos sistemas disminuyeron drásticamente su citotoxicidad lo cual nos indica que la interacción con el sistema se presenta en los grupos amino de ambos polímeros catiónicos. En cuanto a las células CACO-2, se determinó que estas matrices cargadas presentaron una actividad similar al fármaco modelo 5FU, por lo que se infiere que estas matrices poliméricas cargadas con el extracto polifenólico de orégano tienen potencial actividad antineoplásica.

5. RECOMENDACIONES

Con los resultados obtenidos en el presente trabajo es de importancia continuar con el desarrollo de diferentes matrices que ayuden a encapsular este tipo de compuestos, así como llevar la investigación a las siguientes etapas de desarrollo, ya que en los ensayos realizados se observó su posible potencial para desarrollarse como un biofármaco. Determinar si estos compuestos pudieran aumentar su actividad en terapia combinada con un fármaco modelo. Realizar ensayos de permeabilidad celular, para determinar cuáles de estos compuestos pueden atravesar la membrana. Así como realizar ajustes a la concentración de PDEAEM en los bloques obtenidos, para disminuir la citotoxicidad de los mismos.